THE STRATIGRAPHY AND SEDIMENTOLOGY OF THE BLACK REEF QUARTZITE FORMATION, TRANSVAAL SEQUENCE, IN THE AREA OF CARLETONVILLE AND WEST RAND GOLDFIELDS.

Hendrik Petrus Andreas Coetzee

B.Sc., B.Sc. Honours (Geology)

Thesis submitted in the Faculty of Natural Sciences of the Potchefstroomse Universiteit vir Christelike Hoër Onderwys (Potchefstroom University for Christian Higher Education) in partial fulfilment of the requirements for the degree Magister Scientiea in Geology.

Supervisor: Dr. B.G. Els

Co-supervisor: Dr. J.J. Mayer

POTCHEFSTROOM

1996

Abstract

In the study area the Black Reef Quartzite Formation lies unconformably at the base of the early Proterozoic Transvaal Sequence of South Africa. The Formation comprises a succession of interbedded siliceous quartzites and shales with erratically-developed basal grits and conglomerates in the area of the Carletonville and West Rand goldfields. Outcrops are restricted to the topographic ridge formed by the Rand Anticline.

The pre-Transvaal palaeosurface comprises a variety of rock-types. This heterolithic palaeosurface is a result of extensional tectonism which caused the development of horst, graben and half-graben structures.

A thickness study revealed that the thickness of the Formation is very inconsistent and that zones of maximum thickness generally correlate with linear depressions in the palaeosurface. This study also showed that during Black Reef times the palaeorelief of the study area was low.

The typical lithofacies association of the Formation, as determined by Markov analysis, comprises a basal pebbly quartzite unit overlain by a succession of alternating mudstone and quartzite units.

In the study area the Formation mostly has a uni-, bi- and polymodal palaeocurrent distribution. On the Rand Anticline the modes of the unimodal distribution are towards the north, but in the remainder of the study area the modes lie within the second and third azimuth quadrants. For the bi- and polymodal distributions there are no general dominant modes. The orientations of oscillation ripple crests show a general, well-defined east-west trend for most of the study area.

The pebble size and composition of the conglomerates vary significantly throughout the study area. A petrographic study revealed that the quartzites in the Black Reef succession are generally texturally very mature.

It is considered that the basal strata are characteristically bedload deposits, possibly the detritus of a braided stream system. The strata overlying these are characteristic of a tidal flat deposit, signifying a transgression. The sedimentary makeup of the coastal system, in which the upper strata of the Black Reef Quartzite Formation was deposited, probably consisted of estuarine, lagoon bay, tidal inlet, tidal flat and marsh environments. The transgression resulted in a rise in base level causing a decrease in sediment flux, bringing about clear-water conditions for the precipitation of the overlying carbonates of the Malmani Subgroup.

The cause of the transgression was probably post-graben thermal subsidence in a three-stage tectonic model. The proposed thermal subsidence basin led to the opening of a linear, shallow epeiric sea that transgressed over the partly-pediplaned palaeosurface.

Uittreksel

Die Swartrif Kwartsietformasie kom diskordant aan die basis van die Proterosoïese Transvaal Opeenvolging van Suid-Afrika voor. Die Formasie bestaan uit 'n opeenvolging van tussengelaagde silikaryke kwartsiete, skalies en wisselvallig ontwikkelde basale grintstene en konglomerate in die omgewing van die Carletonville- en die Wes-Rand-goudvelde. Dagsome van die Formasie is beperk tot die topografiese rug wat die Rand Antiklien vorm.

Die voor-Transvaal palaeo-oppervlak bestaan uit 'n verskeidenheid gesteentetipes. Hierdie heterogene palaeo-oppervlak is die gevolg van rek-tektonisme wat die ontwikkeling van horst-, graben- en halfgrabenstrukture veroorsaak het.

'n Diktestudie het getoon dat die dikte van die Formasie baie wisselvallig is en dat maksimum diktesones oor die algemeen ooreenstem met liniêre holtes in die vloergesteentes. Die studie het ook getoon dat die paleoreliëf van die Swartrifkwartsietformasie in die studiegebied baie laag is.

Die tipiese litofasie-opeenvolging van die Formasie bestaan uit 'n rolsteen-houdende kwartsiet, oorlê deur 'n opeenvolging van afwisselende moddersteen- en kwartsieteenhede. Die Formasie het 'n uni-, bi- en polimodale palaeostroom-verspreiding in die studiegebied. Op die Rand-Antiklien is die modus van die unimodale verspreidings noord gerig, maar in die oorblywende dele van die studiegebied lê die modusse in die tweede en derde asimutkwadrante. Vir die modusse van die bi- en polimodale verspreidings is daar geen algemene neiging nie. Die oriëntasies van ossilasiekabbelmerkkruine toon 'n goedgedefinieerde oos-wes rigting vir bykans die hele studiegebied.

Die rolsteengrootte en -samestelling van die konglomerate variëer betekenisvol deur die studiegebied. 'n Petrografiese studie het getoon dat die kwartsiete van die Swartrifopeenvolging oor die algemeen tekstureel baie ryp is. Die basale lae is kenmerkend bodemvragafsettings, moontlik die sediment van 'n vlegstroomriviersisteem. Die lae wat hierdie gesteentes oorlê is kenmerkend van 'n getyvlakte-afsetting, wat 'n transgressie impliseer. Die sedimentêre opset van die kusssisteem waarin die boonste lae van die Swartrif Kwartsietformasie afgeset is, het waarskynlik uit estuarium-, strandmeer-, gety-inlaat-, getyvlakte- en moerasomgewings bestaan. Die transgressie het 'n styging in erosiebasis veroorsaak wat 'n afname in sedimenttoevoer tot gevolg gehad het. Die helder watertoestande wat so ontstaan het, was ideaal vir die presipitasie van die karbonate van die Malmani-subgroep.

Die oorsaak van die transgressie was moontlik termiese wegsakking ná graben-vorming in 'n driefase tektoniese model. Die voorgestelde termiese-wegsakkingskom het gelei tot die oopmaak van 'n vlak liniêre binnelandse see, wat oor die gedeeltelik gepediplaneerde palaeolandskap gestoot het.

Table of Contents

Chapter 1 - Introduction 1
1.1 The Black Reef Quartzite Formation - Nature, occurrence and age 1
1.2 Economic significance of the Black Reef in the study area 2
1.3 Previous work on the Black Reef Quartzite Formation 3
1.4 Aims, scope and methods of study 7
1.4.1 Aims of study 7
1.4.2 The study area 7
1.4.3 Study Methods 7

Chapter 2 - General Geology 9
2.1 Geographical distribution 9
2.2 Stratigraphy of the study area and definition of the Black Reef Quartzite Formation 9
2.3 Structure 11
2.4 Outcrops 12

Chapter 3 - The Pre-Transvaal Palaeosurface 14
3.1 Introduction 14
3.2 Geographic distribution of underlying formations 14
3.3 Characteristics of the underlying Archaean rocks 17
3.3.1 The Basement Rocks 17
3.3.2 The Dominion Group 17
3.3.3 The rocks of the Witwatersrand Supergroup 17
3.3.4 The rocks of the Ventersdorp Supergroup 17
3.4 Structure 18
3.5 Crustal evolution and the influence of the character of the pre-Transvaal palaeosurface upon Black Reef sedimentation 19

Chapter 4 - The Black Reef Quartzite Formation 21
4.1 General Lithology 21
4.2 Thickness 23
4.2.1 The Black Reef Quartzite Formation 23
4.2.2 The conglomerate unit 23
4.2.3 Relative thicknesses of the lithological rock types 26
4.2.4 Discussion and interpretation 27
4.3 Lithofacies and lithofacies assemblages 28
4.3.1 Introduction 28
4.3.2 Methods of investigation 29
4.3.3 Description of the lithofacies 29
4.3.4 Lithofacies assemblages and successions 47
4.4 Palaeocurrents 52
4.4.1 Introduction - palaeocurrent indicators 52
4.4.2 Methods and results 52
4.4.3 Discussion and interpretation 56
4.5 Pebble size, pebble lithology and pebble roundness 57
4.5.1 Introduction 57
4.5.2 Pebble size 58
4.5.3 Pebble lithology 59
4.5.4 Pebble roundness 60
4.6 Petrographic aspects of the quartzites 62
4.6.1 Introduction 62

4.6.2 Laboratory procedure 62
4.6.3 Modal analysis: 64
4.6.4 Grain-size analysis 68

Chapter 5 - The overlying dolomitic Malmani Subgroup 70
5.1 Introduction 70
5.2 Lithological and petrographic description 70
5.3 Discussion and interpretation 71

Chapter 6 - Sedimentological Synthesis 74
6.1 Introduction 74
6.2 Palaeo-environmental Classification 74
6.2.1 The Conglomerate unit and immediately overlying quartzites 74
6.2.2 Type of river system 75
6.2.3 The upper quartzite mudstone succession 76
6.2.4 Transition from terrestrial to coastal conditions of the Black Reef Quartzite Formation 77
6.3 The transgression - some considerations 79
6.4 Tectonic and depositional model 81

References 83

Acknowledgements 90

Appendix 1 - Sedimentological profiles 91

Appendix 2 - Ripple marks 106

Appendix 3 - Markov analysis 110

Appendix 4 - Thickness data 113

Appendix 5 - Palaeocurrent data 115

Appendix 6 - Pebble size, pebble composition and pebble roundness 128

Appendix 7 - Modal analysis of quartzites 134

Appendix 8 - Grain-size data 136

List of Figures

1.1. Distribution of the Transvaal Sequence and the locality of the study area....2

2.1. Geological map of the study area. (The names of the gold mines at Carletonville and Westonaria are given on Figure 2.3)....10
2.2. Generalised lithostratigraphic column of the study area. No scale is implied. (After SACS, 1980 and J.J. Mayer, *pers. com.*, 1996).... 11
2.3. The most prominent outcrops of the Black Reef Quartzite Formation in the study area.... 13

3.1. Map showing the geology of the pre-Transvaal palaeosurface and the outcrops of the Black Reef Quartzite Formation....16

4.1. Photograph showing soft-sediment deformation (probably load-cast structures, Collinson & Thompson, 1982) in the shales of the Black Reef Quartzite Formation.... 22
4.2. An isopach map of the total thickness of the Black Reef Quartzite Formation. The data of 181 boreholes were used for the map. (After Visser, 1989).... 24
4.3. Map showing positions of boreholes from which information was obtained.... 25
4.4. Cumulative thicknesses of the rock types constituting the Black Reef Quartzite Formation, calculated from different borehole intersections....26
4.5. Photograph showing the massive sedimentary breccia facies on the farm Bospan 56.... 30
4.6. Photograph showing the planar cross-bedded quartzite facies on the farm Blaauwbank 278....34
4.7. Photograph showing a trough structure on the farm Blaauwbank 255....35
4.8. Photograph showing plane bedding in mature quartzite on the farm Blaauwbank 278....36
4.9. Photograph showing the lateral extent of the plane-bedded lithofacies on the farm Blaauwbank 278....37
4.10. Photograph showing ripple marks on the farm Middelvlei 255....39
4.11. Photograph showing flat-topped ripple marks on the farm Middelvlei 255....39
4.12. Photograph showing large ripple marks, covered with a thin shale bed, on the farm Wildfontein 52....40
4.13. Photograph showing flaser bedding in a drill-hole core....43
4.14. Photograph showing mud layers on cross-bed foresets (Borehole BW1). Stratigraphic bottom is on the left....45
4.15. Diagrammatic interpretation of the situation shown on Fig. 4.14....45
4.16. A path diagram showing the most likely transitions among the rock types of the Black Reef Quartzite Formation....48
4.17. Schematic presentation of the four most likely lithofacies associations of the Black Reef Quartzite Formation. No scale is implied....49
4.18. Map showing palaeocurrent distributions and vectors of cross-bedding measurements....54
4.19. Map showing the distribution of ripple-mark crest orientations....55
4.20. The textural composition of the different arenite units in borehole BL8....63
4.21. Photomicrograph showing dull black carbonaceous material (bottom of picture; top part shows dolomite crystals). The long dimension of the photomicrograph is 1.8 mm.... 64
4.22. Photomicrograph of a very mature quartz arenite. The long dimension of the photomicrograph is 1.83 mm....65
4.23. Textural and sieve-equivalent grain-size parameters of the different quartzite units in borehole BL8.... 67

5.1. Diagram showing the dolomite content of the different units in borehole BL8.... 73

List of Tables

4.1. The occurrence of ripples in different sedimentary environments.....42
4.2. A summary of palaeocurrent patterns and the environments they are related to (Selley, 1982)..... 56
4.3. Mean pebble-roundness for conglomerates from three different locations..... 60

6.1. Characteristics indicative of a fluvial environment and their applicability to the lower part of the Black Reef Quartzite Formation.....75
6.2. Characteristics indicative of a braided-stream deposit and their applicability to the lower part of the Black Reef Quartzite Formation..... 76
6.3. Characteristics indicative of a coastal deposit and their applicability to the upper part of the Black Reef Quartzite Formation.....77

Chapter 1

Introduction

1.1 The Black Reef Quartzite Formation - Nature, occurrence and age

The Black Reef Quartzite Formation comprises a succession of interbedded thin siliceous quartzites and shales with erratically-developed basal grits and conglomerates. The Formation lies at the base of the early Proterozoic Transvaal Sequence and in the study area (the area of the Carletonville and West Rand goldfields, Fig. 1.1) it outcrops on the Rand Anticline (Fig. 2.1).

The name "Black Reef" does not refer to a geographic locality, but is derived from a miner's term for some of the quartzites and auriferous conglomerates of the Formation exhibiting a dark colour (SACS, 1980). This colour is due to the abundance of chlorite and carbonaceous material in these rocks (Liebenberg, 1955).

Button & Tyler (1981) and Frey & Germs (1986) estimate the age of the Black Reef Quartzite Formation at between 2200 Ma and 2300 Ma. Van den Berg (1994) puts the age between 2200 and 2700, based on Van Niekerk & Burger's (1978) dating of the underlying Ventersdorp lavas and Hamilton's (1977) dating of the younger Hekpoort basalts of the Pretoria Group.

A major angular unconformity is present at the base of the Formation. An important consequence of this contact relationship is a depositional surface comprising rocks that range from Archaean Basement to Ventersdorp lava (Fig. 2.2). This aspect of the geology of the Formation is discussed later in some detail.

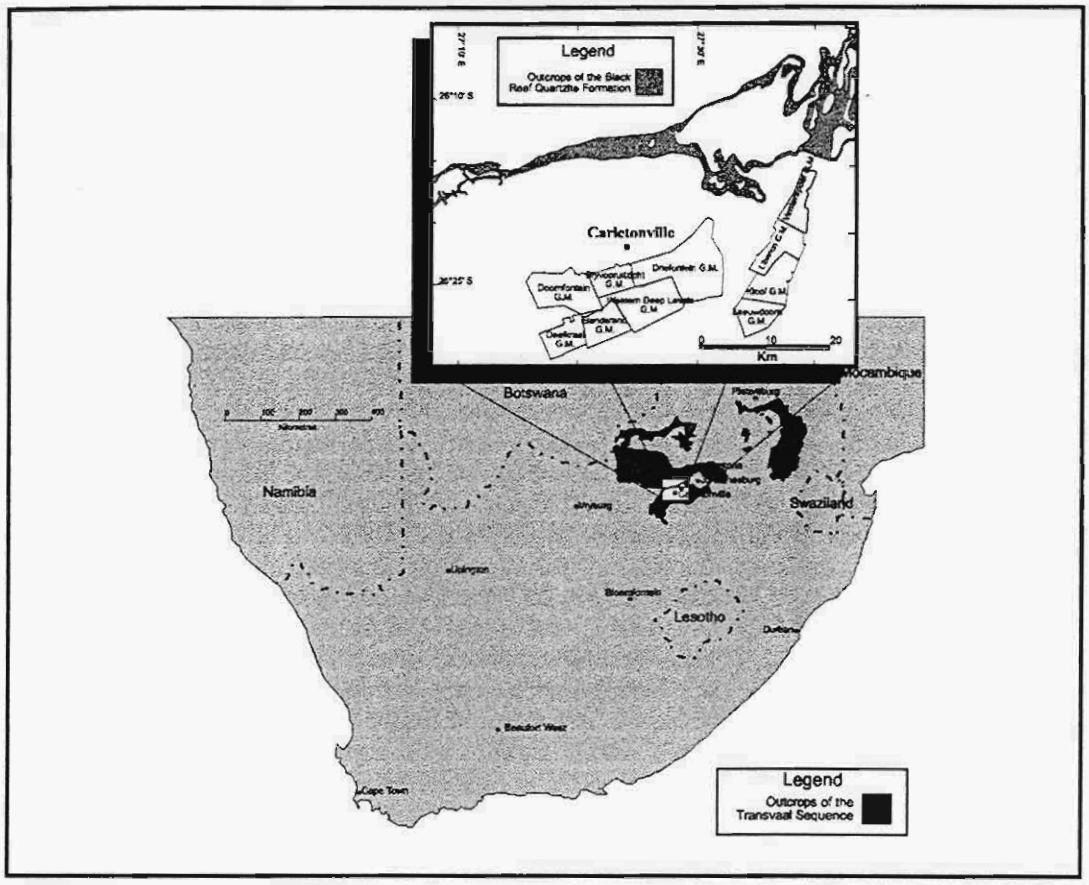

Fig. 1.1. Distribution of the Transvaal Sequence and the locality of the study area.

1.2 Economic significance of the Black Reef in the study area

According to Frey & Germs (1986) the conglomerates of the Black Reef Quartzite Formation are the youngest known gold and uranium-bearing quartz-pebble conglomerates in the world.

The Black Reef placer has been mined for gold at a few locations in the study area; a significant tonnage of low-grade ore was recovered at shallow depths at Randfontein Estates Gold Mine at the town Randfontein (Fig. 2.3) (Papenfus, 1964). An uneven footwall topography, resulting from differential erosion of the various rock types underlying the placer, was thought to have controlled Black Reef deposition and gold concentration in this area. This interpretation is based upon the observation that the most-

persistent pay shoots follow the strike trends of some of the underlying rocks, e.g. the Booysens Shales, the Bird Reefs and the Jeppestown Shales (Papenfus, 1964; Body, 1988). It is thought that the gold mined at Randfontein Estates is mostly of detrital origin (Papenfus, 1964).

A small tonnage of high-grade Black Reef ore was mined near the eastern boundary of the farm Middelvlei 255. The Government Reef conglomerates were presumably the source of the gold for this particular occurrence (Papenfus, 1964).

More recently, the Black Reef has been mined on the farm Drylands 64 (Fig. 2.3). The gold mined here is presumably not of detrital but hydrothermal origin (Body, 1988).

In 1990 Lindum Reefs Gold Mine started to exploit the remaining reserves of the Randfontein section of the Randfontein Estates Gold Mining Company as an open-cast operation. This mining operation is still in progress and by June 1993 some 230 tons of Black Reef had been mined here (Shaw, 1994).

1.3 Previous work on the Black Reef Quartzite Formation

Of the first geological accounts of the Black Reef Quartzite Formation are those by Stonestreet (1898) and Dorfel (1904). Stonestreet (1898) gave a description of the Formation at Natalspruit near the town Alberton, based on his observations of the unit which was exposed in the area due to exploration activities. He concluded his paper with the remark that "this reef and the manner of its deposition seem to be but little understood..." Dorfel (1904) described the Black Reef conglomerate at the Kromdraai Mine, about sixteen kilometres north of Krugersdorp, as "a small pebble banket" (conglomerate), with a low gold content. The upper quartzites of the Black Reef Quartzite Formation (which he did not recognise as being part of the Formation) he described as dense and fine grained. He also remarked that they are

"interbedded". On the shales and the contact between the Formation and the overlying dolomites he wrote: "(the shales) ... are about one hundred feet thick, and form a distinct and reliable horizon between the quartzites and the first bed of dolomite".

The first detailed account of the Black Reef Quartzite Formation in the study area was the landmark paper by Papenfus (1964). He described the lithological characteristics and the main structural features of the Formation and its relationship to the older formations. He also gave a detailed account of the major Black Reef areas mined in the region and he discussed the occurrence and possible origin of gold in the Formation.

Van den Berg (1994) and Els *et al.* (1995) studied the sedimentological characteristics and reviewed the economic aspects of the Black Reef Quartzite Formation in the Western Transvaal. They found the palaeocurrent distribution of the conglomerate unit to be generally unimodal in character, but that of the upper quartzite unit to be bimodal at some locations. Their study also revealed that the arenites, especially those of the upper beds, were very mature. They concluded that the palaeo-topography was the dominant factor that controlled early sedimentation in shallow braided-stream systems. These authors proposed that during a subsequent transgression the fluvial successions became drowned, transgressive estuarine conditions ensued, and was followed by deposition in a shallow marine environment.

Frey & Germs (1986) studied the sedimentological, mineralogical and geochemical characteristics of the Black Reef conglomerates in South Africa and compared their characteristics with those of nearby pre-Transvaal conglomerates of the probable source areas. They found, by way of palaeogeographical reconstruction, that the Black Reef conglomerates were generally deposited in palaeovalleys which formed adjacent to relatively

small palaeo-highs situated on horst blocks of floor strata. Frey & Germs (1986) proposed that despite its textural relationship to epigenetic minerals, the gold of the Black Reef Quartzite Formation is of detrital origin.

The mineralogy of the Black Reef Quartzite Formation has also been extensively discussed by Swiegers (1938, 1939), Frankel (1940a, 1940b), Liebenberg (1955) and Frey & Germs (1986). Swiegers (1938) described the petrographic character of the various lithofacies present in the Black Reef Quartzite Formation in the Randfontein and Klerksdorp areas. In connection with the origin of the Black Reef gold, he concluded that the conglomerate outcrops with a poorer gold content must be ascribed to placer origin, while in the well mineralised areas, where the pyrite content is higher than 30 %, the bulk of pyrite is of hydrothermal origin.

Eriksson (1972), Visser & Grobler (1972), Eriksson & Truswell (1974) and Beukes (1976) described the dolomites of the overlying Malmani Subgroup and reported on the transition from siliciclastic to carbonate sedimentation at the base of the Transvaal Sequence. Beukes (1976) studied this transition in the Northern Cape, in what is now referred to as the Griqualand West Sequence. He concluded that the siliciclastic cycles represent progradational subtidal to tidal flat deposits, and the carbonate cycles represent progradational tidal flat deposits. Beukes (*op. cit.*) proposed that the epiclastic source areas were eventually "eliminated" and carbonate deposition became established. Eriksson (1972) proposed that the carbonaceous shale deposits were strand deposits and these were the first deposits of a transgressing sea. He also studied the thickness of the Black Reef Quartzite Formation in the Carletonville area and came to the conclusion that the zones of maximum thickness have a channelised distribution. Visser (1989) too, studied the thickness of the Formation in the study area from the data of a

number of boreholes, producing a detailed account of the thicknesses of the various lithological units (conglomerate, quartzite and shale).

Various other authors have published papers on the Black Reef Quartzite Formation. The most important of these are Button (1972a, 1972b), Tyler (1979) Clendenin & Charlesworth (1990) and Clendenin *et al.* (1989, 1991). Tyler (1979) studied the depositional environments of the Formation in the west-central Transvaal. He proposed that an early phase of braided stream sedimentation was terminated by a marine transgression, resulting in coastal sands resting directly upon fluvial rocks in the vertical profile. He emphasised the important role storms played in the deposition of the Black Reef Quartzite Formation in this area.

Various authors reporting on gold concentration in the Black Reef (e.g. Nel, 1935; Swiegers, 1939; Papenfus, 1964; Antrobus *et al.*, 1986; Body, 1988; Pouroulis & Austin, 1989; Shaw, 1994; Van den Berg, 1994) remarked on the fact that the Black Reef was only sufficiently robust and auriferous to be mined where it was deposited in fluvial channels cut into pre-existing bedrock or within the vicinity of pre-Black Reef Witwatersrand outcrops. Pouroulis & Austin (1989) suggested that wave action was a secondary sedimentary process involved in the gold distribution of the Black Reef Quartzite Formation at Modderfontein Gold Mine.

Antrobus *et al.* (1986) pointed out the discontinuous nature of the conglomerate facies in the Black Reef Quartzite Formation and its highly erratic gold mineralization was confirmed by Shaw (1994). Stonestreet (1896), in his early description of the Formation, mentioned that in "two holes put down within 200 yards of each other ... the first found the reef, and the second did not." Pouroulis & Austin (1989) concluded that the unpredictability of gold distribution in the Black Reef Quartzite Formation is

the reason why most South African mining houses have tended to avoid exploration of the Formation.

1.4 Aims, scope and methods of study

1.4.1 Aims of study

It is evident from the previous section that there is a general paucity of sedimentological information on the Black Reef Quartzite Formation in the study area.

The primary purpose of this study therefore was to collect data which would lead to an integrated sedimentological model for the Black Reef Quartzite Formation in the Carletonville and Randfontein areas. Another, equally important aim was to compile a representative vertical profile for the Formation in the study area.

1.4.2 The study area

The study area includes the outcrops of the Black Reef Quartzite Formation on the Rand Anticline in the Carletonville and Randfontein districts of South Africa. The area is situated between 27°10' E and 27°40' E longitude, and 26°05' S and 26°30' S latitude.

1.4.3 Study methods

The surface data, for this study, were obtained from sedimentological recordings made on the outcrops. The subsurface data were obtained from sedimentological logs of surface borehole cores.

Data collection comprised the following:

(a) compilation of sedimentological profiles from outcrop exposures and the cores of surface boreholes

(b) determination of palaeocurrent directions, using cross-bedding and ripple marks as indicators

(c) quantitative investigation of pebble size and pebble lithology of the Black Reef conglomerates

(d) investigation of the roundness of Black Reef pebbles

(e) microscopic investigation of the quartzites.

Field data were processed either manually or by computer, using software such as Microsoft Excel 7.0, Statgraphics and Rose 1.0. Graphical map compilation was carried out by application of the Lotus Freelance Graphics 4.0 and CorelDraw! 4.0 software packages.

Chapter 2

General Geology

2.1 Geographical distribution

As shown in Fig. 1.1 the Transvaal Sequence occupies a preserved basin with an east-west elongation in the north-western parts of South Africa and includes the succession in the Potchefstroom synclinorium (SACS, 1980).

2.2 Stratigraphy of the study area and definition of the Black Reef Quartzite Formation

The lithostratigraphic subdivision of the Transvaal Sequence in the study area is shown in Fig. 2.2. Here the Black Reef Quartzite Formation is the basal stratigraphic unit of the Transvaal Sequence. The Formation is separated from the underlying strata by a major unconformity, the second in the total stratigraphic sequence in the area; the first being the unconformity between the Ventersdorp Contact Reef and the underlying Witwatersrand strata (Engelbrecht *et al.*, 1986; Tucker & Viljoen, 1986). The upper contact of the Black Reef Quartzite Formation with the dolomites of the Chuniespoort Subgroup is conformable and transitional (SACS, 1980). Previous investigators, such as Swiegers (1938) and Van den Berg (1994), have taken the upper boundary for the Black Reef Quartzite Formation at the base of the lowermost dolomite bed. This convention is also adopted in this study. **The Black Reef Quartzite Formation is therefore stratigraphically defined as the sedimentary succession between the basal unconformable contact with the older Archaean rocks and the base of the lowermost dolomite bed.**

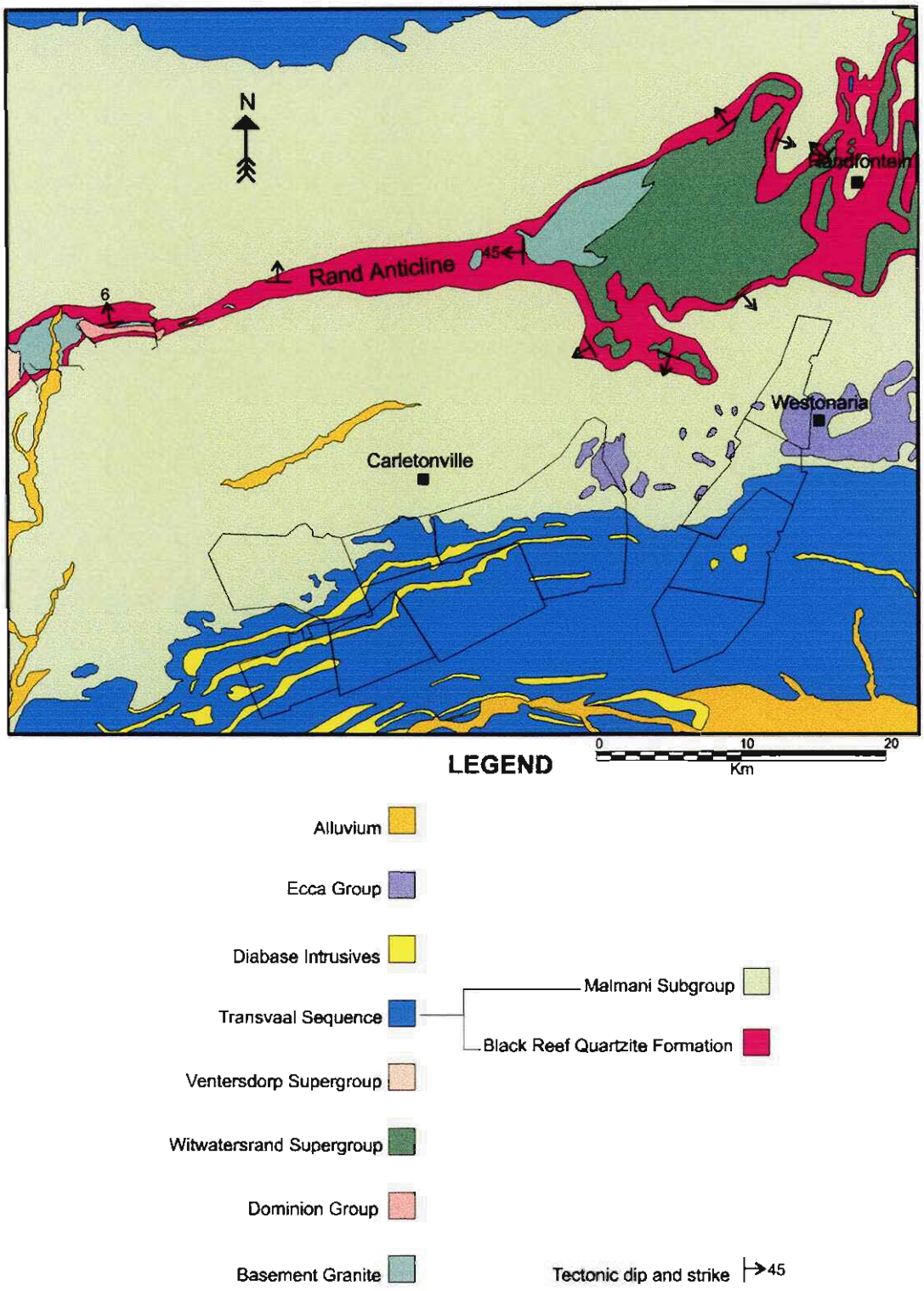

Fig. 2.1. Geological map of the study area. (The names of the gold mines at Carletonville and Westonaria are given on Fig. 2.3)

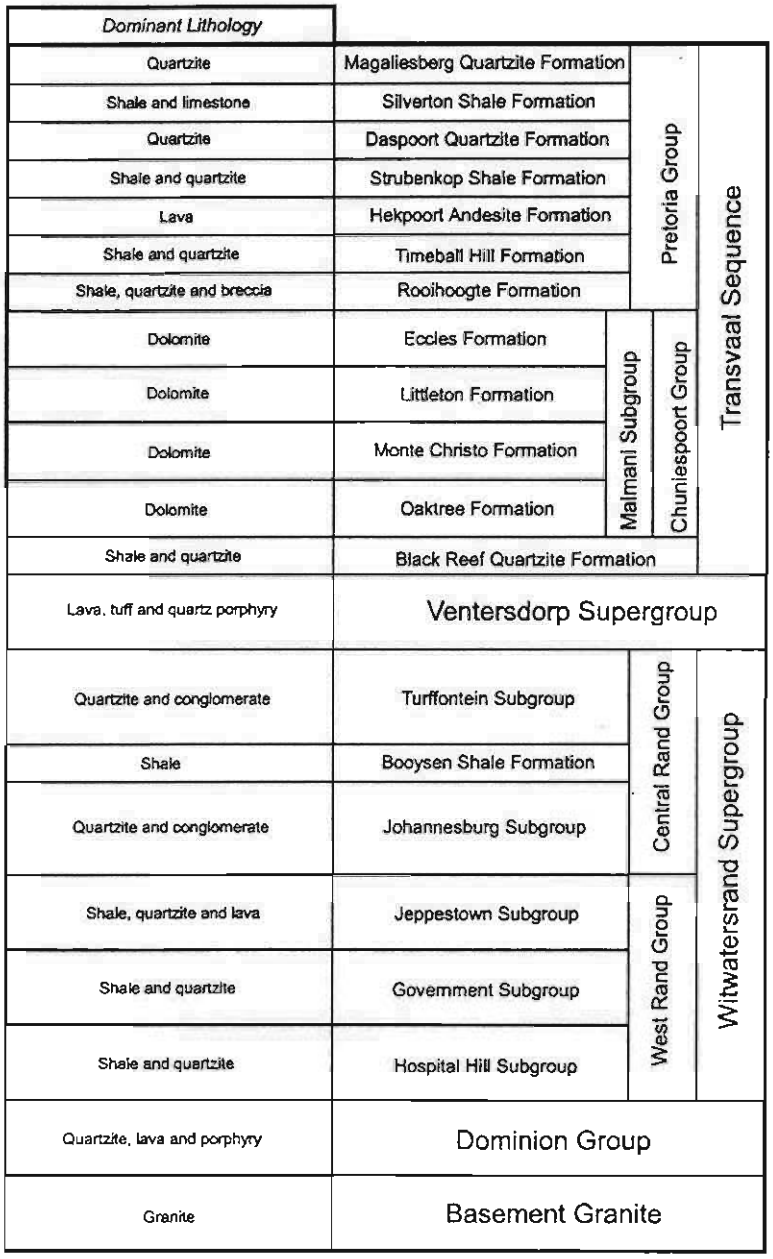

Fig. 2.2. Generalised lithostratigraphic column of the study area. No scale is implied. (After SACS, 1980 and J.J. Mayer, *pers. com.*, 1996)

2.3 Structure

Although the Black Reef Quartzite Formation locally dips gently in various directions due to gentle post-Transvaal folding, it has a general northerly and southerly dip along the structure known as the Rand Anticline between

Randfontein in the east and the Klerkskraal dam in the west (Figs. 2.1 and 2.3).

In general, the Black Reef Quartzite Formation is free of major faulting in the study area. The Formation has not been displaced along the major faults of Ventersdorp or post-Ventersdorp age, but there is evidence of movement on a minor scale along some of the older fault planes during post-Transvaal periods. For example Papenfus (1964) records a displacement of only 3.5m (12 ft) across the major Witpoortjie fault for the Black Reef Quartzite Formation in an opencast working at the Randfontein Estates Gold Mine.

2.4 Outcrops

In the study area the outcrops of the Black Reef Quartzite Formation are restricted to the topographic ridge formed by the Rand anticline (Fig. 2.1). The geological map of Fig. 2.1 may be misleading, because the area shown as being covered by Black Reef Quartzite Formation, has been inferred from data collected at "true outcrops" as well as from evidence of Black Reef intersections in boreholes and the presence of Black Reef rubble in cultured lands. Because of the small thickness of the Formation, its outcrops are typically narrow and limited in areal extent.

The Formation characteristically forms outcrops on the highest topographic points along the ridge formed by the Rand Anticline. In Fig. 2.3 the locations of the most prominent, usable outcrops of the Formation in the study area are indicated and shown in relation to farm boundaries and mining lease areas.

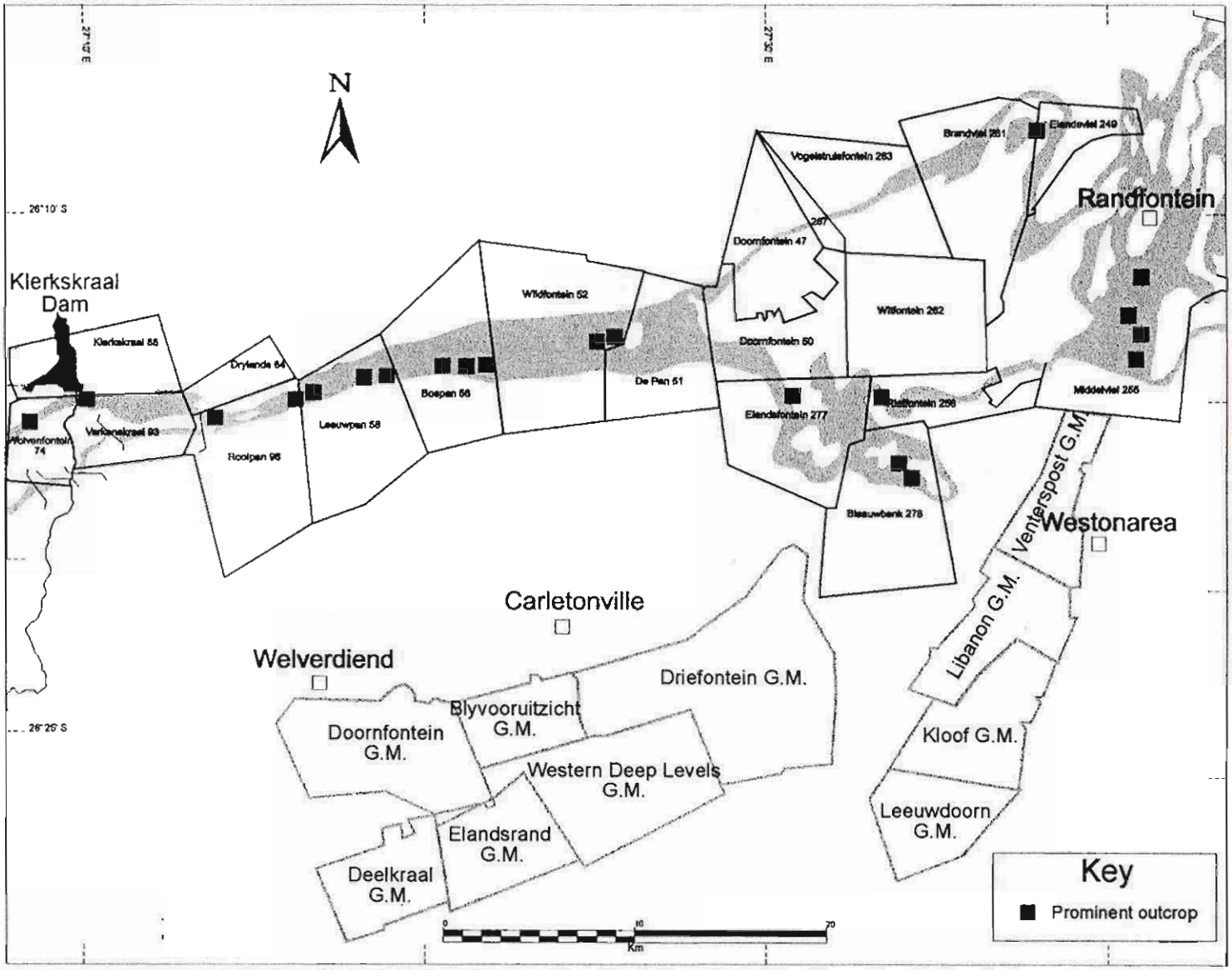

Fig. 2.3. The most prominent outcrops of the Black Reef Quartzite Formation in the study area.

Chapter 3

The pre-Transvaal palaeosurface

3.1 Introduction

To obtain an understanding of the processes that controlled deposition of Black Reef Quartzite Formation, a knowledge of the floor rocks and the geological events leading to their configuration is necessary. It has been shown before that the characteristics of palaeosurfaces play a very important role in controlling sedimentation (e.g. Van den Berg, 1994; Henning, 1992). Factors such as the lithology of the palaeo-bedrock and the structure of the underlying palaeosurface are important parameters determining the palaeorelief . Van den Berg (1994) came to the conclusion that the uneven pre-Transvaal palaeosurface had been the dominant factor controlling the sedimentation of the Black Reef Quartzite Formation. Also, the pre-Black Reef outcrops had been an important source of Black Reef sediment (Van den Berg, 1994).

3.2 Geographic distribution of underlying formations

Figure 3.1 is a map showing the geology of the pre-Transvaal palaeosurface, compiled from data of De Kock (1964), Papenfus (1964), Pretorius (1986), Tucker & Viljoen (1986) and Engelbrecht *et al.* (1986). This diagram shows that in the northern part of the study area the Black Reef Quartzite Formation is generally underlain by Archaean Basement rocks, whereas lavas of the Ventersdorp Supergroup constitute the palaeosurface beneath the Formation in the southern and south-eastern part of the study area. The sedimentary rocks of the Central Rand Group and the West Rand Group of the

Witwatersrand Supergroup underlie the Formation in the central part of the study area.

The outcrops of the Black Reef Quartzite Formation in the western part of the study area are underlain by lavas, tuffaceous sediments and volcanic conglomerates of the Ventersdorp Supergroup. On the farms Varkenskraal 93 and Rooipan 96 in the western regions of the study area (Fig. 2.3) outcrops of the Formation are underlain by Archaean granite and Orange Grove quartzites. Further eastward along the Rand Anticline, up to the farm Doornfontein 50, the Black Reef Quartzite Formation outcrops rest upon Archaean granite. To the east of this point the Formation rapidly transgresses a succession of lower Witwatersrand rocks striking generally at right angles to the outcrops of the Formation. At Middelvlei 255 (Lindum Reefs Mine) outcrops of the Black Reef Quartzite Formation transgressively oversteps, within a short distance, sediments of the Central Rand Group and the Ventersdorp lavas, up to the Witpoortjie fault. Due to the effect of the Witpoortjie, Roodepoort and Doornkop faults there is a rapidly changing succession of steeply inclined West Rand and Central Rand rocks that underlie the Formation in this eastern section of the study area.

Along a stretch of Black Reef outcrops on the ridge of the Rand Anticline a thin fine-grained bed, considered to be a palaeosol, separates the Archaean granite basement from the Black Reef Quartzite Formation.

At a few locations a white quartz unit was found in association with the Basement Granite.

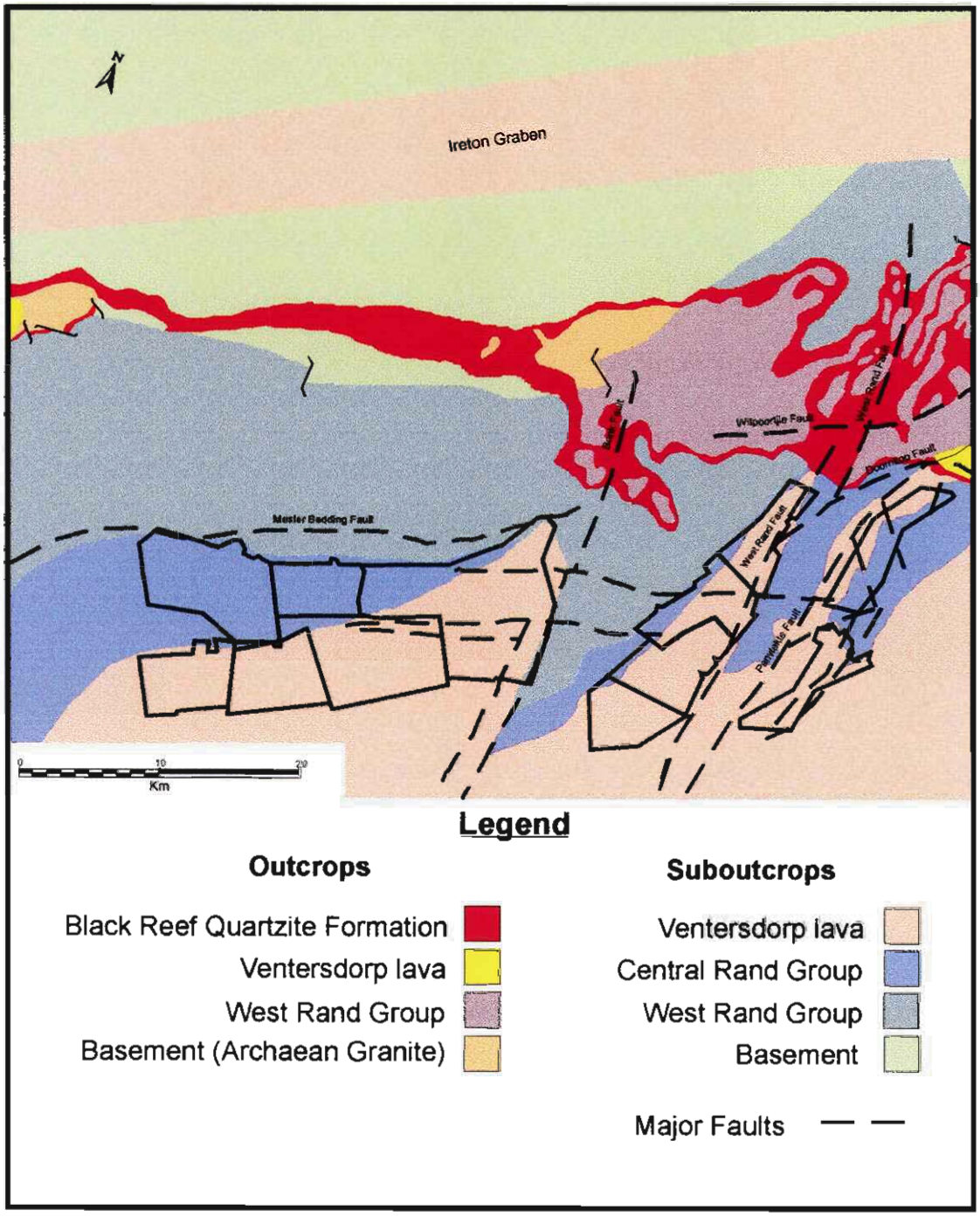

Figure 3.1. Map showing the geology of the pre-Transvaal palaeosurface and the outcrops of the Black Reef Quartzite Formation

3.3 Characteristics of the underlying Archaean rocks

3.3.1 The Basement Rocks

The Basement Granite is typically a coarse-grained granite and is usually traversed by quartz veins. Along the Rand anticline, the Granite underlying the Black Reef Quartzite Formation, is extensively weathered in outcrop and at some localities (e.g. Wildfontein 52) the weathering product shows evidence of crude bedding, indicating that some transportation of material has taken place over short distances. At some localities, e.g. De Pan 51, Wildfontein 52, Bospan 56, Leeuwpan 58 and Rooipan 96, on the Rand Anticline, sizeable outcrops of structureless white quartzite-like rock, were found in association with the Basement Granite.

3.3.2 The Dominion Group

Sedimentary rocks of the Dominion Group overlie the Basement in the far western part of the study area (Fig. 2.1). These strata are not shown on Fig. 3.1. Nowhere else in the study area does the Dominion Group feature as part of the palaeosurface to the Black Reef Quartzite Formation.

3.3.3 The rocks of the Witwatersrand Supergroup

Rocks of the Witwatersrand Supergroup, that underlie the Black Reef Quartzite Formation in the study area, are mostly quartzites and shales. The quartzites are typically mature and are resistant to weathering. The shales, on the other hand, are very susceptible to weathering and shale outcrops are therefore not prominent.

3.3.4 The rocks of the Ventersdorp Supergroup

Rocks of the Ventersdorp Supergroup, in the study area, are mostly lavas. They are typically greenish-grey in colour, fine-grained and in some cases

contain scattered amygdales. In some borehole cores the unconformity between the lava and the Black Reef Quartzite Formation is inconspicuous indicating the possibility of a basal lava palaeosol, and grading upwards into transported detrital material of the Black Reef sediments.

3.4 Structure

The pre-Transvaal rocks are disturbed by folding and faults, some of which have been responsible for major dislocations. Two major folds which have had the greatest influence on the geological history of this area are the Rand and Bank Anticlines. The Bank Anticline was active during Ventersdorp Contact Reef times (Vermaakt & Chunnet, 1994), and probably continued being active till late Ventersdorp Supergroup time (Engelbrect *et al.*, 1986), but warping along the Rand Anticline unabatedly continued until at least late post-Black Reef time (Engelbrecht *et al.*, 1986).

According to Vermaakt & Chunnet (1994) the Bank Anticline was peneplaned before the deposition of the Ventersdorp Contact Reef, but the structure was subsequently re-accentuated by post-Black Reef folding.

According to Engelbrecht *et al.* (1986) the total distance of uplift produced by the Rand Anticline is of the order of 16 Km. This tectonism caused a gradient that was sufficient to initiate gravity gliding which affected even the Gerhardminnebron Graben, and the Bank and West Rand faults. A brecciated zone, recording the cataclastic gravity gliding and later consequential movement, has been termed the Master Bedding Fault. Where it outcrops, as part of the Mooi River Fault Complex, it is responsible for a post-Black Reef stratigraphic displacement of 2000 m, although the fault is largely of proven pre-Black Reef age. A number of faults were generated by the movement on the Master Bedding Fault and a few of these were active during and after the Black Reef period. The West Rand Fault and the

Witpoortjie Fault are also of pre-Black Reef age (Engelbrecht *et al.*, 1986). The Bank Fault, which is tectonically associated with the Bank Anticline, was mainly the result of an east-west compressional event during late-Witwatersrand Supergroup time, followed by an extensional event during early Ventersdorp Supergroup time. Presently, the geometry of the Bank Fault is that of a classic listric normal fault (Vermaakt & Chunnet, 1994).

3.5 Crustal evolution and the influence of the character of the pre-Transvaal palaeosurface upon Black Reef sedimentation

After cratonic stabilisation of the Basement, which was characterised by a decrease in heat flow and an increase in the thickness of the continental crust, supracrustal successions accumulated on top of the Basement (Tankard *et al.*, 1982). The Archaean Granite is, because of its age, structurally very disturbed. On the Rand Anticline, where it outcrops, it is traversed by quartz veins. The vast accumulations of white quartzite, that were found in association with the Basement Granite are interpreted to be recrystallised vein quartz.

Because rocks of the Dominion Group do not feature as an important part of the palaeosurface to the Black Reef Quartzite Formation their role in controlling the sedimentation of the Formation, in the study area was probably insignificant.

The sediments of the Witwatersrand Supergroup, which form important floor rocks to the Black Reef Formation, followed the Dominion Group and were deposited in a foreland basin during the compressional tectonic regime (Winter, 1987). The end of the Witwatersrand sedimentation was reached when a new tectonic cycle, characterised by tensional stresses was initiated in the area. Tensional tectonism was manifested by the outflow of the first andesitic lavas which mark the onset of the Ventersdorp Period. Continental

rifting was the predominant process during the end of Ventersdorp times (Tankard *et al.*, 1982). This rifting caused extensive flooding of large parts of southern Africa by andesitic lavas. The extentional tectonism was responsible for the extensive development of horst, graben and half-graben structures. The Dominion, Witwatersrand, and Ventersdorp successions reflect a progressive increase in tectonic influence from gentle warping to deep crustal fracturing and associated volcanism (Tankard *et al.*, 1982).

The Witwatersrand Supergroup had been greatly affected by faulting and folding prior to the commencement of Black Reef sedimentation. Most of the major faults illustrated in Fig. 3.1 already existed during Black Reef times. The horst and graben structures formed by these faults certainly played a major role during deposition of the Black Reef Quartzite Formation, but during Black Reef time there was a period of tectonic quiescence in which the pre-Transvaal surface was essentially peneplaned. The few active faults may have caused fault-controlled erosion and sedimentation in subsidiary yoked basins. Some authors, e.g. Papenfus (1964) and Van den Berg (1994), regard the sediments of the Black Reef Quartzite Formation to comprise mostly reworked Witwatersrand sediments. Thus, Witwatersrand rocks are considered to be the most important source of the Black Reef sediments and of the gold in the Black Reef Quartzite Formation.

Chapter 4

The Black Reef Quartzite Formation

4.1 General Lithology

The Black Reef Quartzite Formation consists of erratically developed basal grits and conglomerates with thin interbedded quartzites and shales. The shale content of the Formation increases upward. It has a gradational contact with the dolomites at the base of the Malmani Subgroup.

The conglomerates of the Black Reef Quartzite Formation typically have a red-brown colour in weathered outcrop. Their matrix usually comprises a poorly sorted siliceous quartzite whereas the framework consists of predominantly well-rounded quartz pebbles of 15 mm or less in diameter and lesser proportions of quartzite pebbles. However, at some locations the conglomerate contains large pebbles of varying lithologies, depending on the composition of the underlying palaeosurface. The pebbles are usually well-cemented, and the conglomerates typically do not exhibit primary internal structure. At nearly all the outcrops in the study area, where conglomerate is developed, only a single conglomerate bed is present. However, in some boreholes multiple conglomerate beds were transected. The conglomerate beds do not occur at the base of the succession in all cases.

Unweathered, the quartzites of the Black Reef Quartzite Formation have a light to dark grey colour and are red-brown in weathered outcrop. The mature quartzites commonly have a glassy white appearance and are very resistant to weathering. In terms of textural maturity the lithology of the quartzites vary greatly. At some localities both very mature and immature quartzites are found together in the succession. Grit beds occur at different stratigraphic levels. Primary sedimentary structures characterising the quartzites are

trough and planar cross-bedding and plane (horizontal) bedding. The most common preserved bedforms are ripple marks.

In many cases the quartzites contain interbedded and interlaminated lenses of dark grey to black carbonaceous shale, which is yellow to red in weathered outcrop. The less weathered shales in outcrop are seen to be finely laminated. At some localities the shales are very carbonaceous and appear to consist virtually of pure carbon. In some borehole cores soft-sediment deformation structures were noticed (Fig. 4.1), occurring fairly high up in the succession.

Fig. 4.1. Photograph showing soft-sediment deformation (probably load-cast structures, Collinson & Thompson, 1982) in the shales of the Black Reef Quartzite Formation.

4.2 Thickness

4.2.1 *The Black Reef Quartzite Formation*

At most outcrops only either the lower or the upper part of the succession is exposed. No complete vertical profile of the Formation could therefore be compiled from outcrop information. Thickness data for the Black Reef Quartzite Formation, therefore, had to be compiled from information obtained from borehole cores.

Because the complete core of only one borehole (N4), drilled north of the Rand Anticline, was available, very little information on the thickness of the Black Reef Quartzite Formation, in the northern part of the study area, could be obtained.

An isopach map showing thickness variations for the Black Reef Quartzite Formation (Fig. 4.2) was constructed from the data of 181 boreholes, mostly from the southern part of the study area. This map indicates a lensoid-like geometry for the Black Reef Quartzite Formation in this area, with a north-west to south-east trend. A maximum thickness of 65 m for the Formation in the study area is quoted by Visser (1989). Eriksson (1972), who also studied the thickness variations of the Formation in this area, similarly came to the conclusion that areas of maximum thicknesses coincided with linear depressions in the floor .

4.2.2 *The conglomerate unit*

The thickness data for the conglomerate unit were obtained almost exclusively from boreholes drilled in the study area (Figs. 4.3 and 4.4). Only a few borehole cores contain conglomerate; thus conglomerate appears to be developed erratically. In general it was found that the basal conglomerate, if present, is relatively thin in the study area. This finding is

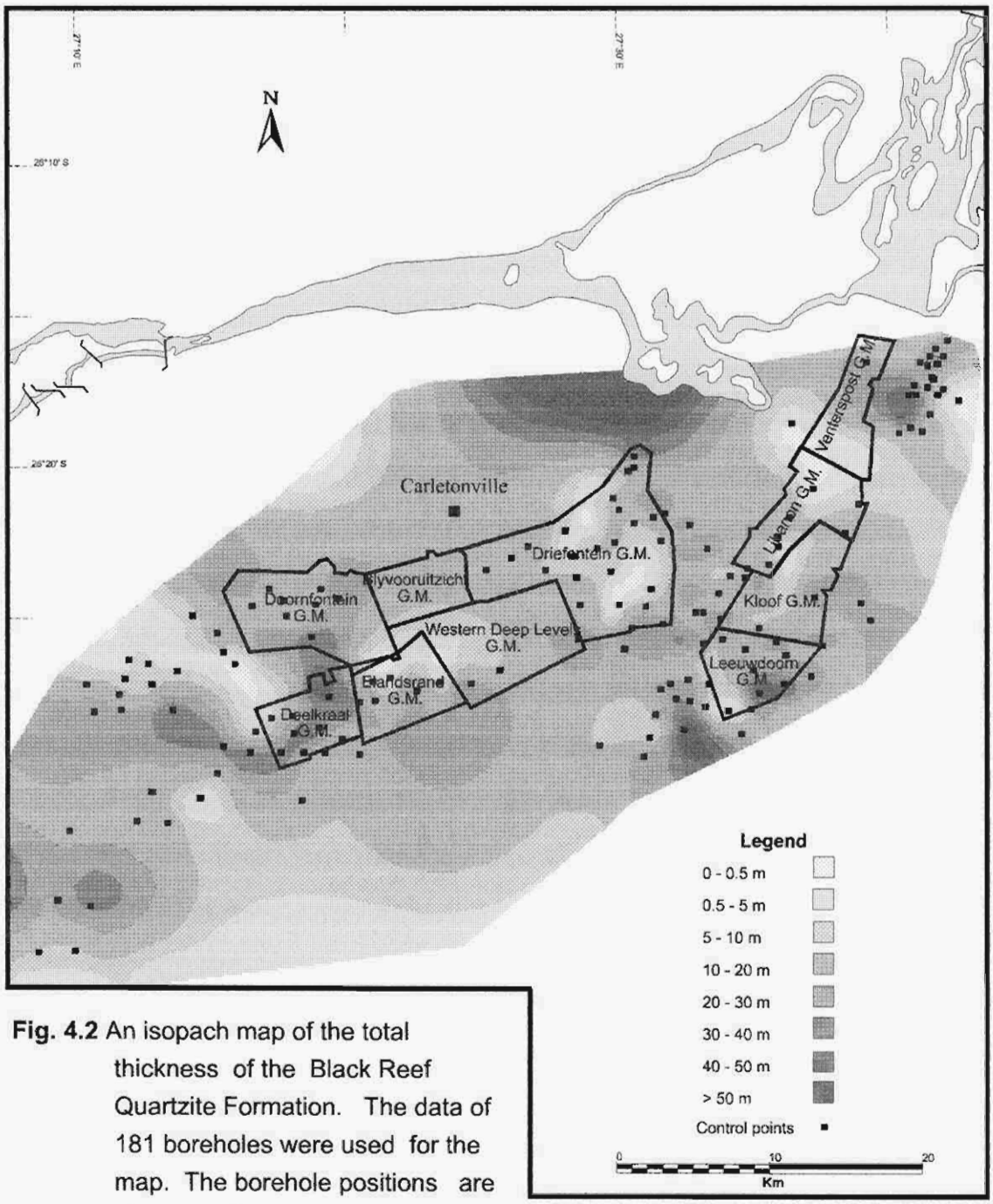

Fig. 4.2 An isopach map of the total thickness of the Black Reef Quartzite Formation. The data of 181 boreholes were used for the map. The borehole positions are shown on the map.
(After Visser, 1989)

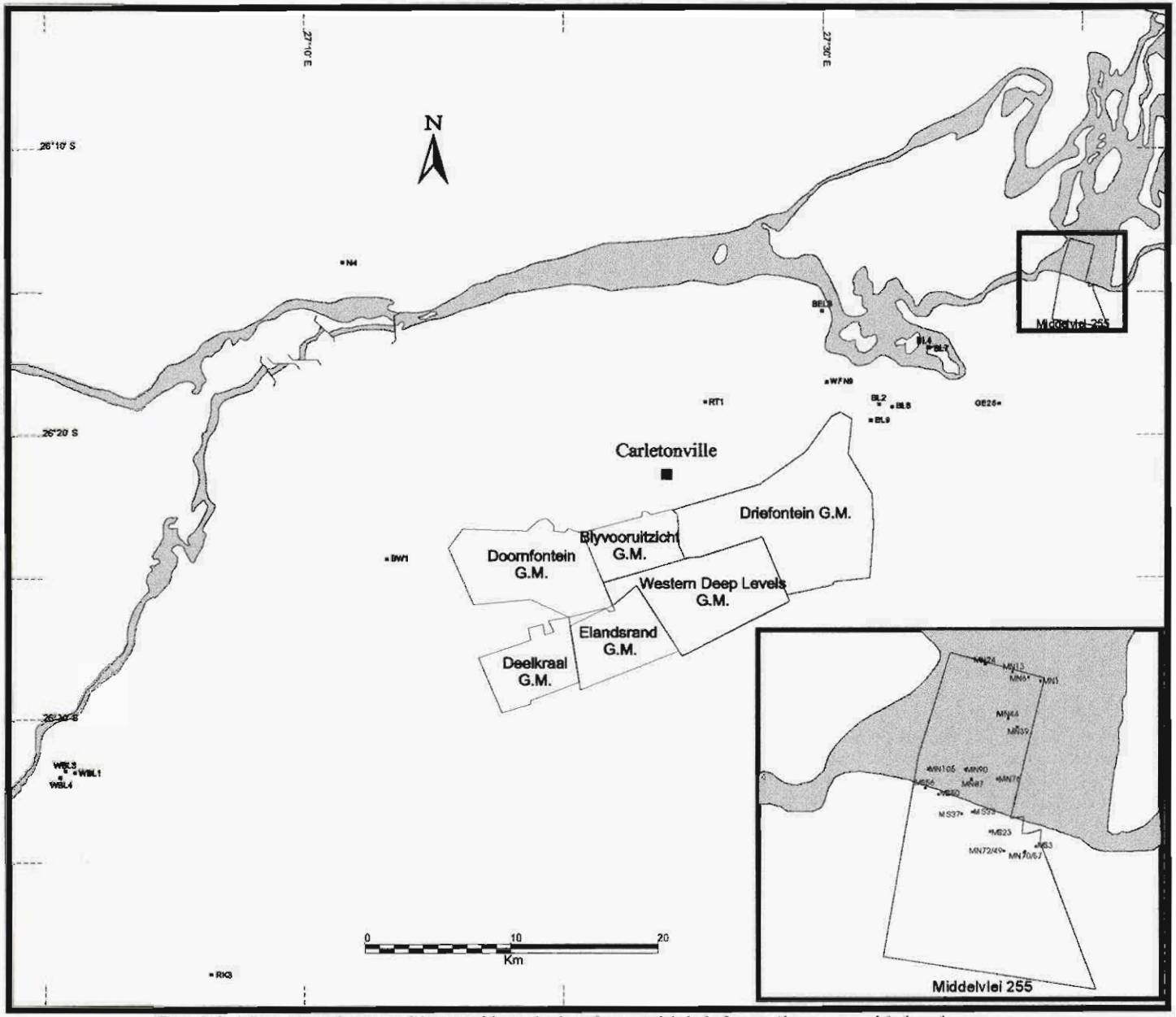

Fig. 4.3. Map showing positions of boreholes from which information was obtained.

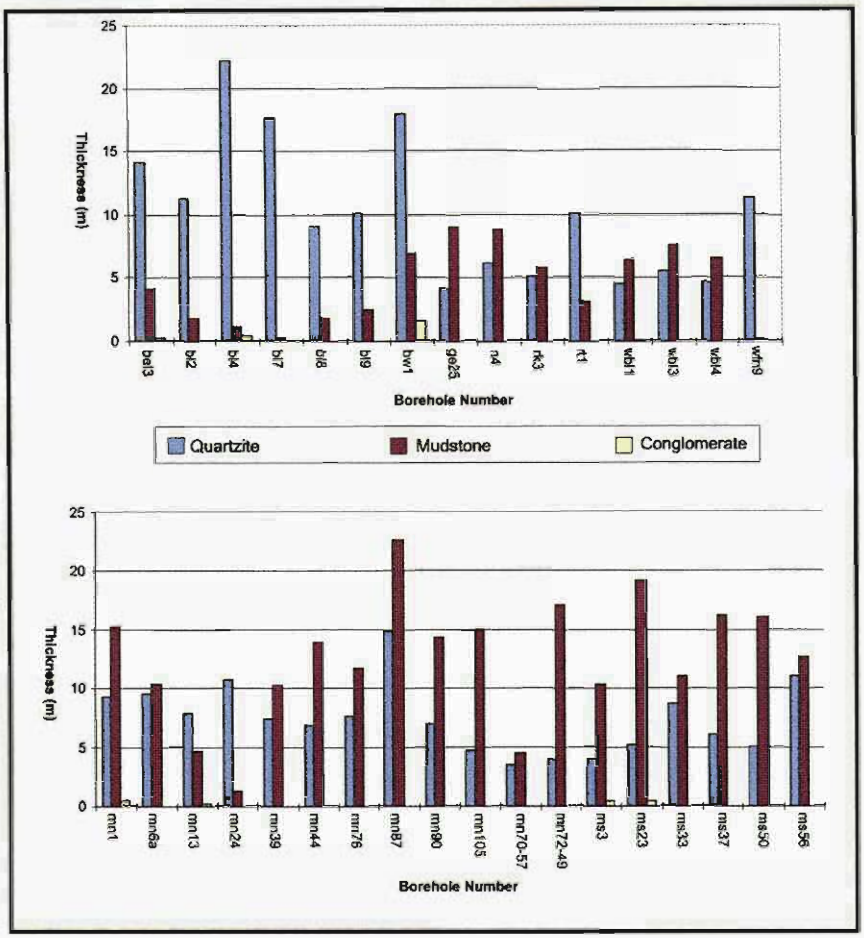

Fig. 4.4. Cumulative thicknesses of the rock types constituting the Black Reef Quartzite Formation, calculated from different borehole intersections.

confirmed by the work of Visser (1989) who states that the conglomerate thickness varied from 0 - 1 m. He concluded that conglomerate thicker than 1 m rarely occurs at few localities, where it is very locally developed, with the greatest thicknesses in the Southwest and Northeast of the study area.

4.2.3 ***Relative thicknesses of the lithological rock types***

The cumulative thicknesses of the different rock types, constituting the Black Reef Quartzite Formation, conglomerate, quartzite and mudstone, were calculated for each borehole (Fig. 4.4).

In this calculation the interbedded quartzite/mudstone units, predominated by quartzite, were grouped with the quartzite units, whereas the interbedded

quartzite/mudstone units, predominated by mudstone, were grouped with the mudstone units.

The calculated mean cumulative thicknesses of the quartzite and mudstone are 8.67 m and 8.86 m, respectively. The average quartzite to mudstone ratio for the borehole intersections is about 1:1.

4.2.4 Discussion and interpretation

The fact that zones of maximum thickness of the Black Reef Quartzite Formation coincide with linear depressions in the underlying palaeosurface (Eriksson, 1972), leads to the conclusion that the lithology and structure of the floor rocks (Fig. 3.1) had had a major influence on the deposition of the Black Reef Quartzite Formation. However, palaeorelief of the depositional surface was probably low. It is thought that during the long hiatus, prior to deposition of the Black Reef Quartzite Formation, the Pre-Transvaal palaeosurface was pediplaned (Button & Tyler, 1981; Vermaakt & Chunnet, 1994), but because of differential weathering of the different rock types depressions formed in the palaeofloor. Such depressions most probably formed over the shale beds of the Witwatersrand Supergroup and the lavas of the Ventersdorp Supergroup, because these rocks are theoretically more susceptible to weathering. Comparison of Figs. 3.1 and 4.2 reveals that the greatest thicknesses are found in areas where the Formation overlies lavas of the Ventersdorp Supergroup. However, there are exceptions, for example in the area of large thickness to the north-east of Carletonville the palaeosurface comprises Basement rocks. Areas where the Formation has a low thickness, or where the Formation is absent, probably indicate palaeohighs on the depositional surface.

The erratic distribution of the Black Reef conglomerates probably suggests deposition in channels. The higher occurrence of Black Reef

conglomerates, overlying Witwatersrand shales and Ventersdorp lavas supports the hypothesis that differential weathering of the pre-Transvaal palaeosurface influenced the sedimentation of the Black Reef Quartzite Formation. Areas of thicker conglomerate beds probably reflect zones where higher flow-conditions reigned for longer times.

The higher quartzite to mudstone ratio, in the vicinity of the farm Blaauwbank 278 and Elandsfontein 277 suggests high-energy flow conditions for more extended periods. These thicker quartzite beds in this area may be ascribed to the close proximity of the nearby Bank Fault, which may have been active during Black Reef times.

4.3 Lithofacies and lithofacies assemblages

4.3.1 Introduction

Moore (1949) used the term "lithofacies" to signify any particular kind of sedimentary rock or distinguishable rock record formed under common environmental conditions of deposition, without regard to age or geologic setting or without reference to designated stratigraphic units, and represented by the sum total of the lithologic characteristics of the rock. According to Miall (1990) each lithofacies represents an individual depositional event. An individual lithofacies is a rock unit defined on the basis of its distinctive lithologic features, including composition, grain size, bedding characteristics, and sedimentary structures. Lithofacies may be grouped into lithofacies associations or assemblages, which are characteristic of particular depositional environments (Miall, 1990).

4.3.2 *Methods of investigation*

A standard recording form was used to record the following sedimentological parameters for each discrete lithological unit:

(a) thickness

(b) general lithology

(c) type and scale of sedimentary structure

(d) nature of the bottom contact

(e) mean maximum grain size of the sand fraction

(f) grading

(g) maturity

(h) maximum clast size

(i) general lithology of clasts.

4.3.3 *Descriptions of the lithofacies*

4.3.3.1 Massive sedimentary breccia

Description:

This lithofacies is a poorly-sorted clast-supported breccia consisting of mostly angular fragments and boulders. In addition to the angular clasts, the breccia also contains some rounded clasts (with roundness of up to 0.6 on Krumbein's, 1941 scale). The pebbles and boulders comprise mostly white quartzite. The clast sizes range from a few millimetres up to 22 cm. The matrix consists of a coarse-grained quartzite apparently composed of the same material as the clasts. This breccia shows no obvious fabric and the clasts display no imbrication. This lithofacies was seen in outcrop only, and found where the Black Reef Quartzite Formation overlies

Basement on the Rand Anticline. One example of this lithofacies unit, on the farm Bospan 56, has a total thickness of almost two metres and a linear lateral extent of 118 metres. Everywhere this facies was seen, it was found in close association with the large occurrences of white recrystallised vein quartz of the Basement.

Fig. 4.5. Photograph showing the massive sedimentary breccia facies on the farm Bospan 56.

Interpretation:

This lithofacies is probably the product of rock avalanches. This type of depositional event occurs most commonly as a rapid downward fall, accompanied by partial to complete disintegration and pulverisation, of a large fractured bedrock cliff (Blair & McPherson, 1994). Rock avalanche deposits can either have brecciated or granular gravel textures containing high to low proportions of cataclastic material. The clast size and matrix

content reflect the degree of weathering and fracturing of the bedrock prior to failure (Blair & McPherson, 1994). Rock avalanche deposits are differentiated from those of other sediment gravity flows by:

(a) the lack of bedding, or large scale of bedding

(b) sheared and angular character of the gravel clasts

(c) poor sorting or lack of sorting, including the presence of large boulders, blocks, or bedrock slabs

(d) general monomictic or zoned composition of clasts

(e) cataclastic rather than pedogenic origin of the matrix fines

(f) very large volume of sediment per depositional event

(g) a distinctive hummocky surface, that may contain ponds

(h) a highly deformed basal zone formed by the rapid and unidirectional emplacement of the mass (Blair & McPherson, 1994).

This breccia of this study conforms to most of the above mentioned characteristics.

The monomict white quartzite pebble composition of this facies can be related to the white quartzitic material found in close association with this facies which was probably the source for the material of this lithofacies. The angular clasts suggest that the source of this material was very proximal.

4.3.3.2 Massive small pebble conglomerate

Description:

This conglomerate lithofacies is usually a small pebble conglomerate containing mostly well-rounded quartz and quartzite pebbles. The average pebble size of this facies is about 8 mm, while the maximum pebble size

varies from 45 mm at Wildfontein 52 to 23 mm at Middelvlei 255. The matrix is usually dense, dark coloured and highly siliceous. In some cases this conglomerate is matrix supported. In most cases it is difficult to establish the presence or absence of imbrication, because of the small size of the pebbles. This conglomerate does not show any obvious other fabric or sedimentary structures. In some cases, especially in the borehole cores, it was possible to observe normal grading within this lithofacies.

Interpretation:

Miall (1992) described such facies as a massive gravel, or one with crude horizontal bedding, displaying imbrication. According to his interpretation this lithofacies forms in longitudinal gravel bars, lag deposits and sieve deposits. Bridge (1993) argued that interpretation as bar deposits requires positive identification of distinctive macrostructures and scaling with channel geometry. According to him this facies can be deposited from low-amplitude bedwaves, e.g. bedload sheets.

4.3.3.3 The quartzite lithofacies

(I) Introduction

These lithofacies were the most common ones encountered in outcrop. The texturally mature Black Reef quartzites have a very distinctive appearance; mostly very mature and with a colour ranging from pure white to bluish-grey. The immature quartzites, however, are typically yellow-brown in colour.

A distinction, based on sedimentary structures, was made between four quartzite lithofacies found in outcrop, i.e. planar cross-bedded quartzite, trough cross-bedded quartzites, flat-bedded quartzites and quartzites containing ripple marks.

Because of the small diameters of borehole cores it was difficult to distinguish between different facies in terms of internal structure. An apparently structureless quartzite lithofacies was commonly found in both outcrop and the borehole cores. However, it was not always possible to establish whether the quartzites were truly massive or not. Some of these quartzites contain pebbles and display grading.

(II) <u>Planar cross-bedded quartzites</u>

Description:

This lithofacies is not as common as trough cross-bedded quartzites in the outcrops. At most locations, except at Randfontein South (Middelvlei 255), these structures were observed in immature quartzite units. This lithofacies is commonly coarse-grained and was mostly observed near the base of the succession. At only two locations (both at Middelvlei 255) could palaeocurrents indicated by the planar cross-bedded quartzites be measured. The set thickness of one of these sets is 46 cm and the corrected average foreset dip angles of the two sets measured were 25° and 22° respectively.

Interpretation:

This facies is commonly deposited by migrating sand waves (Harms *et al.*, 1975). However, it can also be formed by the deltaic growths from older bar remnants on longitudinal bars and straight-crested dunes or bars (Miall, 1992; Bridge, 1993). Sand waves typically indicate lower flow-strength than required for the formation of dunes (Harms *et al.*, 1975).

Fig. 4.6. Photograph showing the planar cross-bedded quartzite facies on the farm Blaauwbank 278.

(III) Trough cross-bedded quartzites

Description:

This lithofacies is found rather commonly in the Black Reef Quartzite Formation of the study area and trough cross-bedding was observed in both mature and immature quartzites. The grain size of the quartzites exhibiting trough cross-bedding varies from medium to coarse sand, and small pebbles were also commonly observed in these quartzites. The lateral trough dimensions range from a few centimetres to about one metre. At Blaauwbank 278, troughs within the same quartzite unit were observed indicating opposite palaeocurrent directions.

Fig. 4.7. Photograph showing a trough structure on the farm Blaauwbank 255.

Interpretation:

The lithofacies is produced by deposition in the lee-side scours of migrating dunes with curved-crests (Miall, 1992; Bridge, 1993). From the bi-directional troughs found at a few locations, such as Blaauwbank 278, it is obvious that reversing currents of probably tidal origin were in operation.

(IV) <u>Plane-bedded quartzites (horizontal bedding)</u>

Description:

Plane-bedded quartzite is very conspicuous at a few locations (especially at Blaauwbank 278) (Figs. 4.8 and 4.9). Here this lithofacies covers a large area, probably in the order of one hectare. It was mostly observed in mature quartzites, but at some locations, e.g. Randfontein South and Leeuwpan 58, plane-bedding is developed in

immature quartzite. At both these locations this facies overlies conglomerate. In many cases this lithofacies is associated with an overlying mature quartzite unit containing ripples, e.g. at Blaauwbank 278. The laminae constituting this lithofacies are usually on average a few millimetres thick and grain-size ranges from fine to medium sand.

Fig. 4.8. Photograph showing plane bedding in mature quartzite on the farm Blaauwbank 278.

Interpretation:

Horizontal stratification develops with upper flow-regime deposition on a flat bed. The flat bed configuration suggests flow velocities higher than those prevailing during the deposition of ripples, sand waves and dunes, and flow depths great enough that in-phase waves (antidunes) are not developed (Harms *et al.*, 1975). An additional lower flat-bed phase exists at low velocities for sand coarser than 0.6 mm. There are, thus, two possible interpretations for plane-bedded coarse sand (Harms *et al.*, 1975).

Fig. 4.9. Photograph showing the lateral extent of the plane-bedded lithofacies on the farm Blaauwbank 278.

Evenly laminated sand, produced in the plane bed phase of the upper flow regime, is invariably associated with parting lineation (Reineck & Singh, 1980).

(V) <u>Quartzite unit with ripple marks</u>

Introduction:

All the ripple marks found during the study appeared to be symmetrical ones, but to confirm this observation a study of ripple marks found at three different locations, i.e. Middelvlei 255, De Pan 51 and Wildfontein 52, was carried out to determine the type of ripple mark. The wavelengths and amplitudes of adjacent ripples were measured and the indices proposed by Tanner (1967) were calculated.

The ripple index (R.I.) is defined as the crest spacing divided by the height of the ripples. The ripple symmetry index (R.S.I.) is the

horizontal distance from the highest point on the crest, along the gentler slope, to the deepest point in the trough, divided by the horizontal distance between crest and trough, taken along the steeper slope (Tanner, 1967).

An attempt was made to calculate additional indices, proposed by Tanner (1967), but due to the small areal extent of the outcrops it was not possible to measure all the required parameters.

The indices for the different measurements were plotted on a graph of R.I. versus R.S.I., proposed by Tanner (1967), for each location (Appendix II).

Description:

A mature quartzite, containing prominent ripple marks, was found mostly as the uppermost unit in outcrop (Figs. 4.10 and 4.12). The grain size of the quartzite unit ranges from medium to coarse sand and the dimensions of the ripple marks vary notably. Their wavelengths range from 2 cm up to half a metre and amplitudes from 0.3 cm to 8 cm. This lithofacies is practically present over the entire study area and shows a ripple-crest orientation that is remarkably constant. The beds, deposited higher up in the succession, were probably less resistant to erosion and were subsequently stripped off in most localities of the study area, to expose this unit.

A number of flat-topped ripple marks were found on the farm Middelvlei 255 (Fig. 4.11). Bates & Jackson (1987) describe this bedform as a ripple mark with a flat wide crest between narrow troughs.

Fig. 4.10. Photograph showing ripple marks on the farm Middelvlei 255.

Fig. 4.11. Photograph showing flat-topped ripple marks on the farm Middelvlei 255.

Fig. 4.12. Photograph showing large ripple marks, covered with a thin shale bed, on the farm Wildfontein 52.

Discussion and interpretation:

The majority of indices calculated for the three locations (Appendix II) plot in the oscillation or wave ripple field proposed by Tanner (1967). The field observation that most ripple marks are symmetrical was thus confirmed by the results of this study.

When classifying ripple marks, and from indices calculated from present dimensions, questions on the dimensional preservation of ripple marks arise. Boersma (1970) for example argued that in ancient sediments ripple size, and therefore the ripple index, would be affected by the compaction. According to Tanner (1967) the height of a ripple-mark crest, above adjacent troughs, can also be reduced, or made to appear to have been reduced, in several different ways. Some of these are enumerated below:

1. Rain splash can round, or spread out, the sand making up the crest.
2. Clay and fine silt settling out of water can concentrate in the trough, raising it's surface without affecting the adjacent crests.
3. Falling water level can plane off ripple crests, moving the sand into adjacent troughs. This process is prevalent on tidal flats and on intermittent sand-floored creek beds.
4. A change in flow regime can result in scouring off sand from crests.
5. Sinking of water into loose sand can reduce the water depth so drastically that the Froude number is increased to above the critical value (F = 0.7), and ripple-type bottom motion is replaced, at least in part, by thin sheet motion.

Ripples with the best preserved form were used for this study. This and the fair number of recordings made give reassurance of the result of the study.

Although many types of ripples may be found in several varied depositional environments, their distribution (especially their relative abundances) may serve to recognise the depositional environment. Reineck and Singh (1980) summarised the occurrence of wave ripples in different sedimentary environments (Table 4.1).

Environment	Wave ripples
River	Rare
Lake	Common
Lake beach	Abundant
Lagoon	Common
Intertidal flat	Abundant
Tidal channel and inlet	Absent
Backshore and foreshore	Abundant
Upper shoreface	Common
Lower shoreface	Common
Transition zone	Common
Muddy shelf	Rare
Sandy shelf	Rare
Continental slope and rise	Absent
Deep sea	Absent
Sandy deep sea	?
Turbidite	Absent
Seamounts	Rare

Table 4.1. The occurrence of ripples in different sedimentary environments.

Thus, according to Reineck & Singh (1980) wave ripples are most abundant on a lake beach, on intertidal flats as well as the back and foreshore.

The unit containing the ripple marks possibly represents a palaeosurface indicating a time interval during which very similar conditions reigned over a wide spread area.

According to Bates & Jackson (1987) flat-topped ripple marks are shallow-water ripple marks the crests of which were planed off during ebb tide or a fall in water level. They therefore indicate a tidal depositional environment.

4.3.3.4 Rhythmic quartzite/mudstone bedding

Introduction:

The descriptive term "rhythmic sand/mud bedding" was proposed by Reineck and Singh (1980) to include all bedding types composed of alternating layers of sand and mud. It includes lenticular and flaser

bedding (Fig. 4.13), coarsely interlayered sand/mud bedding, and thin interlayered sand/mud bedding. All the interlayered quartzite/mudstone units, encountered in the borehole cores, were grouped into this one lithofacies unit. This was done because it is rarely possible to identify the exact bedding type from the borehole core. It might, therefore, be possible that some of the rhythmic units, encountered in the boreholes, could be flat-bedded quartzite laminae.

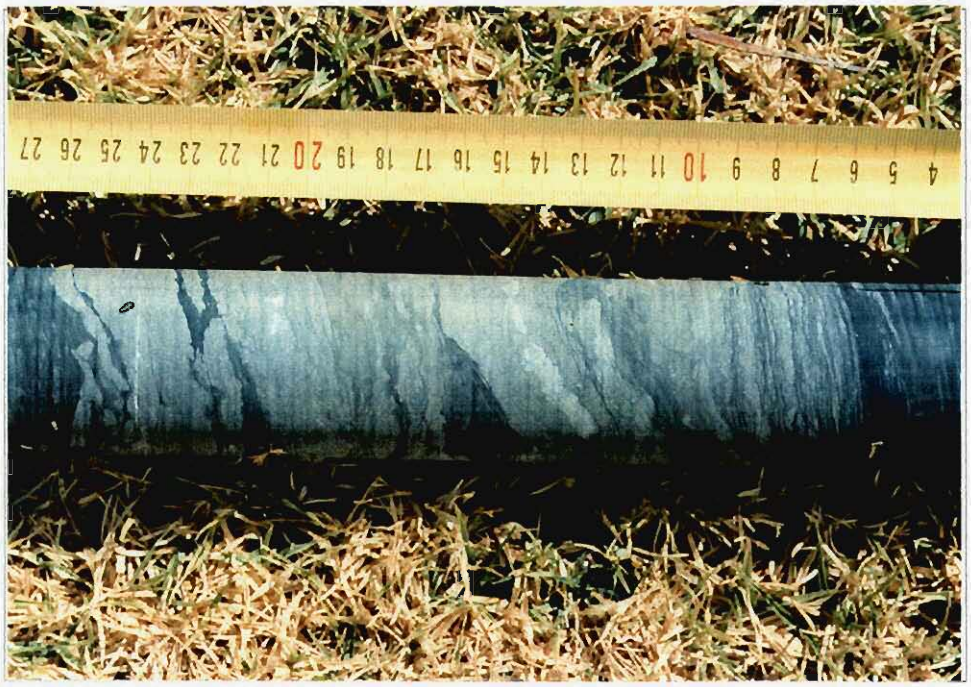

Fig. 4.13. Photograph showing flaser bedding in a drill-hole core.

Description:

Because of the poor outcrop preservation of the upper parts of the Black Reef Quartzite Formation, the rhythmic bedding lithofacies unit was only observed in borehole cores. It consists of alternating mudstone and quartzite layers, the thickness of which range from a few millimetres to a few centimetres. The grain size of the sandy layers was found to range from very fine to coarse. A distinction was made between units in which

quartzite dominates and units in which mudstone is dominant. In the cores of one borehole (BW1) mud laminae separating sandy cross-bed foresets were observed (Figs. 4.14 and 4.15).

Discussion and interpretation:

Because layers of two different kinds of rock types are alternatingly repeated in the rock record, the resultant deposits may be classified as rhythmites. The reason for such rhythmic repetition is a cyclic change in the transport or production of material. Such regular changes may be of short duration e.g., current fluctuations, variation in flow characteristics, tidal changes, or they may be long term changes e.g., seasonal changes caused by changes in weather conditions (Reineck & Singh, 1980).

According to Reineck & Singh (1980) **thinly interlayered** bedding (laminae less than 4 mm) is common on intertidal flats and in river estuaries, but are rare in open shelf environments.

Coarsely interlayered bedding is composed of alternating coarse- and fine-grained layers which are several millimetres to several centimetres thick (Reineck & Singh, 1980). Coarse layers may comprise sand or silt, whereas fine layers may be silt, mud or clay. Occasionally foreset laminae of ripples are recognisable in sand layers, but generally the coarse layers are horizontally laminated (Reineck & Singh, 1980).

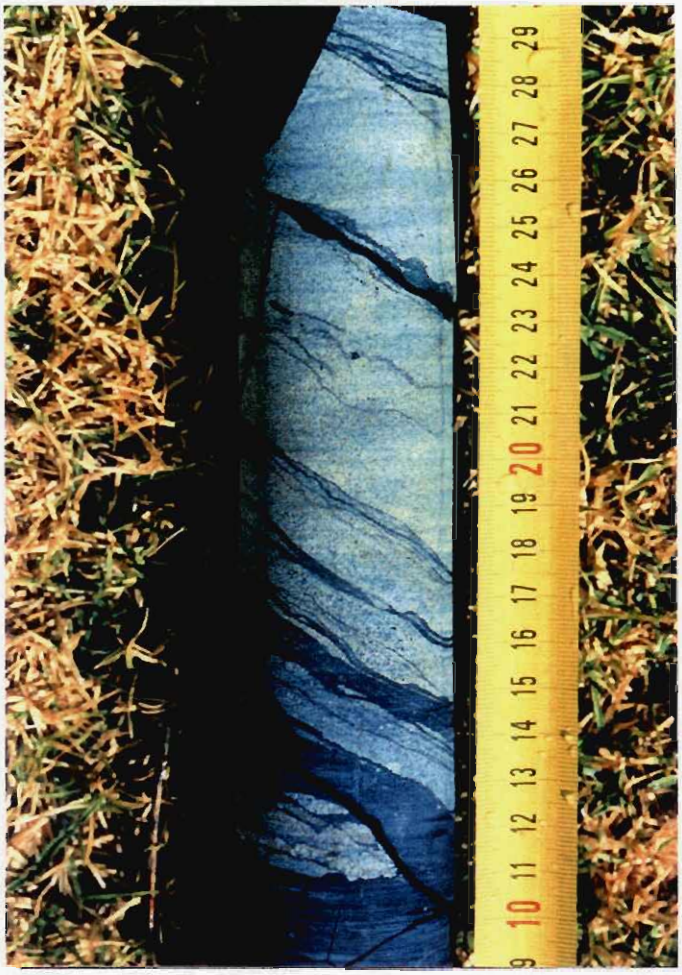

Fig. 4.14. Photograph showing mud layers on cross-bed foresets (Borehole BW1).

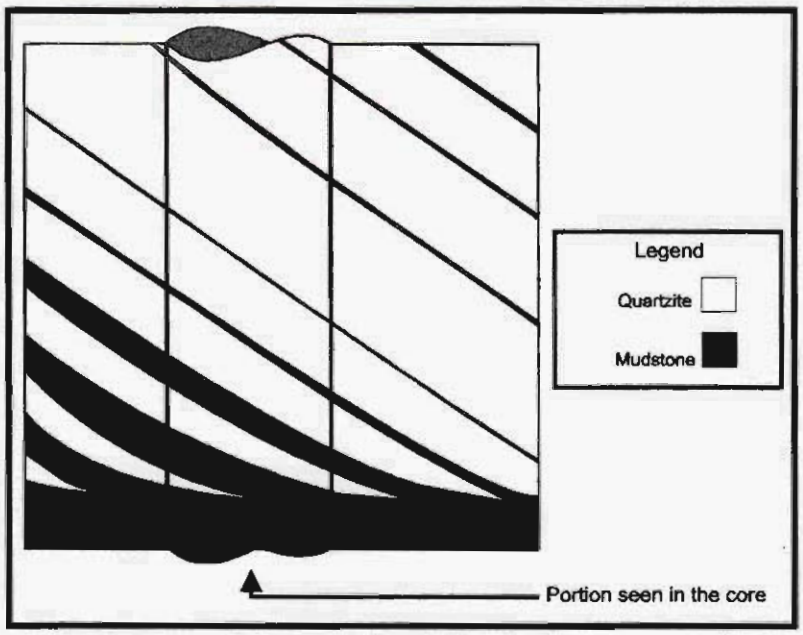

Fig. 4.15. Diagrammatic interpretation of the situation shown on Fig. 4.14.

Depending upon the relative thickness of sand and mud layers, three types of coarsely interlayered bedding can be distinguished (Reineck & Singh, 1980):

(a) sand and mud layers have almost equal thicknesses;

(b) thick sandy layers are separated by thin clayey or fine-grained layers;

(c) thick mud layers alternate with relatively thin sand layers

Coarse interlayered bedding is common in sediments of mixed intertidal flats (Reineck & Singh, 1980).

Flaser, wavy and lenticular bedding constitute another group of interlayered bedding consisting of thick sandstone\mudstone units. Ripple-marked bedding, with numerous mud flasers, is classified as **flaser bedding**, whereas in **lenticular bedding** the ripples or sand lenses are discontinuous and isolated, not only in a vertical but also in a horizontal direction. In **wavy bedding** mud and sand alternate and form continuous layers.

Flaser bedding is produced in environments in which conditions for deposition and preservation of sand are relatively more favourable than for mud. Whereas lenticular bedding is produced under conditions most favourable for the deposition and preservation of mud than for sand. The genesis of wavy bedding requires conditions where the deposition and preservation of both sand and mud are possible (Reineck & Singh, 1980).

According to Reineck & Singh (1980) the main environments where flaser and lenticular bedding may be deposited are subtidal and intertidal zones.

Regardless of the type of rhythmic sandstone/mudstone bedding, this bedding in the Black Reef Quartzite Formation is the product of cyclic

changes in the transport or production of material. These cyclic changes were probably brought about in an environment where tides played an important role.

4.3.3.4 Mudstone

Description:

As mentioned before this lithofacies was not observed in the outcrops and observations were made in the borehole cores. This lithofacies consists of massive to very finely laminated mudstone. The mudstone is typically dark grey to black in fresh exposure and yellow to red when weathered. Some of the beds are highly carbonaceous. Soft-sediment deformation structures are present in some of the beds.

Interpretation:

Miall (1992) describes his lithofacies Fsc as laminated to massive silt and mud. According to Miall's (1992) and Bridge's (1993) interpretation this lithofacies is formed by the episodic deposition of silt and mud from suspended load. It, thus, represents a low energy deposit.

4.3.4 Lithofacies assemblages and successions

4.3.4.1 Introduction

A transition matrix of the different lithofacies was compiled for Markov analyses, as described by Miall (1973) and Davis (1973). A similar approach to that of Van den Berg (1994) was followed, in the sense that the analysis was applied collectively to all the borehole profiles of the Formation, with the aim of determining typical lithofacies successions. The palaeo-depositional surface for each vertical succession was also included in this analysis and treated as a separate "lithofacies". This was done in order to find the most common **basal** lithofacies for the succession. Because the successions recorded in the outcrops were all

incomplete only sequences from borehole cores were used for this analysis. Because of the problem of identifying sedimentary structures in borehole core, no distinction, based on sedimentary structures, was made between the different lithofacies. The different lithofacies used in the analyses are conglomerate, quartzite, pebbly quartzite, mudstone, lenticularly bedded quartzite, pebbly lenticularly bedded quartzite, flaser-bedded quartzite and pebbly flaser-bedded quartzite. Units consisting of interbedded mudstone and quartzite, in which the quartzite is dominant, were considered lenticular bedding, whereas interbedded mudstone and quartzite units, in which the mudstone is dominant, were taken as flaser bedding.

A path diagram was constructed from the results of the Markov analysis (Fig. 4.16). The three most common lithofacies successions for the Black Reef Quartzite Formation were compiled from the analysis (Fig. 4.17).

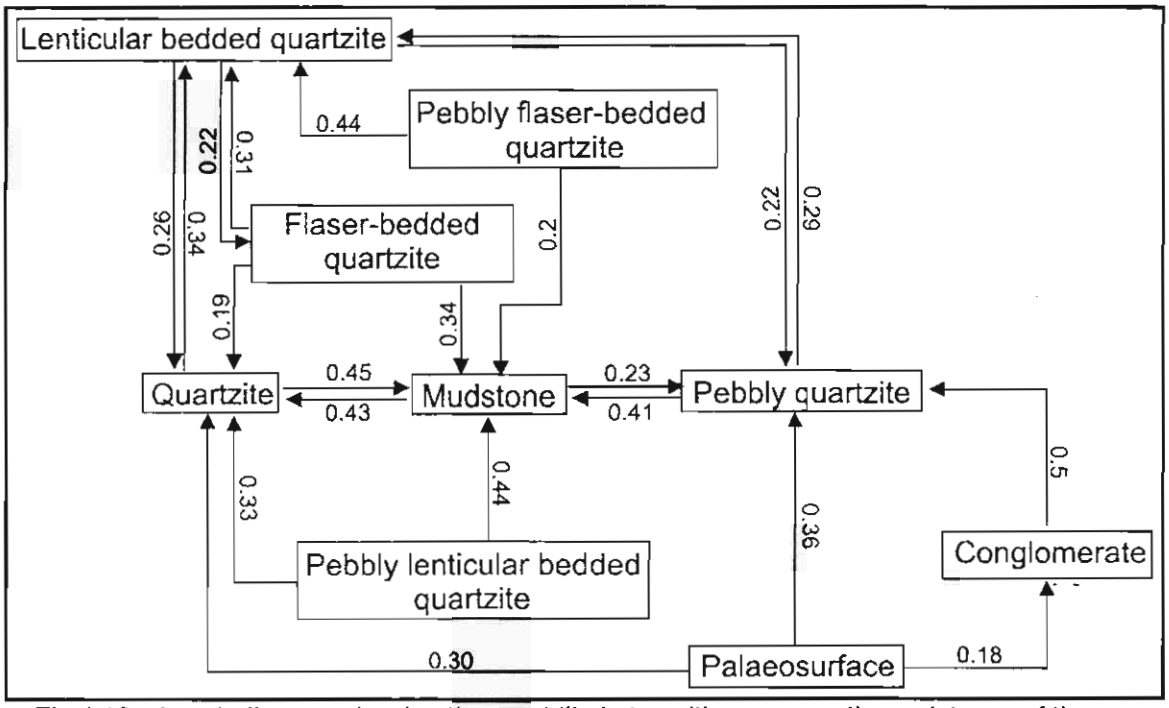

Fig.4.16. A path diagram showing the most likely transitions among the rock types of the Black Reef Quartzite Formation

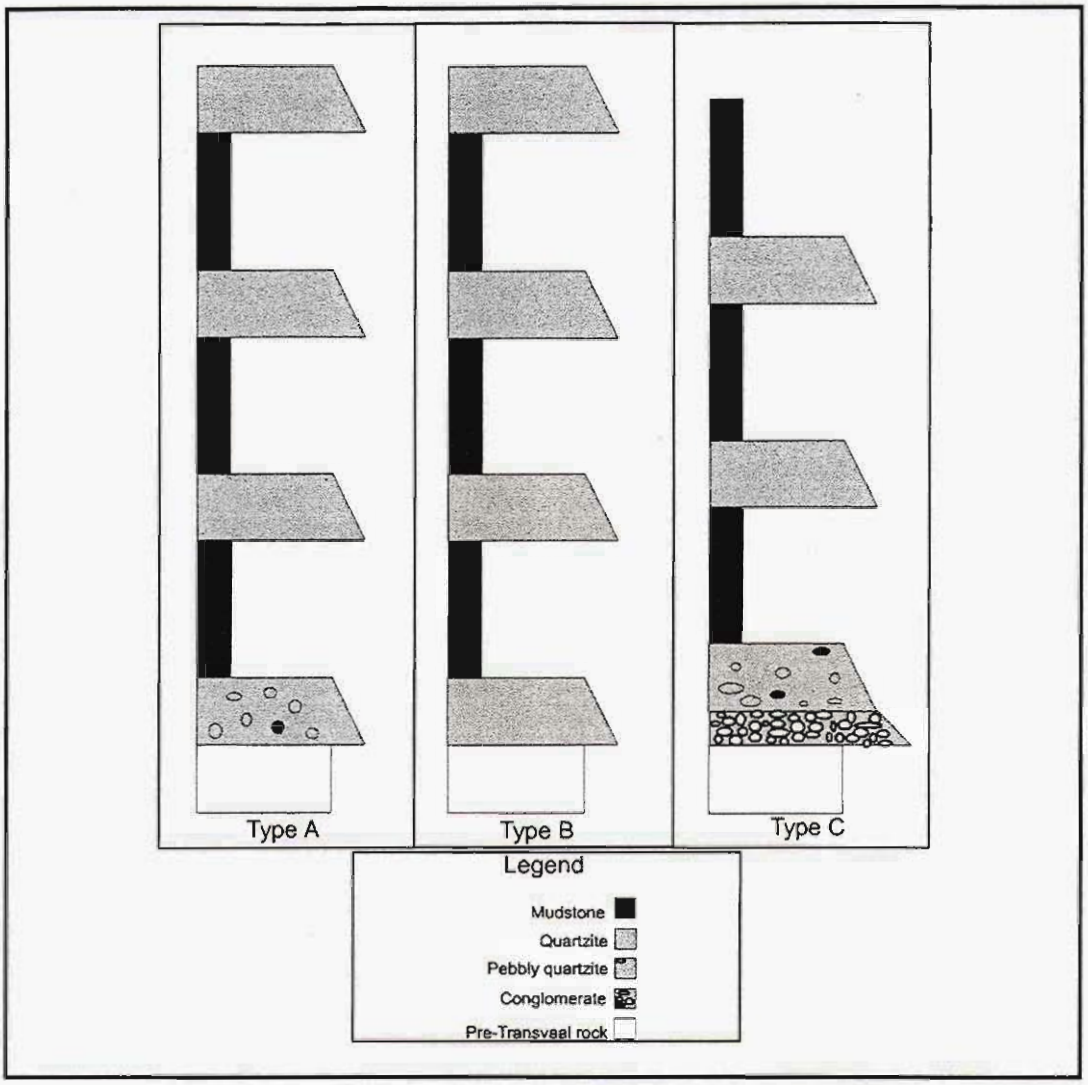

Fig. 4.17. Schematic presentation of the four most likely lithofacies associations of the Black Reef Quartzite Formation. No scale is implied.

4.3.4.2 Type A

Description:

Type A lithofacies assemblage is the most probable succession for the Black Reef Quartzite Formation. A pebbly quartzite unit occurs at the base of this succession and is overlain by a mudstone unit. Following upwards from hereon is a succession of alternating mudstone and quartzite units.

Discussion and interpretation:

The coarse-grained basal lithofacies is clearly a bed-load deposit. Although its internal structure could not be identified this lithofacies may contain any of the sedimentary structures discussed in the previous section, e.g. plane bedding or trough or planar cross-bedding. The overlying mudstone facies is a suspension deposit, probably deposited when flow was terminated or interrupted. The succession of alternating quartzite and mudstone beds therefore indicate cyclic changes of the hydraulic regime; from bedload transport to slack-water deposition. Such cyclic changes are typical of the tidal environment.

By strict application of Walther's Law, the initial facies deposited on a tidal flat, during a marine transgression, is the mudfacies of the supratidal zone, rather than sandstone (Reineck & Singh, 1980; Hallam, 1981). However, the preservation potential of such mudstone units may be low. Reineck & Singh (1980) ascribe the phenomenon of alternating lithological units to the changing lateral morphology of a shallow tidal environment. According to them, a slight change in morphology may transform an area of low energy into a high energy one.

In conclusion, Type A lithofacies assemblage indicate deposition in a tidal environment.

4.3.4.3 Type B

Description:

This lithofacies succession is the next-most probable one. It is virtually identical to the Type A assemblage; the only difference being the absence of pebbles in the basal quartzite unit.

Interpretation:

The absence of pebbles in this hypothetical succession suggests somewhat lower energy conditions than those prevailing during deposition of Type A lithofacies succession. The mudstone facies were, as with Type A, probably deposited on a mudflat in the intertidal zone and the quartzite facies were probably deposited in the subtidal zone and upper shoreface (Reineck & Singh, 1980). It is possible that this entire facies succession is of tidal-flat origin, because the succession, in its entirety, consists of alternating quartzite mudstone units. An alternative to be considered is that the quartzite unit at the base of the facies succession may be of fluvial origin.

4.3.4.4 Type C

Description:

A conglomerate unit forms the base of this succession and is overlain by a pebbly quartzite unit. This is overlain by a mudstone lithofacies unit. Upward from this point in the succession follows an alternation of quartzite and mudstone units.

Interpretation:

The basal conglomerate lithofacies suggests high bed-shear stresses, and could possibly have been deposited as gravel in submerged longitudinal bars or low-height bedwaves as suggested by Bridge (1993). Although these bedforms are characteristic of the fluvial depositional environment, they may also occur in other types of channels, such as tidal creeks. The overlying pebbly quartzite unit indicates a reduction in stream energy, although bed-load motion was still sufficiently energetic to deposit coarse-grained sediment.

As in the cases of the other facies assemblages, the mudstone facies overlying the pebbly quartzite facies, is regarded to represent a suspension deposit, laid down under very low-energy conditions. The cyclic alternation of mudstone and quartzite facies, which constitute the upper part of the assemblage, resembles a tidal flat deposit (Reineck & Singh, 1980).

4.4 Palaeocurrents

4.4.1 *Introduction - palaeocurrent indicators*

Planar and trough cross-bedding were the only palaeocurrent indicators that could be used for determining the palaeocurrent directions. Because of their relative abundance and reliability as palaeocurrent indicator (Miall, 1974) trough-axis orientations were used almost exclusively to determine palaeocurrent directions.

For ripples their crest orientations were recorded. Although the ripples of this study were predominantly of the symmetrical type (oscillation ripples), and having subordinate palaeo-environmental significance, their data were nevertheless collected with a view to their integration and interpretation in the context with more reliable palaeocurrent indicators.

4.4.2 *Methods and results*

The orientations of structures were measured with a magnetic compass and recorded on standard forms. The following parameters were measured for the different sedimentary structures:

a) Trough cross-bedding: The direction and angle of plunge of the trough axis.

b) Planar cross-bedding: The direction and angle of dip of the foresets.

c) Ripple marks: The orientation of the ripple crests, their wavelenghts and amplitude.

For each palaeocurrent measurement the following additional information was recorded:

a) geographic location

b) type of structure

c) dimensions of the structure (where possible)

d) local tectonic dip.

The tectonic dips were recorded with a view to making corrections for the tectonic inclination, but because of the low tectonic dip of the Black Reef strata, 7.9° average for the study area, these corrections were deemed unnecessary.

Selley (1982) suggested that 25 readings are generally sufficient to determine a vector mean with an accuracy of ±30°. However, at many data stations it was not possible to record 25 readings, because of poor outcrops.

Compass roses were constructed for the trough axes. For each data station the vector mean (Fig. 4.18) was calculated and for bimodal distributions two vector means were calculated.

The data of the ripple mark crest orientations are presented by compass roses on a map of the study area (Fig. 4.19). "Mean orientations" were also calculated for the different data stations and shown as discrete "axes" on Fig. 4.19.

The compass roses on Fig. 4.18 show that for Stations 2, 7, 8, 12, 13, 15 and 16 the distributions are unimodal, whereas bimodal distributions were found for Stations 1, 6, 9, 10 and 11. The distributions calculated for

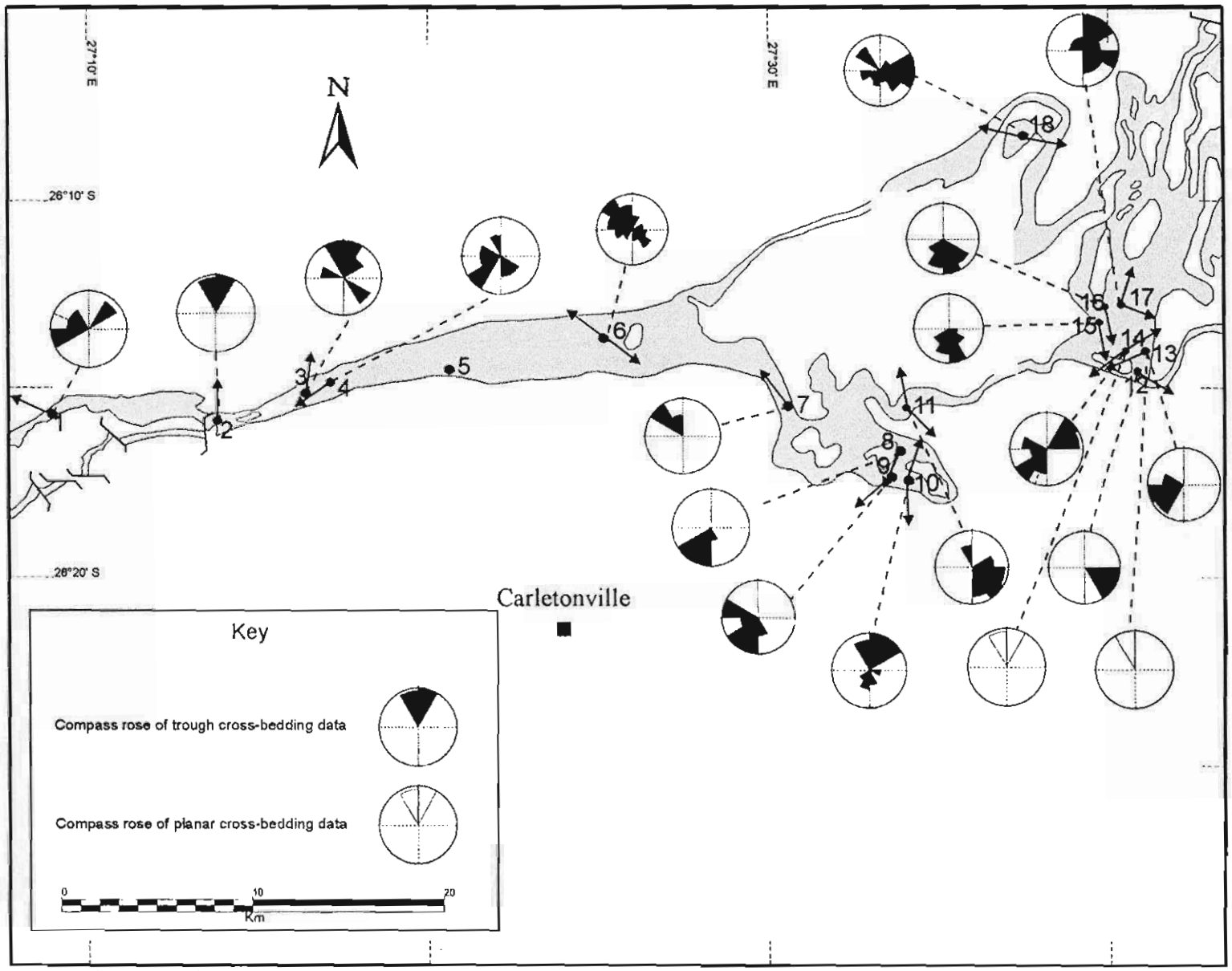

Fig. 4.18. Map showing palaeocurrent distributions and vectors of cross-bedding measurements

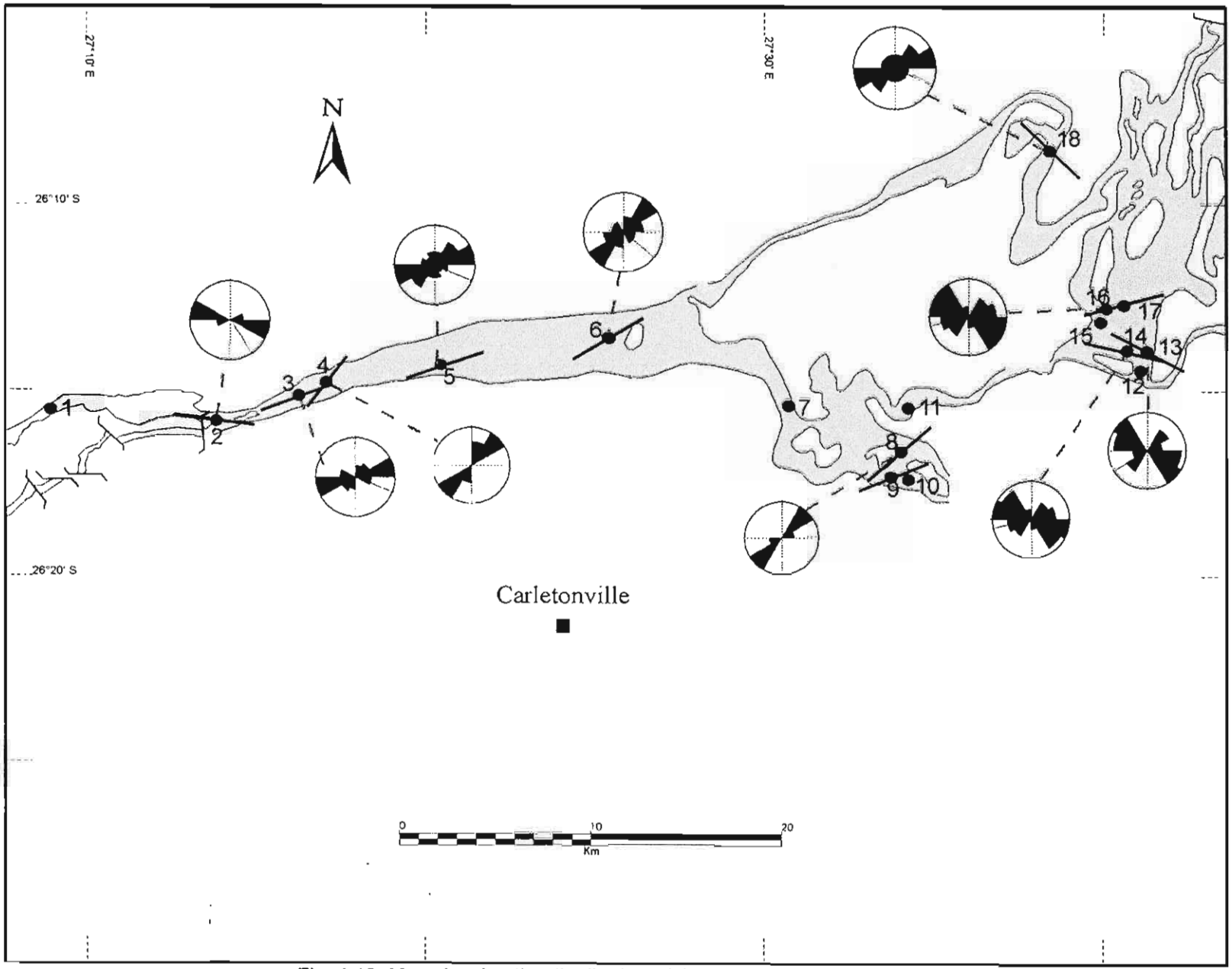

Fig. 4.19. Map showing the distribution of ripple-mark crest orientations

Station 3, 4, 14, 17 and 18 are considered polimodal. Figure 4.18 shows that on the Rand Anticline the modes of the unimodal distributions are towards the north. However in the remainder of the study area, especially in the east, the modes lie within the second and third azimuth quadrants. For the bi- and polimodal distributions there are no general dominant modes.

Figure 4.19, portraying ripple crest orientations, shows that there is a general well-defined east-west orientation of ripple crests for most of the study area.

4.4.3 *Discussion and interpretation*

Selley (1982) classified palaeocurrent patterns as shown in Table 4.2.

Environment	Local current vector	Regional Pattern
Alluvial (braided)	Unimodal, low variability	Often fan-shaped
Alluvial (meandering)	Unimodal, high variability	Slope-controlled often centripetal basin fill
Eolian	Uni-, bi-, or polymodal	May swing round over hundreds of kilometres around high pressure systems
Deltaic	Unimodal	Regionally radiating
Shorelines and shelves	Bimodal or polymodal	Generally consistently orientated on-shore, off-shore or long-shore
Marine turbidite	Unimodal (sometimes exceptions)	Fan shaped, or, on a larger scale, trending into or along trough axes.

Table 4.2. A summary of palaeocurrent patterns and the environments they are related to (Selley, 1982).

Applying the above classification to the data of this study, it may be reasoned that Stations where bimodal, oblique and polymodal current distributions were recorded represent shoreline or shelf environments. This interpretation seems plausible, if the tidal sub-environment is included in Selley's (1982) shoreline and shelf environment. Interpretation of the unimodal distributions of this study is problematic. These distributions may indicate fluvial deposition, but may alternatively represent flood and ebb currents in a tidal setting where either of these were too weak to produce bedforms.

According to Selley (1982) palaeocurrents are slope controlled in fluvial, deltaic and most turbidite environments, whereas palaeocurrents are not related to slope in eolian and marine shoreline environments. Applying this datum to the northern and southern modes of the unimodal distributions of this study, both northerly and southerly sloping palaeosurfaces can be inferred. The fact that these directions are perpendicular to the anticlinal axis of the Rand Anticline leads one to the conclusion that the Rand Anticline existed in Black Reef times and exerted some structural control on the current directions. Van den Berg (1994) indeed postulates a drainage divide along the south-eastern limb of the Rand anticline. The opposed palaeocurrent directions perpendicular to the Rand Anticline may be evidence for this assumption.

4.5 Pebble size, pebble lithology and pebble roundness

4.5.1 Introduction

Pebble size investigations usually provide information on the sorting of the conglomerate, the energy of the stream that deposited the pebbles and the transport distance. Pebble lithology, on the other hand, provides information on the provenance of the pebbles and reflects the maturity of the

conglomerate. Pebble roundness indicates the degree of mechanical abrasion the pebbles were subjected to.

4.5.2 Pebble size

Methods and results:

Because the conglomerates of this study are well-indurated, it is impossible to liberate the pebbles from the matrix. The pebble sizes of the conglomerate samples could therefore not be determined through sieving. Instead conglomerate samples collected for determination of pebble size were cut into slabs and two-dimensional measurements were carried out on the flat-cut surfaces, measuring apparent longer dimension of pebbles. Data were recorded on a standard data sheet making provision for the simultaneous recording of pebble size, pebble lithology and pebble roundness.

The results of these analyses are presented in Appendix VI.

A sample from Leeuwfontein 58 yielded the largest mean pebble size and the poorest sorting, whereas a sample from Middelvlei 255 contained the smallest pebbles with the best sorting.

Discussion and interpretation:

As mentioned before, pebble size indicates the hydraulic energy of the stream that deposited the pebbles. The hydraulic energy (the stream competence) is, among other factors, related to the stream gradient.

The large pebbles found in outcrops at Leeuwfontein 58, indicate high hydraulic energy. For this high-energy deposit a steep slope can be inferred. The same interpretation applies for the coarse-grained conglomerate found at Bospan 56.

The smaller pebbles in the conglomerate of the other two locations indicate a less competent stream (lower bed shear stress), and thus, a less steep slope. In general the pebbles of the Black Reef Quartzite Formation in the study area are rather small, and indicate rather low hydraulic energy conditions.

4.5.3 *Pebble lithology*

Methods and results:

The recorded data on pebble lithology from the three different locations are presented as pie diagrams in Appendix VI.

The pie diagrams display significantly different lithological compositions of the pebble assemblages of the conglomerate samples. The sample from Leeuwfontein 58 had the highest quartzite content, whereas the sample from Middelvlei 255 contained the highest diversity of pebble lithologies.

Discussion and interpretation:

As mentioned before, pebble lithology reflects primarily the provenance of the pebbles. It is obvious that some of the source material would have been derived from the pre-Transvaal rocks constituting the palaeosurface in the study area. However, the possibility does exist that some of the source rocks may have been completely removed by erosion, or occur outside the study area.

The pebble assemblages of conglomerates of the Black Reef Quartzite Formation confirm that the source rocks were predominantly pre-Transvaal rocks found in the study area. The large proportion of white quartzite in the conglomerate at Leeuwfontein 58 can be directly connected to the massive recrystallised quartz found in association with the Archaean Basement. The source of most of these pebbles was therefore very proximal, being the

mentioned white siliceous rocks. The hypothesis of proximal sources is illustrated by the conglomerate at Bospan 56, where it has basically a monomict assemblage reflecting the lithology of the rocks on the depositional surface. It is possible that the many small quartz veins traversing the Archaean Granite in the study area could have served as a source of the quartz pebbles found in the Black Reef Quartzite Formation. The rocks of the Witwatersrand Supergroup surely have been an important source of material, in particular heavy minerals. Workers such as Nel (1935) and Papenfus (1964) have attributed the high gold content of certain parts of the Black Reef Quartzite Formation to the proximity of auriferous Witwatersrand Supergroup placers.

The notable diversity of the pebbles in the conglomerate, found at Middelvlei 255, may be attributed to the marked variety of floor rocks which the Black Reef Quartzite Formation overlie in this area.

4.5.4 *Pebble roundness*

Methods and results:

Pebble roundness deals with the sharpness of the edges and the corners of the pebble (Pettijohn, 1975). In this study roundness of pebbles was determined by way of visual comparison with chart images compiled by Krumbein (1941). The mean pebble roundness, for the different locations used in the study of the conglomerates, are shown in Table 4.3.

LOCATION	MEAN PEBBLE ROUNDNESS
Wildfontein 52	0.472
Leeuwfontein 58	0.430
Middelvlei 255	0.499

Table 4.3. Mean pebble-roundness for conglomerates from three different locations.

The pebbles of the conglomerate sample collected from Middelvlei 255 had the highest mean roundness whereas the sample from Leeuwfontein 58 had

the lowest mean roundness. However, considering the range of Krumbein's (1941) scale (0.1 - 0.9) the difference among the samples of Table 4.3 is small and probably not statistically significant.

Discussion and interpretation:

The roundness of a pebble increases with the duration of transport, during which it is subjected to mechanical abrasion, and is thus related to the distance travelled. Because pebbles of different lithologies have different abrasion coefficients pebble roundness is also influenced by pebble lithology. To illustrate, Sneed & Folk (1958) found that quartz, in the Colorado River of Texas, became well rounded in less than 160 kilometres, whereas limestone pebbles had already attained their maximum roundness by the time they reached the main stream.

Pettijohn (1975) reasoned that most of the observed rounding of pebbles is acquired in the first few kilometres of transport. An implication of this hypothesis is that an angular to subangular pebble could not have been moved more than two or three kilometres.

The highest value of mean pebble roundness for the study area, as shown by pebbles at Middelvlei 255, may suggest the longest transport distance, whereas the lower roundness of the pebbles at Leeuwpan 58 suggests a shorter transport distance. However, as pointed out earlier, the difference in roundness between these samples is small.

When relating transport distance to mean pebble roundness of the Black Reef Quartzite Formation it should be kept in mind that much of the sediments of the Black Reef may represent reworked sediment. Many of the pebbles that are now found in the Black Reef Quartzite Formation may have been derived from Witwatersrand conglomerates. Van den Berg (1994) quantitatively inferred transport distances from pebble roundness of

pebbles of the Black Reef Quartzite Formation. His study revealed that the long transport distances, calculated for some of the pebbles, are anomalous, and concluded that these pebbles have been subjected to abrasion during more than one geological cycle.

4.6 Petrographic aspects of the quartzites

4.6.1 *Introduction*

The petrographic composition and size parameters of quartzite samples, taken at different stratigraphic levels from cores of borehole BL8 were investigated in a petrographic study. The objectives of this study were:

(a) to classify the different quartzite units, according to the system of Pettijohn *et al.* (1972);

(b) to investigate the grain-size distributions of the quartzites, with the aim of interpreting a depositional environment;

(c) to investigate possible lithological variations in the vertical profile;

(d) to study a possible upward increase in dolomite content in the Black Reef Quartzite Formation (discussed in a later section).

4.6.2 *Laboratory procedure*

Nineteen samples (not all true quartzites) were taken at different depths from cores of borehole BL8. Thin sections were prepared from these samples and stained, applying the methods described by McManus (1988). The purpose of staining was to facilitate the identification of potassium feldspar grains.

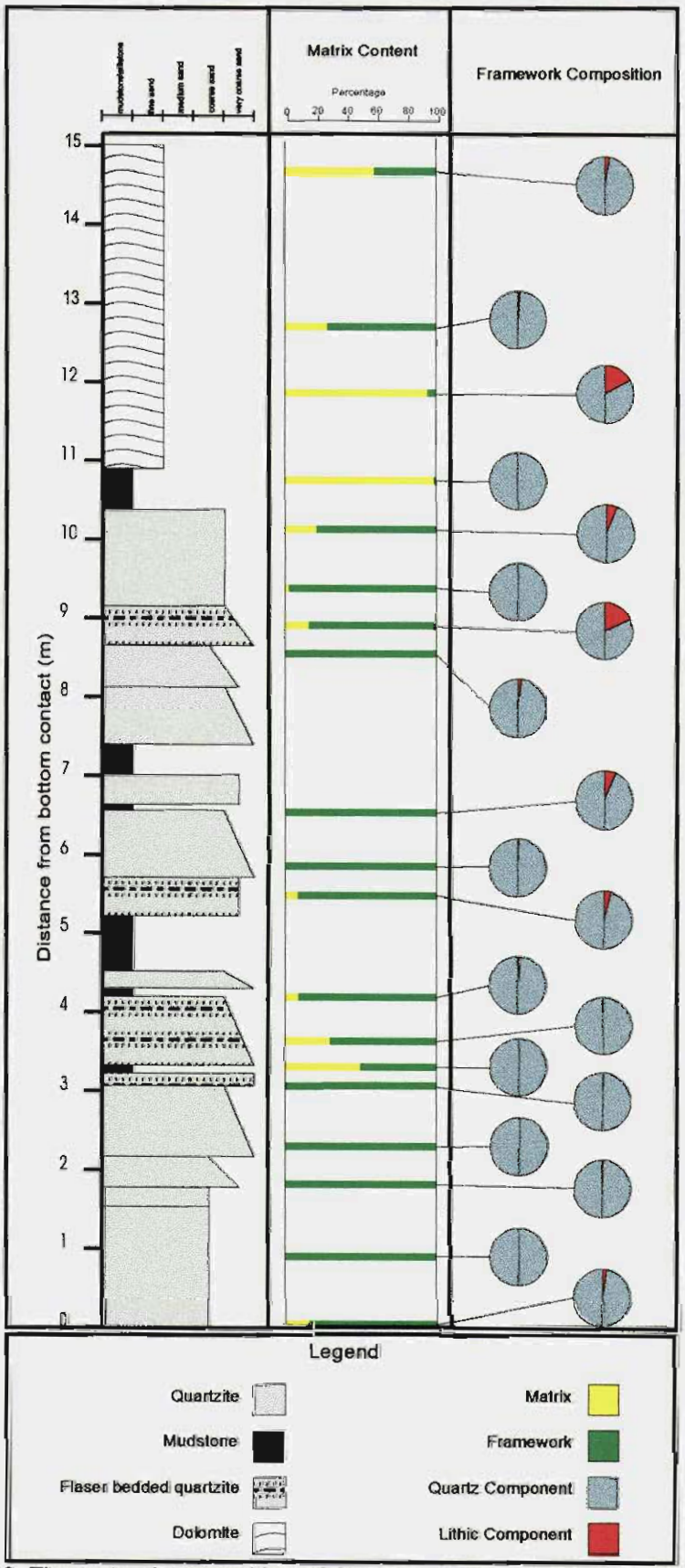

Fig. 4.20. The textural composition of the different arenite units in borehole BL8

4.6.3 *Modal analysis:*

Methods and results:

The textural and mineralogical composition of the sampled quartzite units were determined by standard point-counting techniques, as described by Galehouse (1971).

The main constituent minerals, identified in the microscopic study, were quartz (polycrystalline and monocrystalline), dolomite, chert, sericite, sulphides (mostly pyrite), chlorite and a dark, silt-like material. The latter was noticed to have replaced the quartz grains along their margins and also occupies the interstices. This dull black material consists mostly of fine-grained phyllosilicates that are highly impregnated and obscured by finely dispersed carbon (Frankel, 1940a). Liebenberg (1955) suggested that the carbonaceous material is a non-graphitic amorphous hydrocarbon.

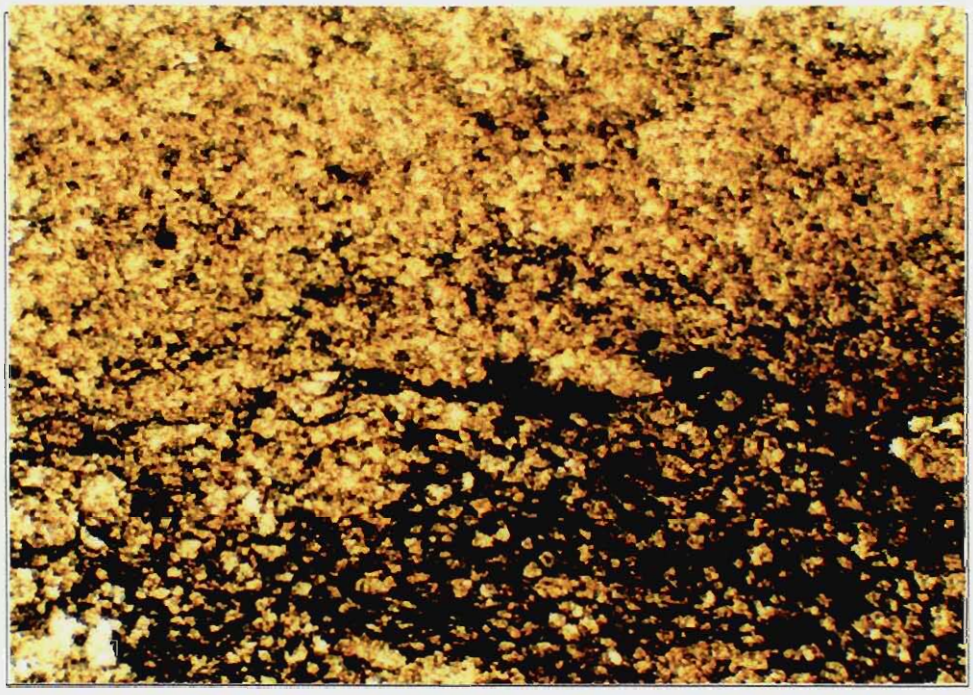

Fig.4.21. Photomicrograph showing dull black carbonaceous material (bottom of picture; top part shows dolomite crystals). The long dimension of the photomicrograph is 1.8 mm.

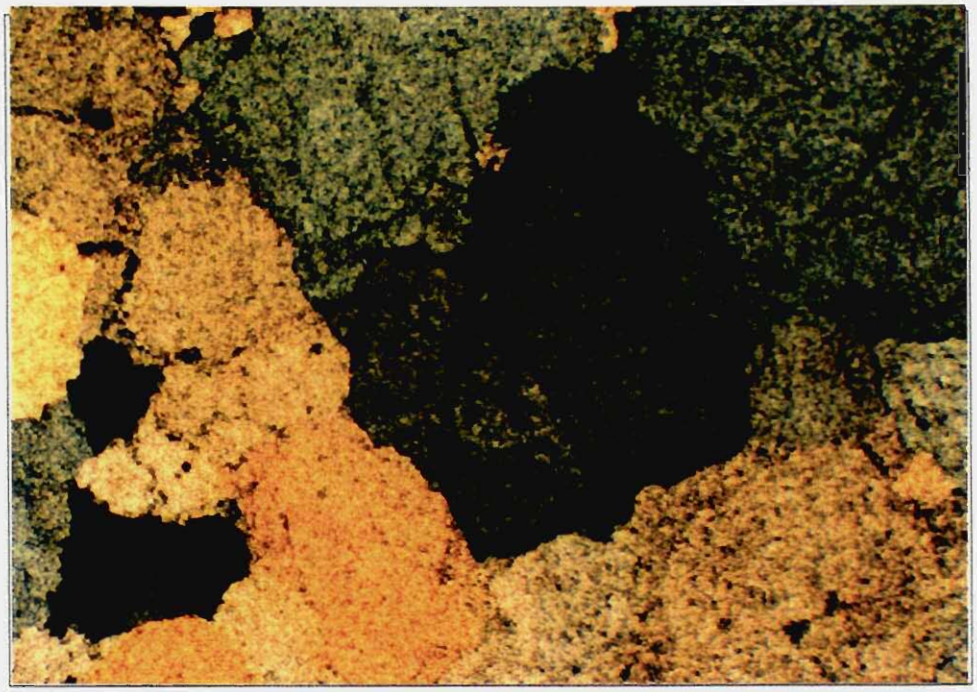

Fig.4.22. Photomicrograph of a very mature quartz arenite. The long dimension of the photomicrograph is 1.83 mm.

All quartz grains observed show undulatory extinction. The results (Appendix VII) show that the quartzite units are mostly very mature quartz arenites (up to 100% quartz content). The succession of the various arenites in the vertical profile in Fig. 4.20 is interesting. The lowermost unit is a quartzwacke, overlain by a number of quartz arenites followed by quartz wackes, a lithic greywacke, a lithic arenite and mudstones. The matrices of the quartz wackes, the lithic greywacke and mudstones consist mostly of siltstone and the black carbonaceous material. The dolomite content of the succession in the borehole increases upward, as would be expected (Fig. 4.20).

Discussion and interpretation:

The black carbonaceous material, the sericite and chlorite is considered to be of diagenetic origin. Many of the pyrite grains appear to have a detrital

origin but at some positions pyrite occurs as veins, suggesting hydrothermal replacement.

The mainly orthoquartzitic sandstones (quartz arenites), indicative of a high degree of textural and mineralogical maturity, represent the final product of protracted and profound weathering, sorting and abrasion (Pettijohn, 1975). Pettijohn (1975) suggests that it is imperative for the formation of these rocks that their source area and the site of deposition be tectonically very stable, or alternatively that the sand goes through several cycles of sedimentation. He concludes that it is improbable that quartz arenites, of the type found in the geologic record, could ever be produced by river action. Pettijohn (1975) further concludes that sand of this maturity can only be formed in an aeolian environment or in the surf zone, where repeated washing and winnowing matures the sand.

Lithic arenites generally reflect an extensive provenance area - that of a large drainage basin, which most likely has a diverse bedrock lithology (Pettijohn, 1975). He suggested that lithic arenites are the deposits of large rivers.

Van den Berg (1994) attributed the paucity of feldspar grains in the quartzites to sediment recycling. A higher original feldspar content is expected if one considers the fact that the Black Reef Quartzite Formation overlies Basement rocks in many areas. The granite rocks must have supplied not only quartz to the Black Reef, but feldspar too.

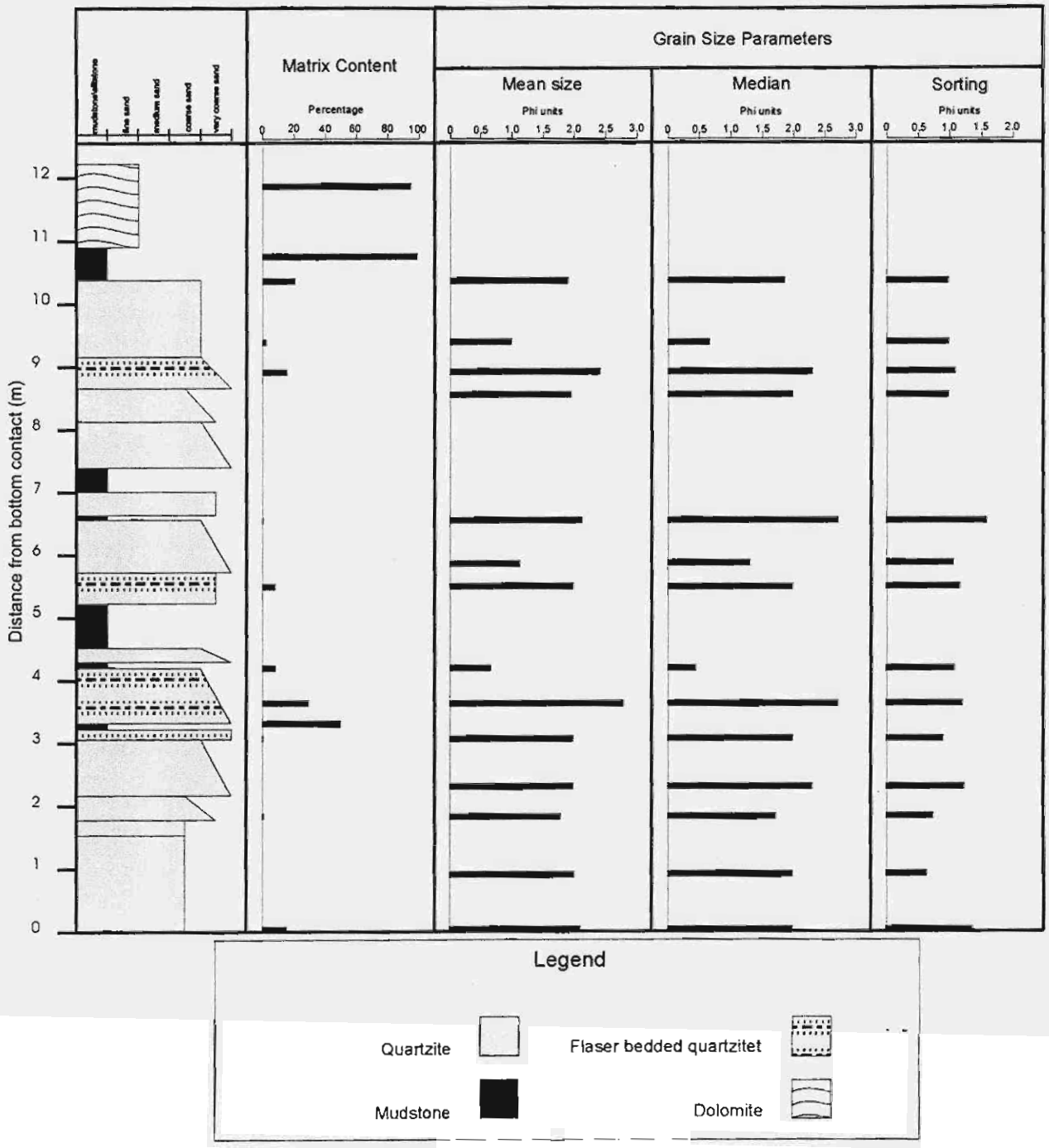

Fig.4.23. Textural and sieve-equivalent grain size parameters of the different quartzite units in borehole BL8

4.6.4 *Grain-size analysis*

Methods and results:

For the grain-size analysis the apparent long and short dimensions of grains, were measured, using a calibrated ocular.

The various percentiles, mean grain-sizes and standard deviations, calculated by computer (Statgraphics software) from the data, were converted to sieve-equivalents by employing linear regression equations proposed by Harrel & Eriksson (1979). Only the quartzites, containing 70 % or more framework grains, were considered for this study. Cumulative frequency curves, of the sieve equivalent percentiles, were plotted for the different samples (Appendix VIII).

Discussion and interpretation:

Various authors have identified ancient environments on the basis of grain-size studies, e.g. Moss (1962) and Visher (1965). Friedman (1967) argued that "no single approach can uniquely define depositional environment in ancient equivalents; but size-frequency studies, if properly applied and if their limitations are realised, can help in upgrading the odds in environmental interpretation". Well-indurated sandstones are problematic for this type of study, because it is virtually impossible to liberate individual sand grains for the purpose of sieving. For this reason Harrell & Eriksson (1979) have derived, via linear regression analysis, thin-section-to-sieve empirical conversion equations for several graphic size-distribution statistics. However, they recommend only their conversion equations for the median (correlation coefficient, r = 0.958) and graphic mean (r = 0.944) for general use. For the purpose of this study the correlation coefficient (r = 0.786), of the standard deviation conversion equation was deemed sufficiently reliable.

No obvious trend could be established for the converted standard deviations of the different quartzite units. However, the basal quartzite unit has one of the highest converted standard deviations (1.44 ϕ). This unit is, according to Johnson's (1994) verbal classification system, a very poorly-sorted sand. Surprisingly however, the quartzite unit immediately overlying the former-mentioned one has one of the lowest standard deviations in the succession with a value of 0.64 ϕ, and would be classified as a moderately sorted sandstone.

According to Middleton (1976) logarithmic-probability cumulative frequency plots that consist of two or three straight-line segments are indicative of a fluvial environment. Such segmented cumulative frequency distributions were found for some of the units investigated (Appendix VIII). However in the light of evidence cited earlier in this dissertation, the arenites studied are not likely to be of fluvial origin.

Chapter 5

The overlying dolomitic Malmani Subgroup

5.1 Introduction

Although the rocks of the Malmani Subgroup were not studied in any detail, their characteristics are summarised here with a view to better understanding the sedimentological setting of the underlying Black Reef Quartzite Formation. The dolomites of the Malmani Subgroup are among the oldest known carbonate deposits. In the study area the Subgroup is subdivided into four Formations; the Oaktree, Monte Christo, Lyttleton and Eccles Formations (J.J. Mayer, *pers. com.*, 1996; SACS, 1980). The lower part of the Malmani Subgroup, the Oaktree Formation, consists predominantly of finely bedded to massive dark dolomite (Eriksson, 1972). Carbonaceous shale and quartzite is abundant near the base. Stromatolites and chert are rare in this lower part of the Malmani Subgroup. (Eriksson, 1972).

5.2 Lithological and petrographic description

In fresh outcrop the dolomite has a light-grey colour, but weathers to a distinctive brown colour. Stylolitic structures are commonly observed and are distinctive of the dolomite. The dark grey to black mudstones in the lower part of the Malmani Subgroup are lithologically identical to those of the underlying Black Reef Quartzite Formation (Van den Berg, 1994).

Under the microscope the dolomite appears to be extensively fractured. A multitude of fine veins criss-cross to divide the rock into intermedial sections which are seemingly undisturbed. These sections, demarcated by nets of fine dark lines, thin calcite veins and blotches of coarse crystalline sparry calcite,

comprise a mosaic of irregular interlocking dolomite grains varying in grain size from 0.04 - 0.1 mm. The latter texture undoubtedly represents one which has resulted from the recrystallization of an original extremely fine-grained micritic carbonate precipitate.

As indicated earlier the dolomite content of the different stratigraphic units in borehole BL8, was determined by means of modal analysis. The dolomite content, expressed as percentages, were plotted as a function of depth on Fig. 5.1. This diagram shows that there is a general upward increase in dolomite content. The dolomite content is very low for the lower part of the succession, but at a level of approximately 4 m a sharp increase is noticed.

5.3 Discussion and interpretation

The fact that dolomite grains are also present in the quartzites of the Black Reef Quartzite Formation indicates that there is not a sharp contact between the Black Reef Quartzite Formation and the overlying Malmani Subgroup. Instead a conformable transition is indicated. This transitional relationship is probably one reason why it is difficult to define the Black Reef Quartzite Formation stratigraphically and to demarcate its top. Additional proof of the conformable transition is the fact that quartzite and mudstone beds also occur above the stratigraphic boundary between the Black Reef Quartzite Formation and the Malmani Subgroup, suggesting a **gradual** decrease in clastic sedimentation.

For a better comprehension of the transition from clastic deposition to carbonate precipitation the general sedimentological controls for the precipitation of modern carbonate sediments are listed (Beukes, 1986):

(a) Temperate to warm water

(b) Clear water

(c) Effective agitation of the water

(d) Effective evaporation

All these conditions are best attained in shallow water, typically 10 - 15 metres deep, with an absolute maximum of 100 - 250 metres (Beukes, 1986).

Applying these criteria to the Transvaal Sequence, it can be inferred that, with the commencement of precipitation of the Malmani dolomites, the clastic sediment supply diminished drastically, bringing about the required clear water conditions. Occasional influxes of clastic sediment interrupted precipitation of the dolomites for brief periods.

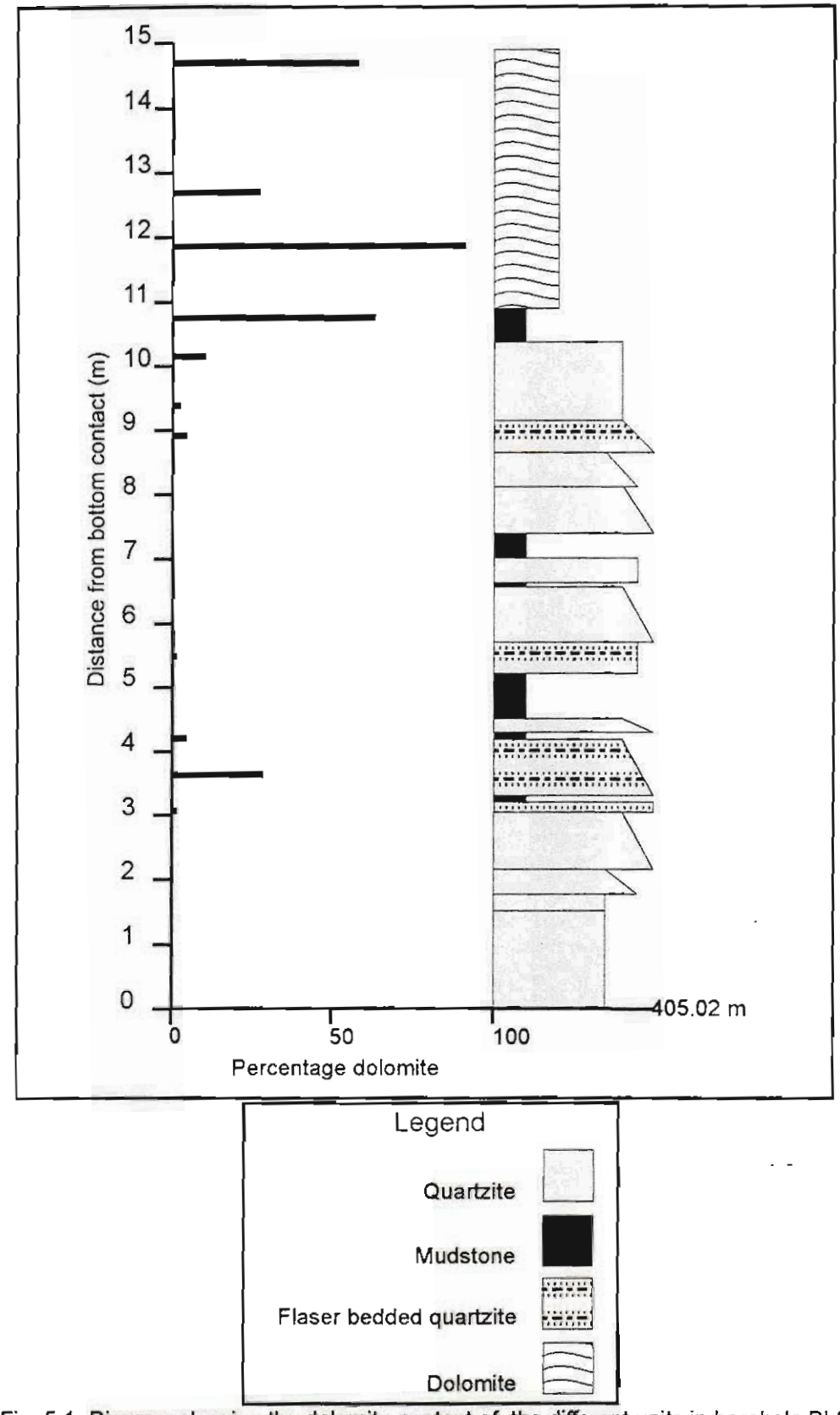

Fig. 5.1. Diagram showing the dolomite content of the different units in borehole BL8

Sedimentological synthesis

6.1 Introduction

Application of the principle of uniformitarianism is fundamental in a sedimentological synthesis. However, it is possible that no modern analogues of some ancient systems exist. Fuller (1985), for instance, noted that no modern analogues of fluvial systems, on the same scale as those inferred for pre-Devonian times exist. It is with this restriction in mind that this environmental interpretation of the Black Reef Quartzite Formation is approached.

6.2 Palaeo-environmental Classification

6.2.1 *The Conglomerate unit and immediately overlying quartzites*

The characteristics indicative of a fluvial environment and their applicability to the Black Reef Quartzite Formation are listed in Table 6.1.

As indicated, some of these characteristics apply to the lower, arenaceous part of the Black Reef Quartzite Formation. It can thus be deduced that this part of the Formation was deposited by fluvial processes. However, for some basal units found in borehole cores and outcrops the listed criteria do not seem to apply. This fact leads to the conclusion that the true basal part of the Formation is absent in parts of the study area due to a channelised distribution. Eriksson (1972), after a thickness study of the Formation,

concluded that maximum thicknesses of the Formation coincided with linear depressions denoting fluvial drainage lines in the floor rocks.

Characteristics	Applicability
• Unidirectional palaeocurrents (Visher, 1972; Long, 1978; Selley,1982)	Uncertain
• Channels and scours (Visher, 1972; Friend, 1978; Rust & Koster, 1984)	Uncertain
• Repetitive fining upward sedimentary cycles (Selley, 1982; Ethridge & Westcott, 1984; Nemec & Steele, 1984; Pettijohn, 1975)	Uncertain
• Dominance of large and medium scale trough and planar cross-beds (Long, 1978)	Yes
• Segmented log-probability cumulative curves (Visher, 1972; Middleton, 1976)	Yes
• Large grain-size variations (Visher, 1972)	Yes
• Presence of sublithic arenites (Pettijohn, 1975)	Yes
• High standard-deviation (sorting) of grain size (Friedman, 1967)	Yes
• Textural immaturity (Pettijohn *et al.*, 1972)	
• Channelised conglomerate bodies (Rust and Koster, 1984)	Yes
• Variable thickness of deposits, and total absence at places, implying deposition in channels (Rust & Koster, 1984)	Yes

Table 6.1. Characteristics indicative of a fluvial environment and their applicability to the lower part of the Black Reef Quartzite Formation

6.2.2 *Type of river system*

Presently, four principal river types are recognised, i.e. meandering, braided, straight and anastomosed (Allen & Allen, 1990). Schumm (1968) proposed that during pre-vegetation times, essentially all rivers were braided streams. Fuller (1985) supports this statement and further points to the problem of mistakenly interpreting pre-Devonian braided river deposits as marine deposits, because of the absence of channel margins.

The lower Black Reef fluvial deposits can thus be interpreted as braided river deposits. The characteristics of braided river deposits and their applicability to features of the Black Reef Quartzite Formation are enumerated in Table 6.2. As indicated, these criteria all seem applicable to the lower fluvial part of the Formation, where present.

Characteristics	Applicability
• Coarse sediments (Selley, 1982; Rust & Koster, 1984)	Yes
• A haphazard (random) vertical sequence of subfacies (Selley, 1982; Collinson, 1978)	Yes
• Unimodal palaeocurrents, with low variability (Collinson, 1978; Selley, 1982)	Yes
• Paucity of typical point bar structures and sequences (Miall, 1977)	Yes
• Large-scale trough cross-bedding very common (Rust & Koster, 1984)	Yes
• Small proportion of mudstone or shale in the vertical profile (Rust & Koster, 1984)	Yes

Table 6.2. Characteristics indicative of a braided stream deposit and their applicability to the lower part of the Black Reef Quartzite Formation.

6.2.3 *The upper quartzite-mudstone succession*

The characteristics of coastal deposits and their applicability to the upper part of the Black Reef Quartzite Formation are listed in Table 6.3. From the listed criteria it can be concluded that the upper part of the Black Reef Quartzite Formation was deposited in a tidal environment. The lack of occurrences of herringbone cross-bedding in the arenites of the Formation is not considered problematic, because this structure is typically developed only in cases where flood and ebb currents have the same competency. This situation is seldom found in tidal settings (Nio & Yang, 1991).

Characteristics	Applicability
• Alternation of bedload and suspension deposits (Reineck & Wunderlich, 1968; Walker, 1984; Klein, 1985)	Yes
• Very mature quartz arenites (Pettijohn ,et al. 1972, 1975; Klein, 1970)	Yes
• Oscillation ripple marks in quartz arenites (Miall, 1990)	Yes
• Flat-topped ripples with eroded crests (Tanner, 1958; Klein, 1971)	Yes
• Bi- and poli-modal palaeocurrent directions indicating tidal influence (Walker, 1984; Long, 1978, Davis, 1985, Selley, 1982)	Yes
• Shale (mudstone) as dominant sediment (Pettijohn, 1975)	Yes
• Well to very well-sorted sands (Davis, 1985)	Yes
• Herringbone cross-bedding indicating tidal influence (Boothroyd, 1985)	No
• Reactivation surfaces (Klein, 1985, Nio & Yang, 1991)	No
• Flat-topped ripple marks (Bates & Jackson, 1987)	Yes
• Mudlayers on foresets (Visser, 1980, Nio & Yang, 1991)	Yes

Table 6.3. Characteristics indicative of a coastal deposit and their applicability to the upper part of the Black Reef Quartzite Formation.

6.2.4 *Transition from terrestrial to coastal conditions of the Black Reef Quartzite Formation*

It has been proposed that the basal facies of the Black Reef Quartzite Formation is of fluvial origin. There can be no doubt that the overlying dolomites of the Malmani Subgroup formed in a shallow marine environment. This change of palaeo-environmental setting implies that a marine transgression had taken place. Shifts in the position of a shoreline depend on a combination of three factors:

(a) eustatic sea-level change

(b) vertical movement of the land

(c) rate of sedimentation (Clifton, et al., 1988).

It is impossible to confidently separate the possible effects of eustatic sea level change from the above-mentioned remaining factors, because no

detailed sea-level curve is available for the Late Archaean (Els & Mayer, 1992).

In vertical sequences estuarine deposits may mark transitions between fluvial and marine environments. Nichols & Biggs (1985) suggest that estuaries figure significantly in the sedimentary makeup of a coastal system, i.e. lagoon, bay, tidal inlet, tidal flat and marsh. It is difficult to distinguish estuarine deposits from other shallow marine deposits, because of their ephemeral character, their limited areal extent, and their lack of distinctive features (Schubel & Hirschberg, 1978). Regardless of the source of sediment supplied to an estuary, the axial sequence of lithofacies is: (a) estuarine fluvial, (b) estuarine, and (c) estuarine marine (Nichols & Biggs, 1985). According to the latter authors estuaries form transgressive sequences interfingering between fluvial and marine deposits. Such interfingering makes it difficult to identify specific estuarine deposits in the Black Reef Quartzite Formation, but it is feasible to accept that certain deposits in the Black Reef Quartzite Formation are of estuarine origin, especially in areas of unambiguous earlier fluvial activity.

The upper part of the Black Reef succession implies a tidal-flat origin. The very mature nature of the quartzites of the uppermost part of the Black Reef Quartzite Formation, coupled with the interbedded quartzite-mudstone units, the cross-bedded quartzites and the bimodal current distribution indicate a tidal flat environment during late stages of deposition of the Formation. Some of the mudstone deposits may indicate deposition in the supratidal zone or may be representative of the mud flat of the intertidal zone, or may even represent marsh deposits. The interbedded quartzite-mudstone units were also probably deposited in the intertidal zone on the mixed flat. The laminated and cross-bedded mature quartzites were probably deposited in the subtidal zone or the upper shoreface. The absence

of evidence for tidal channels suggests that such channels were possibly of minor importance as is the case in the present day Wash area (Evans, 1965). Another reason for this may be the absence of plant life on the banks of tidal channels; a situation resulting in shallow, very wide channels (Schumm, 1968).

Because of the low preservation potential of a barrier system (Oost, 1995), this sedimentary environment was not considered, but it is not completely excluded as a possible integral part of the sedimentary make-up of the Black Reef Quartzite Formation.

6.3 The transgression - some considerations

Bates & Jackson (1987) define a transgression as "the spread or extension of the sea over land areas, and the consequent evidence of such advance (such as strata deposited unconformably on older rocks, especially where the new marine deposits are spread far and wide over the former land surface)." Posamentier & James (1993) stress that a relative sea-level rise does not necessarily imply a transgression, because the direction of shoreline movement is a function of the balance between sediment flux and space available for sediment to fill. Applying the definition of Bates & Jackson (1987) to the Black Reef Quartzite Formation and the dolomites of the Malmani Subgroup, which conformably overlie the Formation, there is sufficient evidence of a marine transgression. The shales in the Black Reef Quartzite Formation provides further evidence of a transgression. Hallam & Bradshaw (1979) proposed that black shales (bituminous shales) tend to occur near the base of transgressive sequences.

Transgressive shoreline deposits generally have a low preservation potential Wood *et al.* (1993). Els & Mayer (1992) suggested that preservation of shoreline deposits in the Turffontein Subgroup is probably due to the

abundant sediment supply to pre-Devonian shorelines. However, the low clastic input during the precipitation of the dolomites of the Malmani Subgroup implies that the sediment supply to the Black Reef Quartzite Formation decreased considerably during the later stages of Black Reef sedimentation, probably because of a rise in base level (Posamentier & James, 1993). In conclusion, the reason for the preservation of the Black Reef deposits is uncertain.

Another important question concerns the rate of transgression. Was this a rapid, or prolonged process? This is a difficult question to answer with the currently available information on the Black Reef Quartzite Formation. Wood *et al.* (1993) reason that during a slow transgression sediments have a longer period to accumulate resulting in thicker deposits, but they also stress that these deposits have a low preservation potential. However, during a rapid transgression thinner deposits are formed, with a better preservation potential. From this reasoning it can be assumed that the Black Reef transgression was a relatively rapid one.

It is not possible to infer the general palaeoslope of the depositional surface from the palaeocurrent data. However, Eriksson & Truswell (1974) proposed that the transgression was a south-west to north-west invasion of land by sea.

Eriksson (1972) who studied cyclic sedimentation in the dolomites of the Black Reef Quartzite Formation and the Malmani Subgroup is of opinion that this succession represents a continuous transgressive cycle up to the columnar stromatolites of the Malmani Subgroup. Above the columnar stromatolite zone, the sequence is representative of a regressive cycle.

6.4 Tectonic and depositional model

A broader perspective is necessary to answer questions about the nature of Black Reef deposition in space and time. Selley (1982) states that: "sedimentation needs subsidence". According to Miall (1990) the most important result of basin analysis is the documentation of the subsidence history and palaeogeographic evolution of a sedimentary basin.

Clendenin *et al.* (1988) propose a simple three-stage divergent rift system model for the evolution of the Kaapvaal Craton; a pre-graben proto-basin, a graben basin, and a post-graben thermal subsidence basin. According to this tectonic model deposition of the Black Reef Quartzite Formation was preceded by active graben development during Ventersdorp times. The Black Reef Quartzite Formation was deposited in a post-graben thermal subsidence basin, which is marked by the overstepping of older tectonic margins. During this stage, tectonic re-adjustment took place. Button & Tyler (1981) proposed that, preceding this period, a tectonic quiescence prevailed during which the palaeosurface was extensively weathered and the landscape essentially peneplaned. According to Clendenin *et al.* (1988) the expanding development of the proposed thermal subsidence basin led to the opening of a shallow epeiric sea. Van den Berg (1994) proposed that continued lithospheric stretching resulted in the creation of a linear sea.

Sedimentation of the Black Reef Quartzite Formation commenced with clastic deposition in a number of sub-basins; probably in the form of eroded remains of graben structures. Sedimentation processes were initially characterised by braided streams on an uneven palaeosurface with some palaeohighs. Locally the Rand Anticline, or certain parts thereof, and possibly the palaeo-drainage divide proposed by Van den Berg (1994),

represented a palaeohigh. The massive sedimentary breccia facies found indicates prominent relief at localities along the Rand Anticline.

Continued overall subsidence of the Transvaal basin resulted in the flooding of the entire basin, resulting in the formation of an epeiric sea.

References

Allen, P.A. & Allen, J.R. (1990). *Basin Analysis: Principles and Applications*. Blackwell Scientific Publications, Oxford, 451pp.

Antrobus, E.S.A., Brink, W.C.J., Caulkin, M.C., Hutchison, R.I., Thomas, D.E., Van Graan, J.A. & Viljoen, J.J. (1986). The Klerksdorp Goldfield. In: Anhaeusser, C.R. & Maske, S. (Eds.). *Mineral Deposits of Southern Africa, 1*. Geol. Soc. S. Afr., Johannesburg, 549 - 598.

Bates, R.L. & Jackson, J.A. (1987). *Glossary of Geology, 3rd Edition*. American Geological Institute, Alexandria, 788 pp.

Beukes, N.J. (1976). Transition from siliciclastic to carbonate sedimentation near the base of the Transvaal Supergroup, Northern Cape Province, South Africa. *Sedim. Geol.*, **18**, 201-221.

Beukes, N.J. (1986). *Introduction to Sedimentology of Precambrian Carbonates. Short Course notes*. Rand Afrikaans University, Johannesburg, 199 pp.

Blair, T.C. & McPherson, J.G. (1994). Alluvial fans and their natural distinction from rivers based on morphology, hydraulic processes, sedimentary processes, and facies assemblages. *Journal of Sedimentary Research*, **A64 (3)**, 450-489.

Boersma, J.R. (1970). *Distinguishing Features of Wave-ripple Cross-stratification and Morphology*. Unpubl. Ph.D. Thesis, University of Utrecht, 65 pp.

Body, J.L.F.E. (1988). *The Black Reef on the Witwatersrand and adjacent areas: its mining history, geology and economic potential*. Gold Fields of South Africa, Unpubl. Int. Rep., 41 pp.

Bridge, J.S. (1993). Description and interpretation of fluvial deposits: a critical perspective. *Sedimentology*, **40**, 801-810.

Button, A. (1972a). The stratigraphic history of the Malmani Dolomite in the Eastern and Notheastern Transvaal. *Inform. Circ. Econ. Geol. Res. Unit*, Univ. Witwatersrand, Johannesburg. **73**, 23 pp.

Button, A. (1972b). The depositional history of the Wolkberg Proto-basin, Transvaal. *Inform. Circ. Econ. Geol. Res. Unit*, Univ. Witwatersrand, Johannesburg, **71**, 17 pp.

Button, A. & Tyler, N. (1981). The character and economic significance of Precambrian Paleoweathering and Erosion surfaces in Southern Africa. *Econ. Geol.*, **75th Ann. Vol.**, 179-213.

Clendenin, C.W. & Charlesworth, E.G. (1990). Depositional facies of the Black Reef Quartzite Formation in the eastern Transvaal. *Geocongress '90 Abstracts*, 230-233.

Clendenin, C.W., Charlesworth, E.G. & Maske, S. (1988). An early Proterozoic three-stage rift system, Kaapvaal Craton, South Africa. *Tectonophysics*, **145**, 73-86.

Clendenin, C.W., Henry, G. & Charlesworth, E.G. (1989). Characteristics of and influences on the Black Reef Quartzite stratigraphic package in the Eastern Transvaal. *Inform. Circ. Econ. Geol. Res. Unit*, Univ. Witwatersrand, Johannesburg. **214**, 12 pp.

Clendenin, C.W., Henry, G. & Charlesworth, E.G. (1991). Chracteristics of and influences on the Black Reef depositional sequence in the Eastern Transvaal. *S. Afr. J. Geol.* **94**, 321-327.

Clifton, H.E. & Gardner, J.V. (1988). Analysis of eustatic, tectonic, and sedimentological influences on transgressive and regressive cycles in the Upper Cenozoic Merced Formation, San Francisco, California. In: Kleinspehn, K.L. & Paola, C. (Eds.) *New Perspectives in Basin Analysis*, Springer-Verlag, New York, 109-128.

Collinson, J.D. (1978). Alluvial sediments. In: Reading, H.G. (Ed.). *Envronments and Facies.* Elsevier, New York, 15-60.

Collinson, J.D. & Thompson, D.B. (1982). *Sedimentary Structures*. George Allen & Unwin, London, 194 pp.

Davis, J.C. (1973). *Statistics and Data Analysis in Geology*. John Wiley and Sons, Inc., New York, 550pp.

Davis, R.A. (Jr.) (1985). Beach and nearshore zone. In: Davis, R.A. (Jr.) (Ed.). *Coastal Sedimentary Environments, Second Edition.* Springer-Verlag, New York, 379-444.

De Kock, W.P. (1964). The geology and economic importance of the West Wits Line, 328-386. In: Haughton, S.H. (Ed.) *The geology of some ore deposits in Southern Africa, I.* Geol Soc. S. Afr., Johannesburg, 625 pp.

Dorfel, D. (1904). The Kromdraai Quartz Reef and its geological association. *Trans. geol. Soc. S. Afr.*, **6**, 101-103.

Els, B.G. & Mayer, J.J. (1992). Transgressive and progradational beach and nearshore facies in the Late Archaean Turffontein Subgroup of the Witwatersrand Supergroup, Vredefort area, South Africa. *S. Afr. J. Geol.*, **95**, 60-73.

Els, B.G., Van den Berg, W.A. & Mayer, J.J. (1995). The Black Reef Quartzite Formation in the Western Transvaal: sedimentological and economic aspects, and significance for basin evolution. *Mineral. Deposita*, **30**, 112-123.

Engelbrecht, C.J., Baumbach, G.W.S., Matthysen, J.L. & Fletcher, P. (1986). The West Wits Line. In: Anhaeusser, C.R. & Maske, S. (Eds.). *Mineral Deposits of Southern Africa.* Geol. Soc. S. Afr., Johannesburg, 599-648.

Eriksson, K.A. (1972). Cyclic sedimentation in the Malmani Dolomite, Potchefstroom Synclinorium. *Trans. geol. Soc. S. Afr.*, **75**, 85-97.

Eriksson, K.A. & Truswell, J.F. (1974). Stratotypes from the Malmani Subgroup north-west of Johannesburg, South Africa. *Trans. geol. Soc. S. Afr.*, **77**, 211-222.

Ethridge, F.G. & Westcott, W.A. (1984). Tectonic setting, recognition and hydrocarbon reservoir potential of fan delta deposits. In: Koster, E.H. & Steel, R.J. (Eds.). *Sedimentology of Gravels and Conglomerates*. Mem. Can. Soc. Petrol. Geol., **10**, 217-235.

Evans, G. (1965). Intertidal flat sediments and their environments of deposition in the Wash. *Q. J. Geol. Soc. London*, **121**, 209-245.

Frankel, J.J. (1940a). Notes on some minerals in the Black Reef Series. *Trans. geol. Soc. S. Afr.*, **43**, 1-9.

Frankel, J.J. (1940b). Observations on the mineralogy and treatment of auriferous rocks of the Black Reef Series from the New Machavie Mine. *Journal of the Chemical and Metallurgical and Mining Society of South Africa*, **XL (3)**, 321-322.

Frey, M. & Germs, G.J.B. (1986). Some sedimentological observations on the conglomerates of the Black Reef Formation, Transvaal Supergroup, South Africa. *Geocongress '86 Extended Abstracts*, 993-995.

Friedman, G.M. (1967). Dynamic processes and statistical parameters compared for size frequency distribution of beach and river sands. *J. Sedim. Petrol.*, **37**, 327-354.

Friend, P.F. (1978). Distinctive Features of some ancient river systems. In: Miall, A.D. (Ed.) *Fluvial Sedimentology*. Mem. Can. Soc. Petrol. Geol., **5**, 531-542.

Fuller, O.A. (1985). A contribution to the conceptual modeling of pre-Devonian fluvial systems. Pres. Address. Geocongress '84. *Trans. geol. S. Afr.*, **88 (1)**, 189-194.

Galehouse, J.S. (1971). Point counting. In: Carver, R.E. (Ed.) *Procedures in sedimentary petrology*. Wiley-Interscience, New York, 385-407.

Hallam, A. (1981). *Facies Interpretation and the Stratigraphic Record*. W.H. Freeman and Company, Oxford, 291 pp.

Hallam, A. & Bradshaw, M.J. (1979). Bituminous shales and oolitic sandstones as indicators of transgressions and regressions. *J. Geol. Soc. Lond.*, **136**, 157-164.

Hamilton, J. (1977). Sr isotope and trace element studies of the Great Dyke and Bushveld mafic phase and their relation to early Proterozoic magma genesis in South Africa. *J. Petrol.*, **18**, 24-52.

Harms, J.C., Southard, J.B., Spearing, D.R. & Walker, R.G. (1975). *Depositional environments as interpreted from primary sedimentary structures and stratigraphic sequences, Lecture notes for Short Course No. 2*. Soc. Econ. Paleont. Miner., Dallas, 161pp.

Harrel, J.A. & Erikson, K.A. (1979). Empirical conversions for thin section and sieve derived size distribution parameters. *J. Sedim. Petrol.*, **49**, 273-280.

Henning, L.T. (1992). *The palaeotopography of the Ventersdorp Contact Reef at Western Deep Levels South Gold Mine, Carletonville, R.S.A.*. Unpubl. M.Sc. Thesis, Potchefstroom University for Christian Higher Education, 143 pp.

Johnson, H.D. (1978). Shallow Siliciclastic Seas. In: Reading, H.G. (Ed.), *Sedimentary Environments and Facies*. Elsevier, New York, 207-257.

Johnson, M.R. (1994). Thin section grain-size analysis revisited. *Sedimentology*, **41**, 985-999.

Klein, G. de V. (1970). Depositional and dispersal dynamics of intertidal sand bars. *J. Sedim. Petrol.* **40**, 1095-1127.

Klein, G. de V. (1971). A sedimentary model for determining paleotidal range. *Geol. Soc. Am. Bull.*, **82**, 2585-2592.

Klein, G. de V. (1985). Intertidal flats and intertidal sand bodies. In: Davis, R.A. (Jr.) (Ed.). *Coastal Sedimentary Environments, Second Edition.* Springer-Verlag, New York, 187-224.

Krumbein, W.C. (1941). Measurements and geological significance of shape and roundness of sedimentary particles. *J. Sedim. Petrol.*, **11**, 64-72.

Liebenberg, W.R. (1955). The occurrence and origin of gold and radioactive minerals in the Witwatersrand System, the Dominium Reef and the Black Reef. *Trans. geol. Soc. S. Afr.*, **58**, 101-223.

Long, D.G.F. (1978). Proterozoic stream deposits: some problems of recognition and interpretation of ancient sandy fluvial systems. In: Miall, A.D. (Ed.). *Fluvial Sedimentology*. Can Soc. Petrol. Geol. Mem., **5**, 313-342.

Miall, A.D. (1973). Markov chain analysis applied to an ancient alluvial plain succession. *Sedimentology*, **20**, 347-364.

Miall, A.D. (1974). Paleocurrent analysis of alluvial sediments: A discussion of directional variance and vector magnitude. *J. Sedim. Petrol.*, **44**, 459-483.

Miall, A.D. (1977). A review of the braided-river depositional environment. *Earth. Sci. Rev.*, **13**, 1-62.

Miall, A.D. (1990). *Principles of Sedimentary Basin Analysis, Second Edition*. Springer-Verlag, New York, 668pp.

Miall, A.D. (1992). Alluvial Deposits. In: Walker, R.G. & James, N.P. (Eds.). *Facies Models: Response to Sea-level Change*. Geol. Ass. Can., 119-142.

McManus, J. (1988). Grain-size determination and interpretation. In: Tucker, M. (Ed.). *Techniques in Sedimentology*. Blackwell Scientific Publications, Oxford, 394 pp.

Middleton, G.V. (1976). Hydraulic interpretation of sand-size distribution. *J. Geol.*. **84**, 405-426.

Moore, R.C. (1949). Meaning of facies. *Geol. Soc. of Am., Memoir 39*, 1-34.

Moss, A.J. (1962) The physical nature of common sandy and pebbly deposits, Part 1. *Am. Jour. Sci.*, **260**, 337-373.

Nel, L.T. (1935). *The Geology of the Klerksdorp - Ventersdorp Area.* Explan. Of Geological Map No. 9., Govt. Printer, Pretoria, 130 pp.

Nemec, W. & Steel, R.J. (1984). Alluvial and coastal conglomerates: their significant features and some comments on gravelly mass-flow deposits. In: Koster, E.H. & Steel, R.J. (Eds.). *Sedimentology of Gravels and Conglomerates*. Mem. Can. Soc. Petrol. Geol., **10**, 1-31.

Nichols, M.M. & Biggs, R.B. (1985). Estuaries. In: Davis, R.A. (Jr.) (Ed.). *Coastal Sedimentary Environments, Second Edition*. Springer-Verlag, New York, 77-186.

Nio, S.D. & Yang, C. (1991). Diagnostic attributes of clastic tidal deposits: a review. In: Smith, D.G., Reinson, G.E., Zaitlin, B.A. & Rahmani, R.A. (Eds.). *Clastic Tidal Sedimentology*. Mem. Can. Soc. Petrol. Geol., **16**, ix - xv.

Oost, A.P. (1995). Sedimentological implications of morphodynamic changes in the ebb-tidal delta, the inlet and the drainage basin of the Zoutkamperlaag tidal inlet (Dutch-Wadden Sea), induced by a sudden decrease in the tidal prism. In: Flemming, B.W. & Bartholomä, A. (Eds.). *Tidal Signatures in Modern and Ancient Sediments*. Spec. Publ. int. Ass. Sediment., **24**, 101-120.

Papenfus, J.A. (1964). The Black Reef Series within the Witwatersrand Basin, with special reference to its occurence at Government Gold Mining areas. In: Haughton, S.H., (Ed.). *The geology of some ore deposits in Southern Africa.* Geol. Soc. S. Afr., Johannesburg, 191-218.

Pettijohn, F.J. (1975). *Sedimentary Rocks, Third Edition*. Harper & Row Publishers, New York, 628 pp.

Pettijohn, F.J., Potter, P.E. & Siever, R. (1972). *Sand and Sandstone*. Springer-Verlag, New York, 618 pp.

Posamentier, H.W. & James, D.P. (1993). An overview of sequence-stratigraphic concepts: uses and abuses. In: Posamentier, H.W., Summerhayes, C.P., Haq, B.U. & Allen, G.P. (Eds.). *Sequence Stratigraphy and Facies Associations.* Spec. Publ. int. Ass. Sediment., 18, 3-19.

Pouroulis, S. & Austin, M.A. (1989). The Geology of the Black Reef at North East Prospect Shaft Consolidated Modderfontein Mines (1979) Limited. In: (Uned.) *Other Reefs Symposium*, 99-104.

Pretorius, D.A. (1986). The goldfields of the Witwatersrand basin. In: Anhausser, C.R. Maske, S. (Eds.). *Mineral Deposits of Southern Africa, I.* Geol. Soc. S. Afr., Johannesburg, 489-494.

Reineck, H.E. & Singh, I.B. (1980). *Depositional Sedimentary Environments, Second Edition.* Springer-Verlag, Berlin, 549 pp.

Reineck, H.E. & Wunderlich, F. (1968). Classification and origin of flaser and lenticular bedding. *Sedimentology*, **11**, 99-104.

Rust, B.R. & Koster, E.H. (1984). Coarse alluvial deposits. In: Walker, R.G. (Ed.). *Facies Models, Second Edition*. Geol. Ass. Can., Newfoundland, 53-77.

(South African Committee for Stratigraphy) SACS (1980). Stratigraphy of South Africa. Part 1. (Comp. L.E. Kent). Lithostratigraphy of the Republic of South Africa, South West Africa/Namibia and the Republics of Bophuthatswana, Transkei and Venda. Hand. *Geol. Surv. S. Afr.*, **8**, 690 pp.

Schubel, J.R. & Hirschberg, D.J. (1978). Estuarine graveyards, climatic change, and the importance of the estuarine environment. In: Wiley, M.L. (Ed.). *Estuarine Interactions*. Academic Press, New York, 285-303.

Schumm, S.A. (1968). Speculations concerning paleohydraulic controls of terrestrial sedimentation. *Geol. Soc. Am. Bull.*, **79**, 1573-1588.

Selley, R.C. (1982). *An Introduction to Sedimentology*. Academic Press, London, 417 pp.

Shaw, M.B. (1994). Geology and evaluation of Black Reef open- cast mining at Lindum Reefs Gold Mine: A case study. *XVth CMMI Congress*, SAIMM, Johannesburg. **3**, 85-94.

Sneed, E.D. & Folk, R.L. (1958). Pebbles in the lower Colorado River, Texas - a study in partical morphogenesis. *Jour. Geol.*, **66**, 144-150.

Stonestreet, C.D. (1898). Notes on the Black Reef at Natal Spruit. *Trans. geol. Soc. S. Afr.*, **2**, 53-55.

Swiegers, J.U. (1938). A study of the Black Reef Series in the Klerksdorp and Randfontein areas. *Trans. geol. Soc. S. Afr.*, **41**, 177-191.

Swiegers, J.U. (1939). Gold, carbon, pyrite and other sulphides in the Black Reef. *Trans. geol. Soc. S. Afr.*, **42**, 35-45.

Tankard, A.J., Jackson, M.P.A., Eriksson, K.A., Hobday, D.K., Hunter, D.R. & Minter, W.E.L. (1982). *Crustal Evolution of Southern Africa - 3.8 Billion Years of Earth History*. Springer-Verlag, New York, 523 pp.

Tanner, W.F. (1958). An occurrence of flat-topped ripple marks. *J. Sedim. Pet.*, **28**, 95-96.

Tanner, W.F. (1967). Ripple mark indices and their uses. *Sedimentology*, **9**, 89-104.

Tucker, R.F. & Viljoen, R.P. (1986). The geology of the West Rand Goldfield, with special reference to the Southern limb. In: Anhaeusser, C.R. & Maske, S. (Eds.). *Mineral Deposits of Southern Africa*. Geol. Soc. S. Afr., **1**, 649-688.

Tyler, N. (1979). Depositional sedimentary environments within the Black Reef Quartzite of the West Central Transvaal. *Inform. Circ. Econ. Geol. Res. Unit*, Univ. Witwatersrand, Johannesburg, **132**, 11 pp.

Van den Berg, W.A. (1994). *The Stratigraphy and Sedimentology of the Black Reef Quartzite Formation, Transvaal Sequence, in the Klerksdorp, Potchefstroom and Ventersdorp Districts.* Unpubl. M.Sc. Thesis, Potchefstroom University for Christian Higher Education, 131 pp.

Van Niekerk, C.B. & Burger, A.J. (1978). A new age for the Ventersdorp acidic lavas. *Trans. geol. Soc. S. Afr.*, **82**, 155-163.

Vermaakt, D.T. & Chunnett, I.E. (1994). Tectono-sedimentary processes which controlled the deposition of the Ventersdorp Contact Reef within the West Wits Line. *XVth. CMMI Congress*, SAIMM, **3**, 117-130.

Visher, G.S. (1965). Use of vertical profile in environmental reconstruction. *Amer. Assoc. Petrol. Geol.*, **49**, 41-61.

Visher, G.S. (1972). *Physical characteristics of fluvial deposits.* Soc. Econ. Paleont. Miner., Special Publication **16**, 84-97.

Visser, J.N.J. & Grobler, N.J. (1972). The transition beds at the base of the Dolomite Series in the Northern Cape Province. *Trans. geol. Soc. S. Afr.*, **75**, 265-274.

Visser, M.J. (1980). Neap spring cycles reflected in Holocene subtidal large-scale bedform deposits: a preliminary note. *Geology*, **8**, 543-546.

Visser, W.J. (1989). *Sedimentologiese Ondersoek van die Swartrif Kwartsiet Formasie in die Verre-Wes Rand.* Gold Fields of South Africa, Unpub. Int. Rep., 29 pp.

Walker, R.G. (1984). Shelf and shallow marine sands. In: Walker, R.G. (Ed.). *Facies Models, Second Edition.* Geoscience Canada, Newfoundland, 141-170.

Winter, H. de la R. (1987). A cratonic foreland model for Witwatersrand Basin development in a continental back-arc, plate-tectonic setting. *S. Afr. J. Geol.*, **90(4)**, 409-427.

Wood, L.J., Ethridge, F.G. & Schumm, S.A. (1993). The effects of rate of base-level fluctuation on coastal-plain, shelf and slope depositional systems: an experimental approach. In: Posamentier, H.W., Summerhayes, C.P., Haq, B.U. & Allen, G.P. (Eds.). *Sequence Stratigraphy and Facies Associations.* Spec. Publ. int. Ass. Sediment., **18**, 43-55.

Acknowledgements

I would like to thank the following:

My promoter, Dr. B.G. Els, and co-promoter, Dr. J.J. Mayer, for their guidance.

The Management of Gold Fields of South Africa for their financial support and permission to use the information.

My family and friends for their sustained encouragement and interest.

The Lord Almighty for the strength and perseverance to bring this project to its conclusion.

Appendix 1

Sedimentological profiles

Sedimentary profiles recorded from surface borehole cores

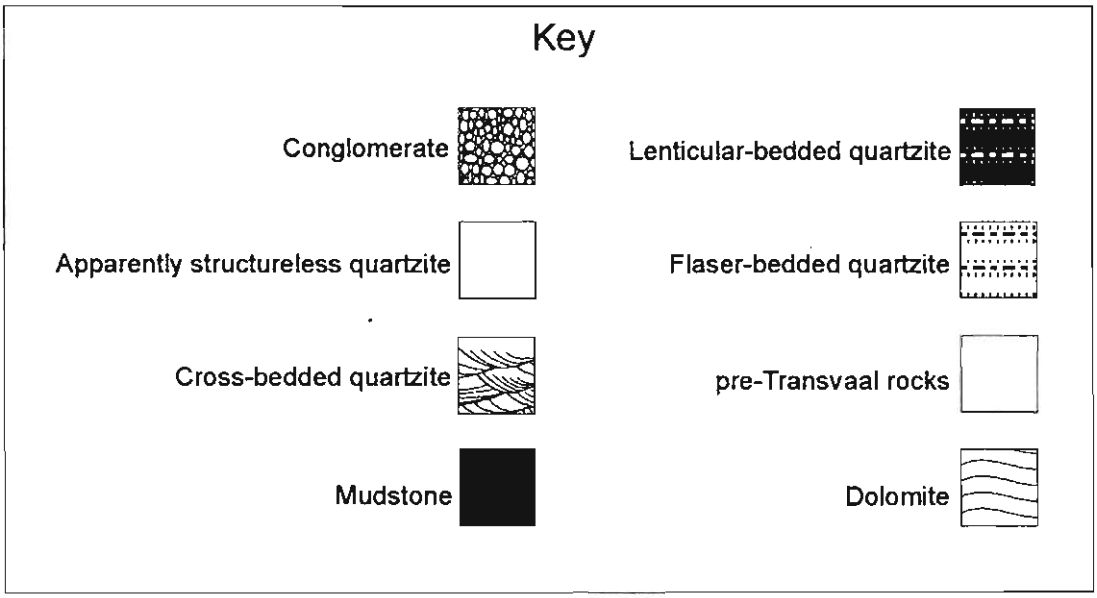

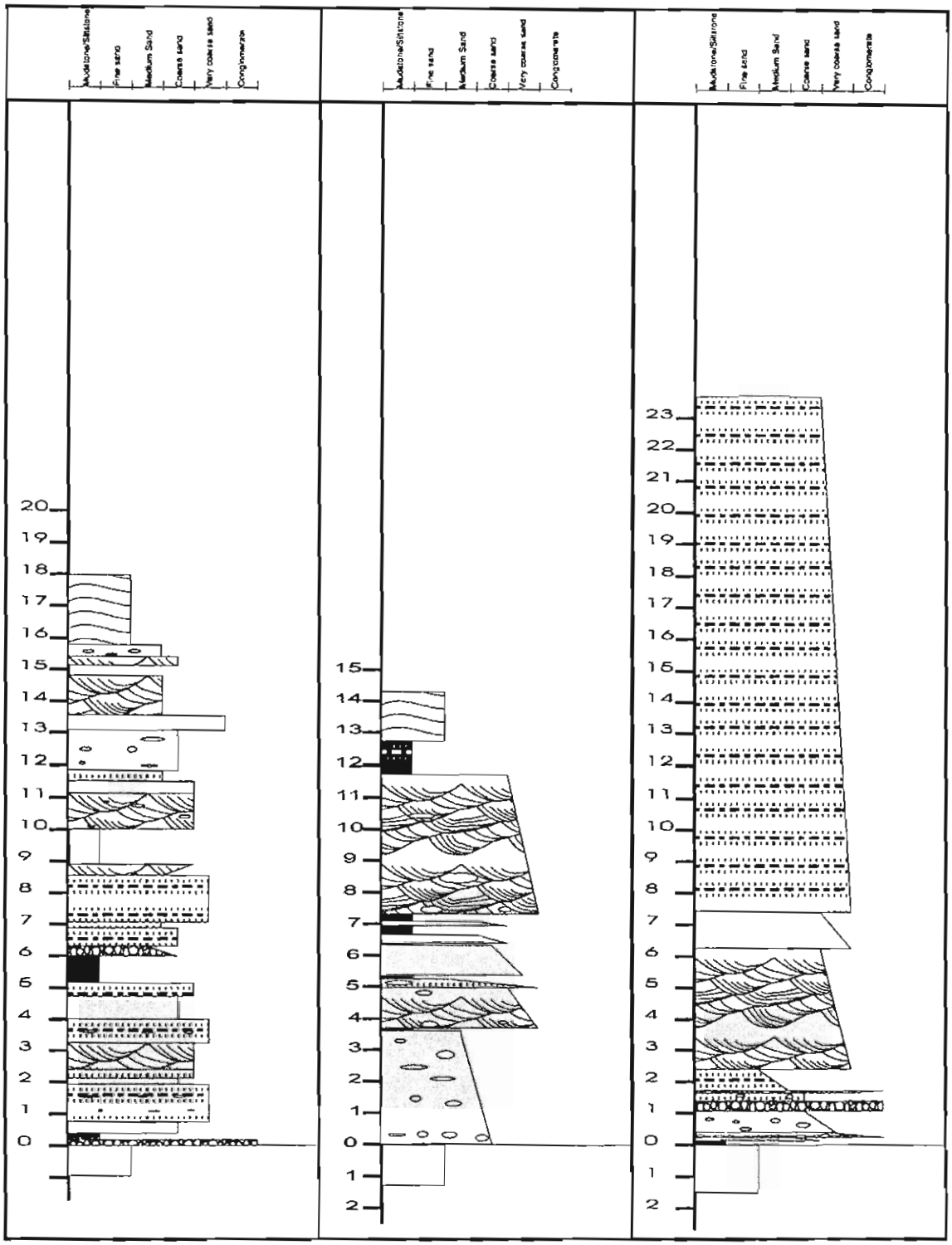

BEL3		BL2		BL4	
Depth of bottom contact = 191.43		Depth of bottom contact = 460.70		Depth of bottom contact = 30.80	
Borehole Position		Borehole Position		Borehole Position	
X = 2904967.8	Y = -49735.5	X = 2911086.57	Y = -53568.9	X = 2907352.1	Y = -56609.1

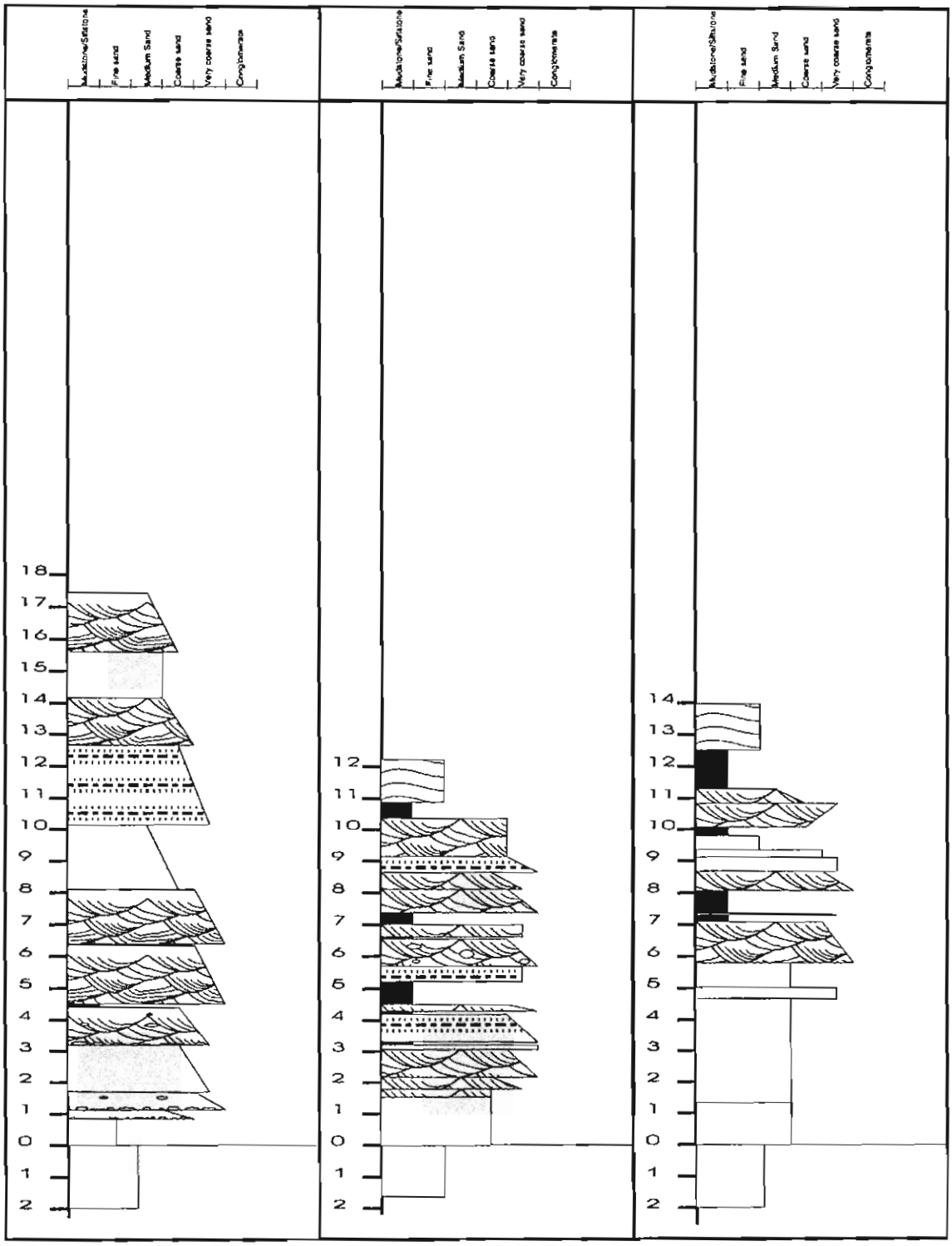

BL7		BL8		BL9	
Depth of bottom contact = 30.30 m		Depth of bottom contact = 405.02 m		Depth of bottom contact = 551.65 m	
Borehole Position		Borehole Position		Borehole Position	
X = 2907414.9	Y = -56710.6	X = 2911233.38	Y = -54265.3	X = 2912218.3	Y = -52884.4

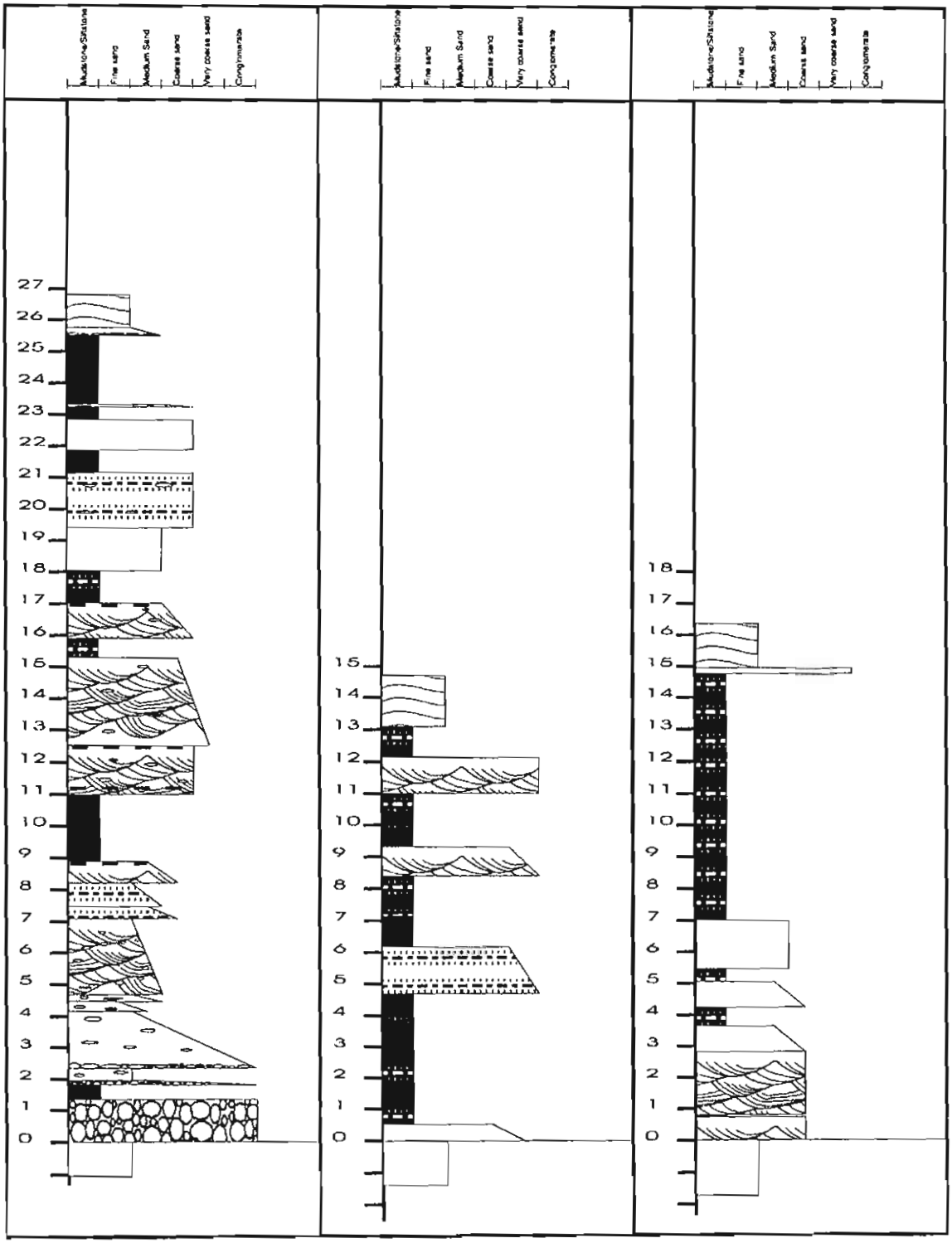

BW1	GE25	N4
Depth of bottom contact = 414.89 m	Depth of bottom contact = 490.00 m	Depth of bottom contact = 581.77 m
Borehole Position	Borehole Position	Borehole Position
X = 2921157.6 Y = -21508.9	X = 2911112.56 Y = -81183.8	X = 2901816.5 Y = -18886.4

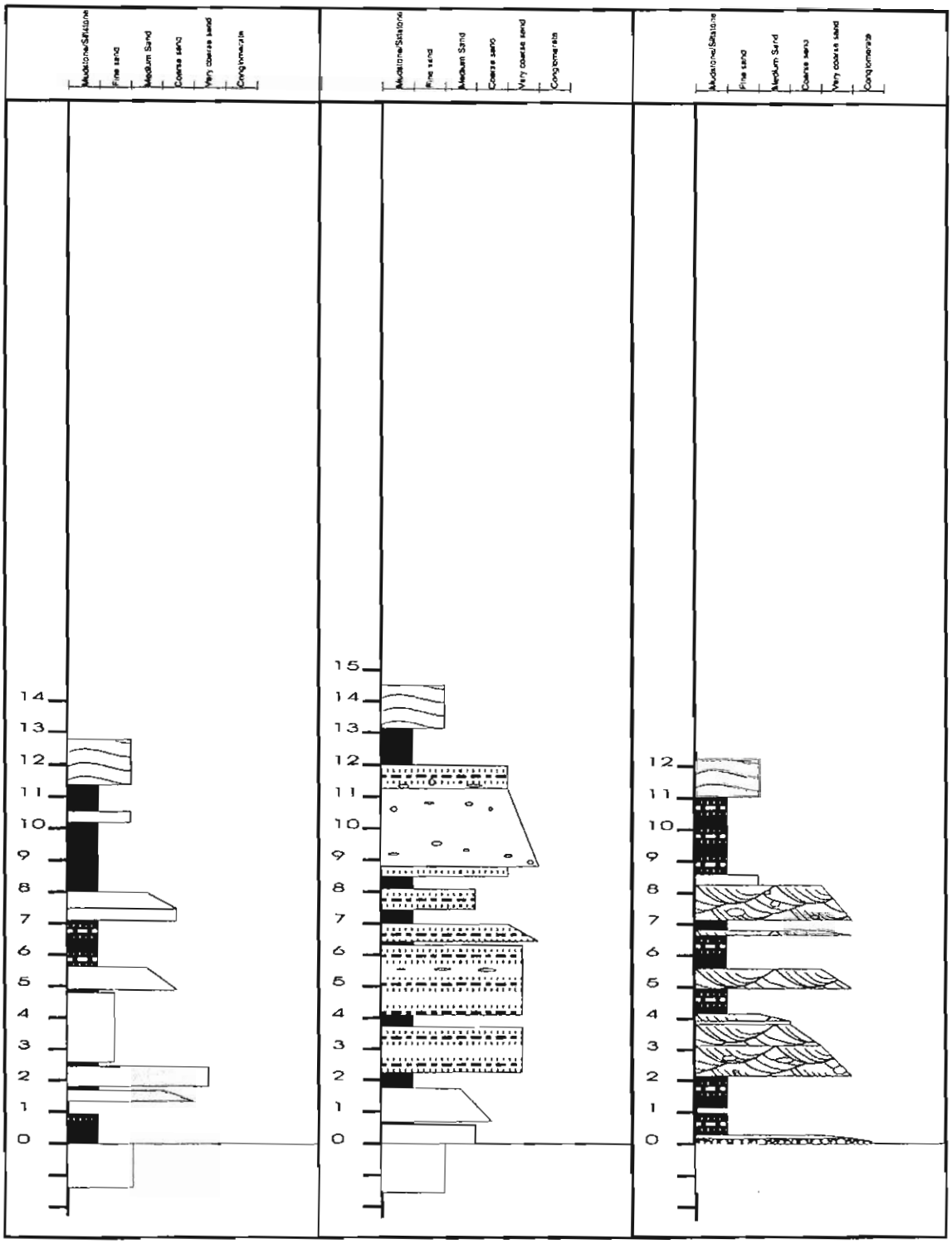

RK3		RT1		WBL1	
Depth of bottom contact = 134.5 m		Depth of bottom contact = 335.15 m		Depth of bottom contact = 224.78 m	
Borehole Position		Borehole Position		Borehole Position	
X = 2948286.6	Y = -10117.4	X = 2910879.32	Y = - 421323	X =2935085.5	Y = -1374.6

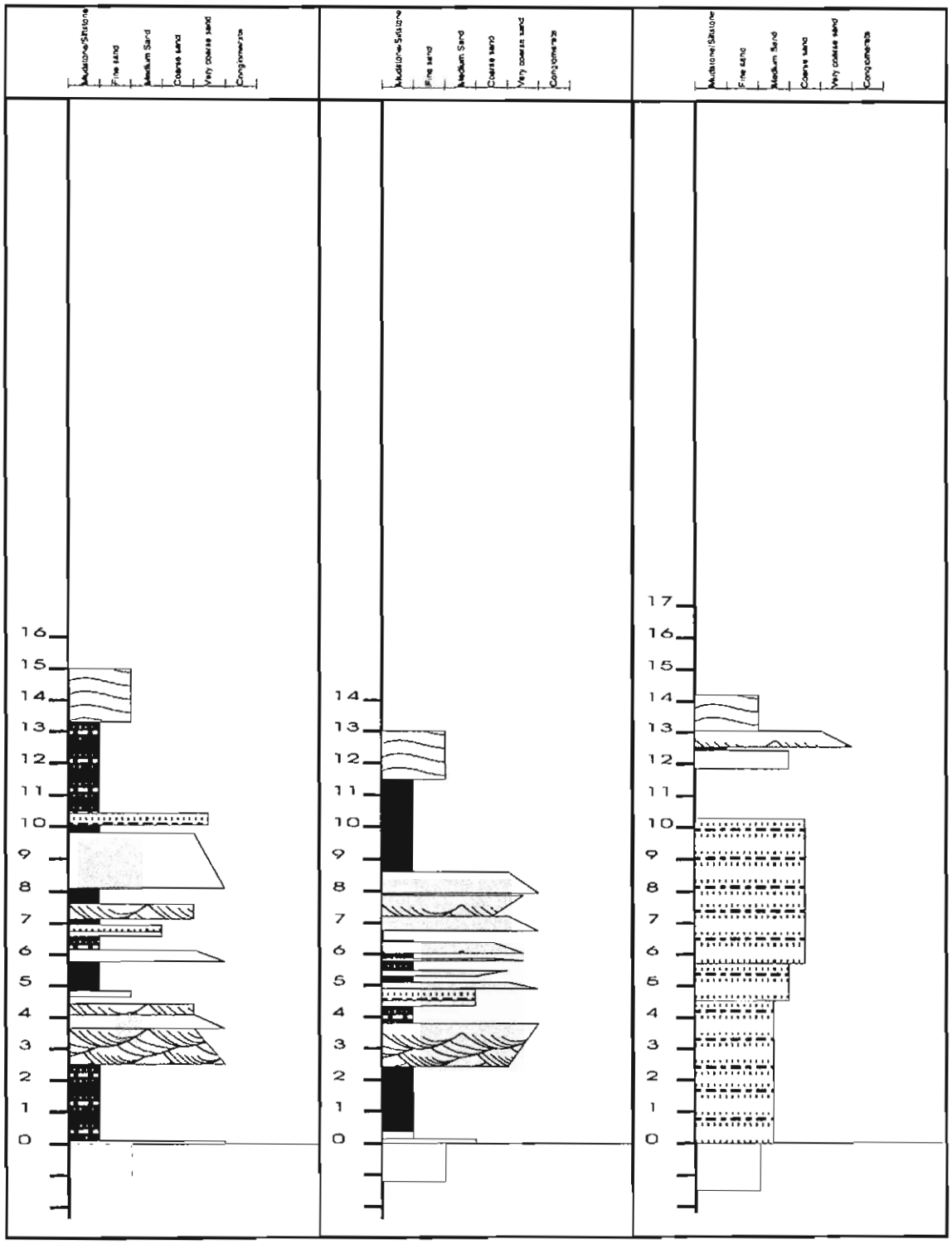

WBL3		WBL4		WFN9	
Depth of bottom contact = 207.82 m		Depth of bottom contact = 128.36 m		Depth of bottom contact = 257.96 m	
Borehole Position		Borehole Position		Borehole Position	
X = 2934953.7	Y = -639.1	X = 2935380.2	Y = -293.4	X = 2909892.2	Y = 50050.8

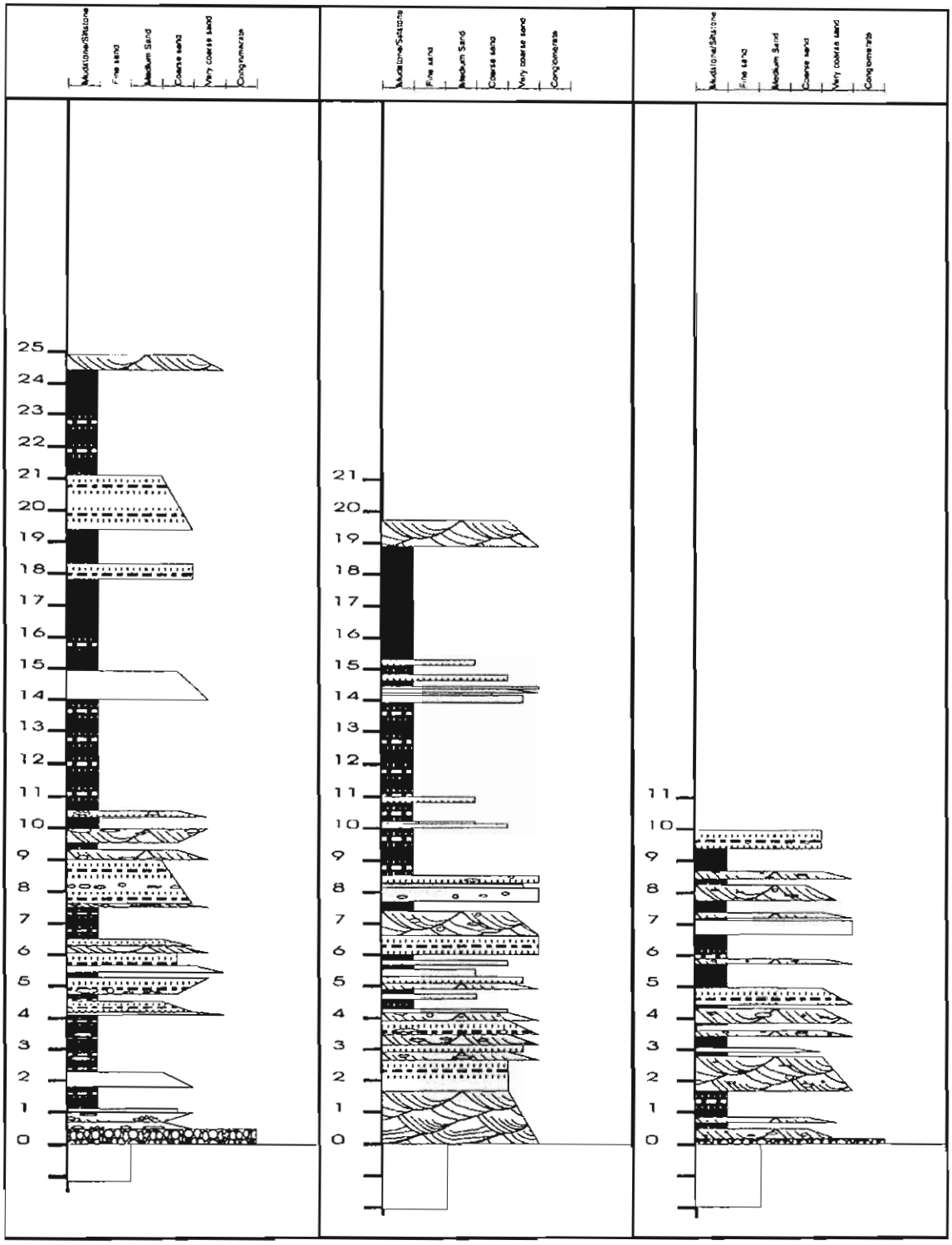

MN1		MN6a		MN13	
Depth of bottom contact = 25.89 m		Depth of bottom contact = 28.21 m		Depth of bottom contact = 19.99 m	
Borehole Position		Borehole Position		Borehole Position	
X = 2900774.28	Y = -87257.22	X = 2900714.04	Y = -87086.59	X = 2900628.42	Y = -86798.8

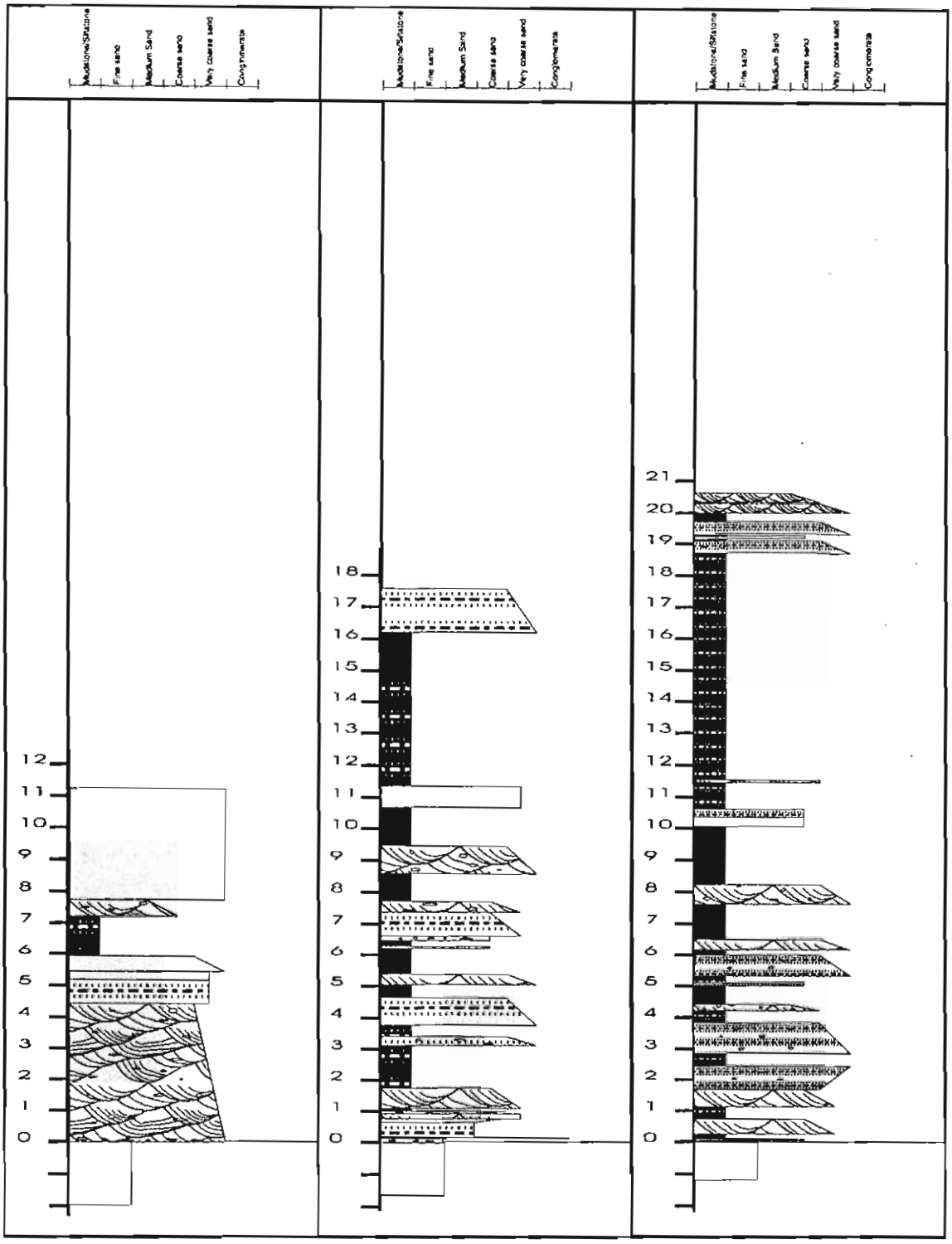

MN24		MN39		MN44	
Depth of bottom contact = 11.24 m		Depth of bottom contact = 38.82 m		Depth of bottom contact = 35.48 m	
Borehole Position		Borehole Position		Borehole Position	
X = 2900495.18	Y = -66376.0	X = 2901531.55	Y = -66877.5	X = 2901397.3	Y = -66730.319

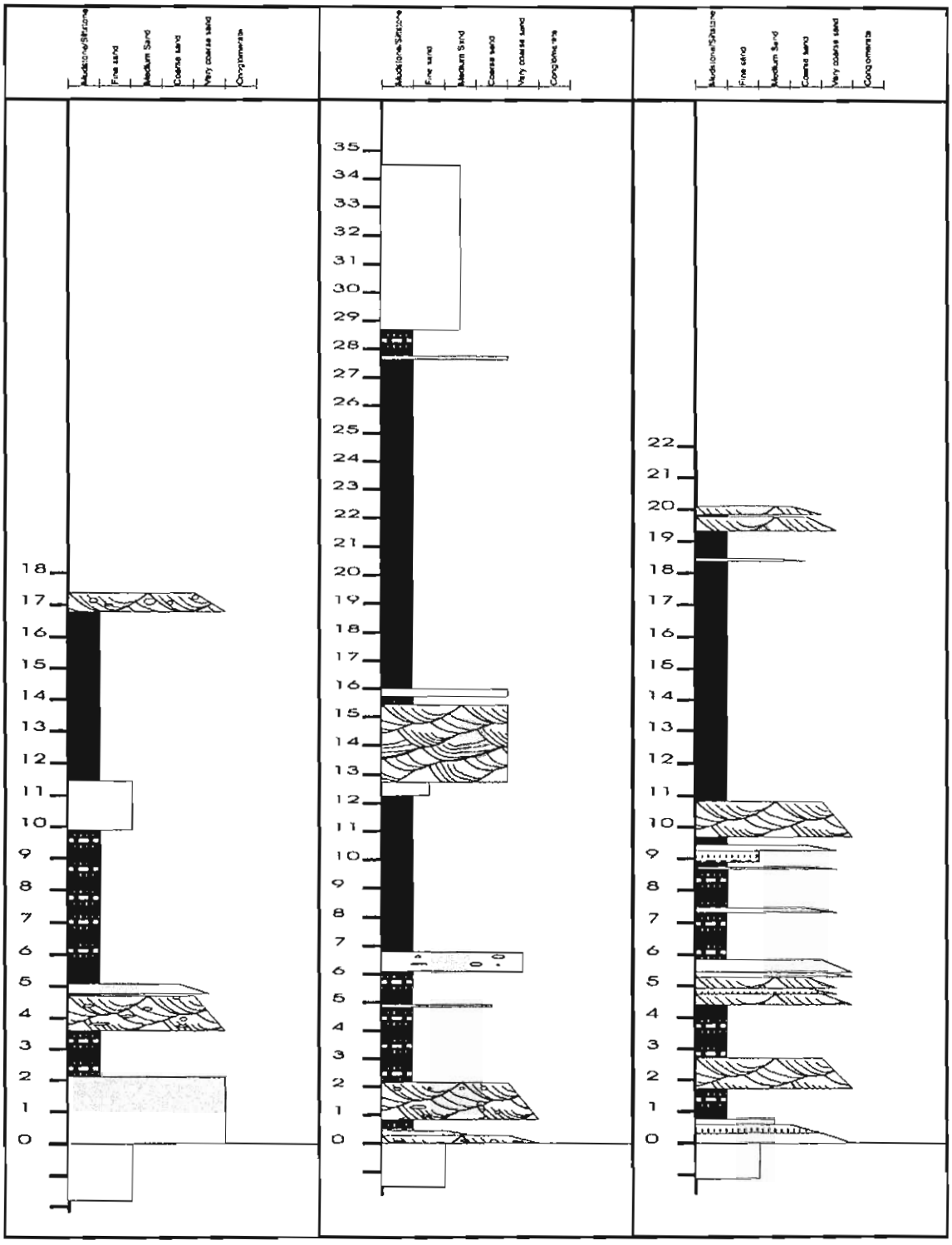

MN76		MN87		MN90	
Depth of bottom contact = 23.38 m		Depth of bottom contact = 37.31 m		Depth of bottom contact = 37.29 m	
Borehole Position		Borehole Position		Borehole Position	
X = 2902385.766	Y = -66551.0	X = 2902400.0	Y = -66127.18	X = 2902233.08	Y = -66025.56

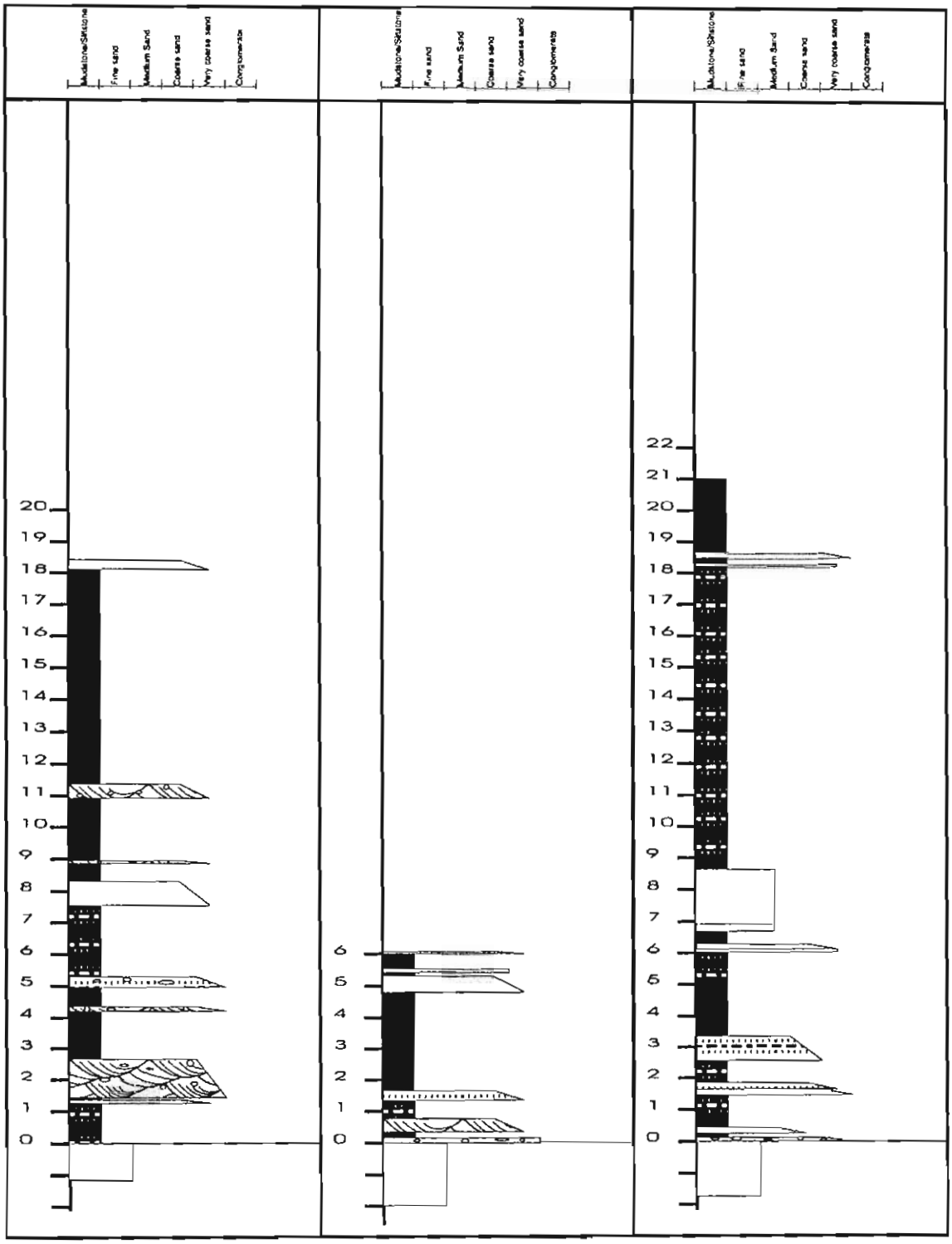

MN105		MN70\57		MN72\49	
Depth of bottom contact = 21.57 m		Depth of bottom contact = 20.02 m		Depth of bottom contact = 21.57 m	
Borehole Position		Borehole Position		Borehole Position	
X = 2902226.12	Y = -65422.41	X = 2903586.96	Y = -66999.5	X = 2903571.4	Y = -66665.388

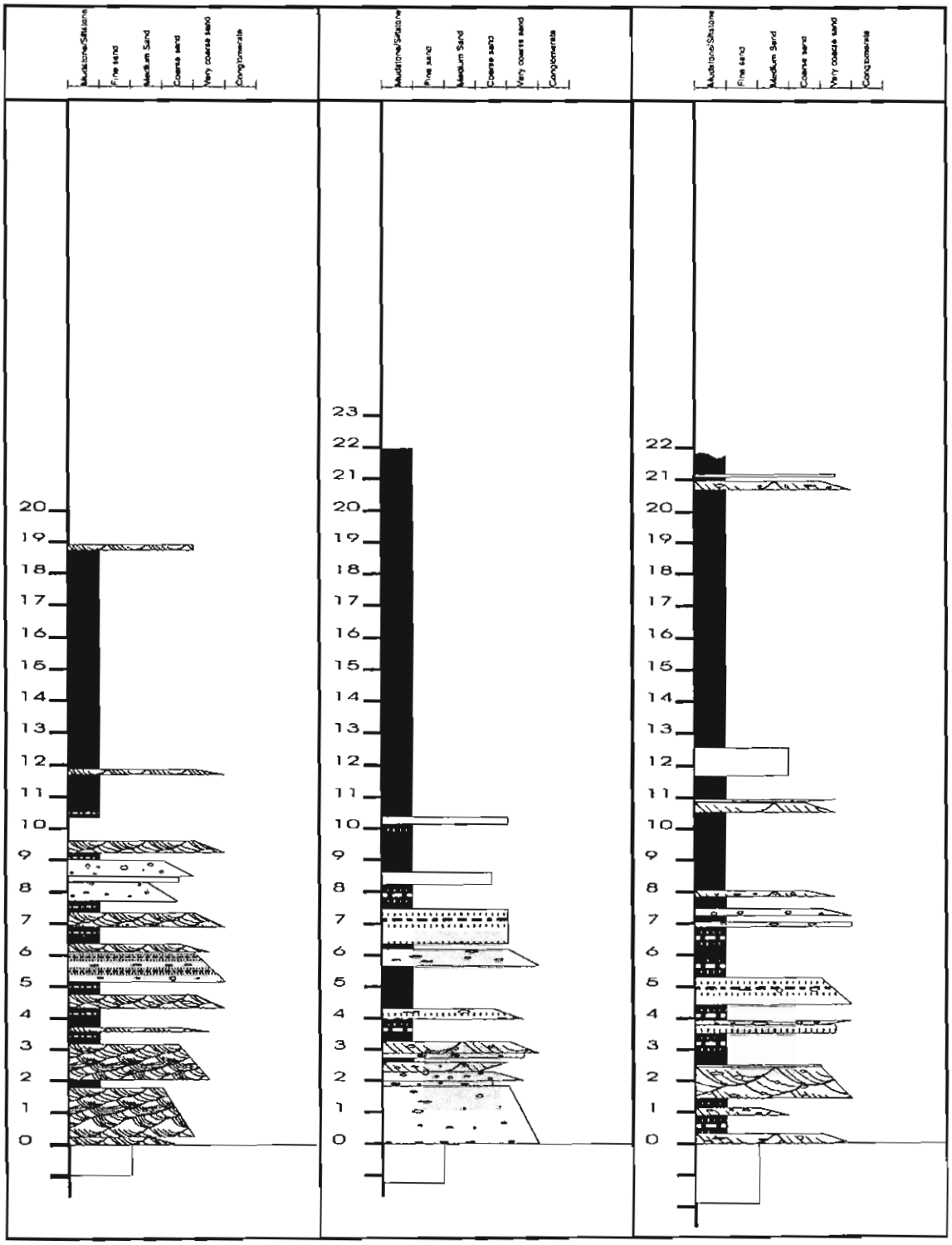

MS33		MS37		MS50	
Depth of bottom contact = 25.14 m		Depth of bottom contact = 26.95 m		Depth of bottom contact = 25.05 m	
Borehole Position		Borehole Position		Borehole Position	
X = 2902924.07	Y = -66149.54	X = 2902961.887	Y = -65971.455	X = 2902638.5	Y = -65578.98

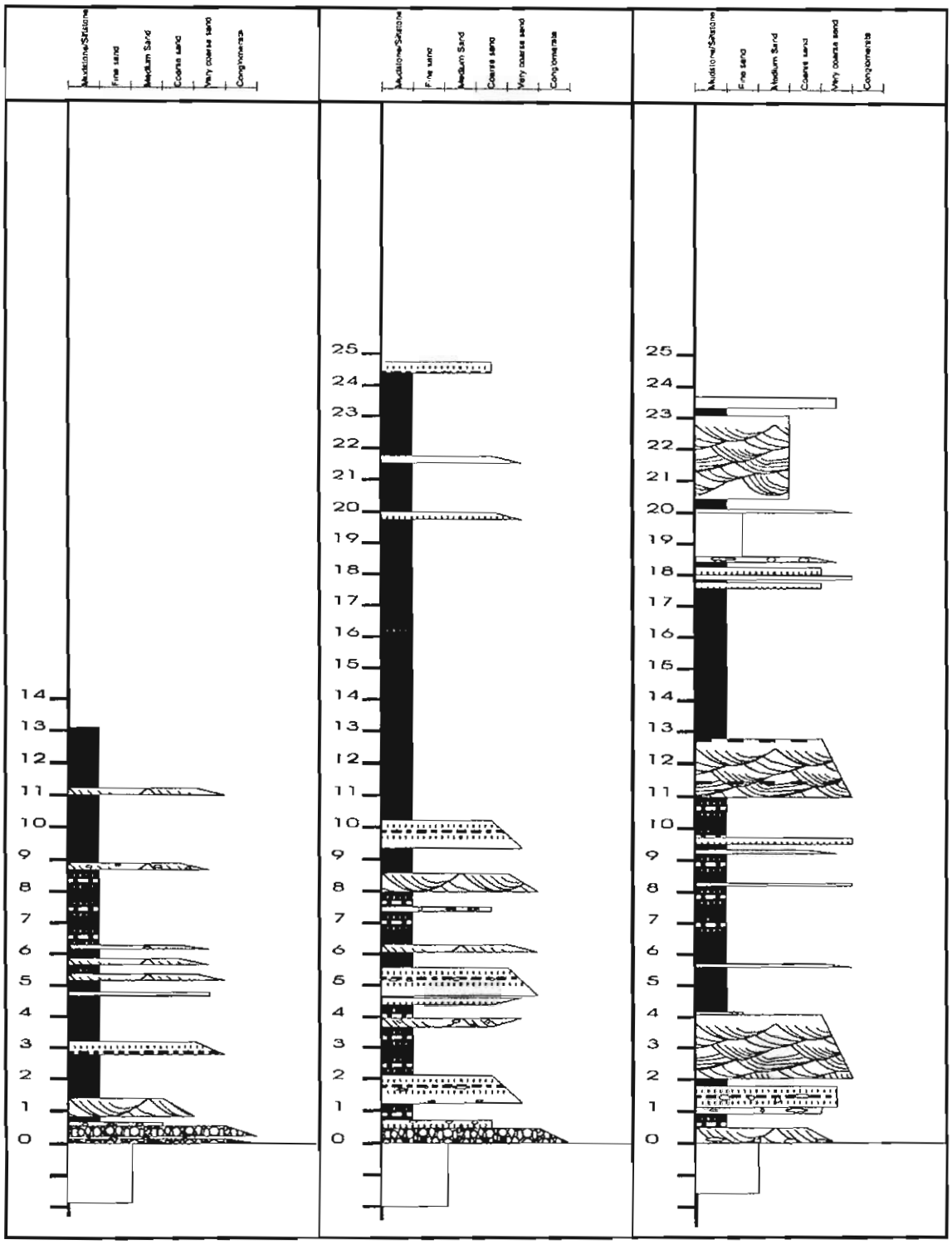

MS3		MS23		MS56	
Depth of bottom contact = 16.12 m		Depth of bottom contact = 37.46 m		Depth of bottom contact = 35.54 m	
Borehole Position		Borehole Position		Borehole Position	
X = 2903507.28	Y = -67187.3	X = 2903251.5	Y = -66432.37	X = 2902531.4	Y = -65365.85

Sedimentological profiles recorded from outcrop exposures

Wildfontein 52

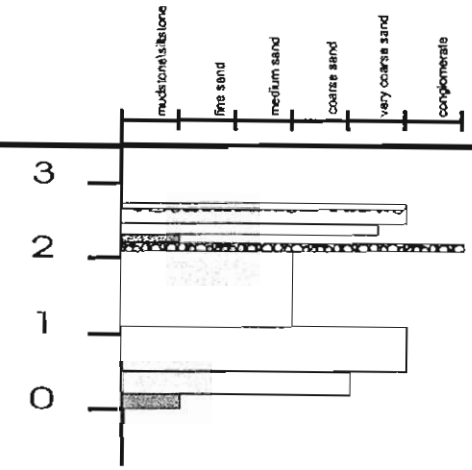

Comments
Mature flat-bedded quartzite with ripples at the top
Mature flat-bedded quartzite
Average pebble size is 1cm and the largest pebble size is 5cm
Argillaceous yellow-green sediment
Immature argillaceous sediment
Petrified green mudstone

Middelvlei 255

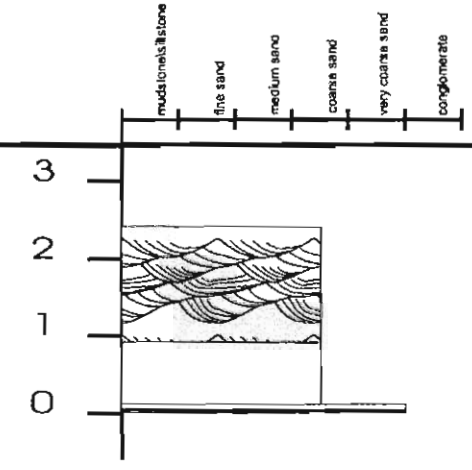

Comments
Mature trough cross-bedded quartzite, with ripples at the top.
Argillaceous "sandstone"
Flat-bedded and planary cross-bedded immature quartzite (weathered) containing one layer of pebbles. The average pebble size is 5mm and the largest pebble size is 15 cm.

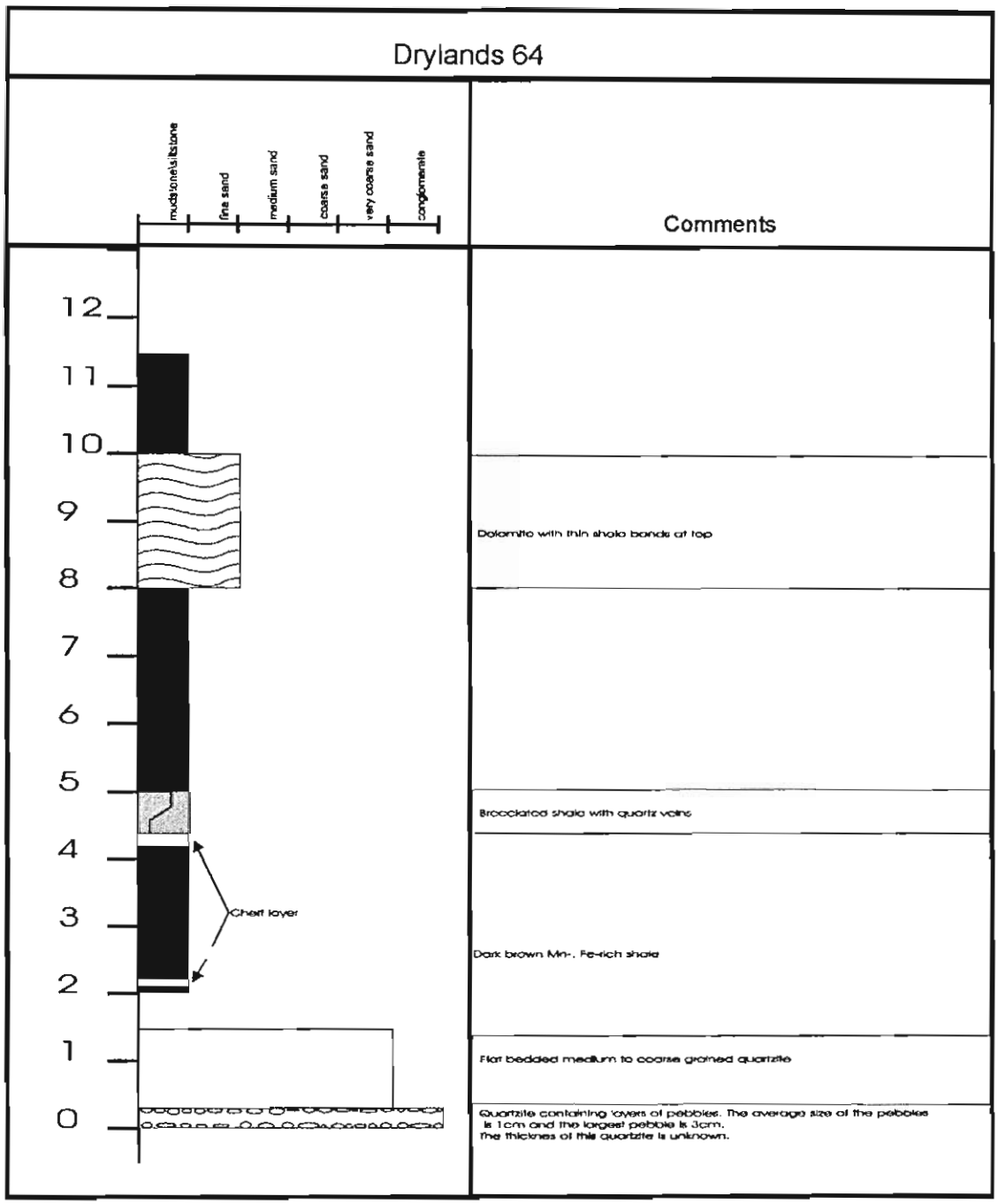
Drylands 64
mudstone/siltstone
fine sand
medium sand
coarse sand
very coarse sand
conglomerate
Comments
12
11
10
9
8
7
6
5
4
3
2
1
0
Chert layer
Dolomite with thin shale bands at top
Brecciated shale with quartz veins
Dark brown Mn-, Fe-rich shale
Flat bedded medium to coarse grained quartzite
Quartzite containing layers of pebbles. The average size of the pebbles is 1cm and the largest pebble is 3cm.
The thickness of this quartzite is unknown.

Appendix 2

Ripple marks

Ripple mark indices

Data Station 9: Middelvlei 255

h	la	lb	s	RSI	RI
31	100	93	193	1.08	6.2
40	112	96	208	1.17	5.2
36	97	86	183	1.13	5.1
35	100	100	200	1.00	5.7
24	116	110	226	1.05	9.4
28	95	88	183	1.08	6.5
26	90	75	165	1.20	6.3
71	79	75	154	1.05	2.2
21	93	82	175	1.13	8.3
24	63	60	123	1.05	5.1
18	80	64	144	1.25	8.0
20	85	78	163	1.09	8.2
19	76	60	136	1.27	7.2
31	69	56	125	1.23	4.0
23	56	48	104	1.17	4.5
14	66	56	122	1.18	8.7
14	89	73	162	1.22	11.6
34	65	65	130	1.00	3.8
28	91	83	174	1.10	6.2
24	78	74	152	1.05	6.3
3	17	15	32	1.13	10.7
1	16	15	31	1.07	31.0
22	74	63	137	1.17	6.2
24	69	56	125	1.23	5.2
18	82	73	155	1.12	8.6
11	61	51	112	1.20	10.2
9	59	52	111	1.13	12.3
32	65	58	123	1.12	3.8
18	64	60	124	1.07	6.9
15	44	42	86	1.05	5.7
17	44	34	78	1.29	4.6
23	127	89	216	1.43	9.4
27	130	83	213	1.57	7.9
23	136	118	254	1.15	11.0
26	102	87	189	1.17	7.3
24	117	101	218	1.16	9.1
11	33	30	63	1.10	5.7
13	36	31	67	1.16	5.2
11	36	33	69	1.09	6.3
8	30	30	60	1.00	7.5
11	30	28	58	1.07	5.3
10	32	29	61	1.10	6.1
6	22	21	43	1.05	7.2

$$RI = {}^{s}/_{h}$$

$$RSI = {}^{l_a}/_{l_b}$$

Data Station 13 Wildfontein 52

h	la	lb	s	RSI	RI
13	130	116	246	1.12	18.9
10	109	102	211	1.07	21.1
19	105	94	199	1.12	10.5
10	130	99	229	1.31	22.9
4	13	12	25	1.08	6.3
4	12	10	22	1.20	5.5
4	12	12	24	1.00	6.0
3	16	14	30	1.14	10.0
5	14	14	28	1.00	5.6
5	12	9	21	1.33	4.2
4	12	9	21	1.33	5.3
4	16	14	30	1.14	7.5
4	14	13	27	1.08	6.8
4	11	9	20	1.22	5.0
4	12	12	24	1.00	6.0
4	18	16	34	1.13	8.5
4	21	19	40	1.11	10.0
4	23	20	43	1.15	10.8
3	25	22	47	1.14	15.7
4	26	25	51	1.04	12.8
4	42	35	77	1.20	19.3
4	30	28	58	1.07	14.5
9	33	30	63	1.10	7.0
6	41	30	71	1.37	11.8
9	74	74	148	1.00	16.4
10	66	53	119	1.25	11.9
7	65	64	129	1.02	18.4
24	160	155	315	1.03	13.1
19	153	150	303	1.02	15.9
22	131	115	246	1.14	11.2
14	110	102	212	1.08	15.1
42	170	160	330	1.06	7.9
29	160	118	278	1.36	9.6

Data Station 5: Bospan 56

h	la	lb	s	RSI	RI
10	97	80	177	1.213	17.7
18	72	65	137	1.108	7.611
20	79	74	153	1.068	7.65
15	58	55	113	1.055	7.533
19	105	105	210	1	11.05
21	110	100	210	1.1	10
24	104	95	199	1.095	8.292
20	82	74	156	1.108	7.8
14	79	72	151	1.097	10.79
21	106	91	197	1.165	9.381
10	96	83	179	1.157	17.9
20	109	99	208	1.101	10.4
20	104	92	196	1.13	9.8
8	51	42	93	1.214	11.63
27	105	103	208	1.019	7.704
10	63	52	115	1.212	11.5
23	106	79	185	1.342	8.043
19	107	102	209	1.049	11
31	111	105	216	1.057	6.968
14	67	57	124	1.175	8.857
27	120	103	223	1.165	8.259
19	74	68	142	1.088	7.474
19	107	90	197	1.189	10.37
16	91	69	160	1.319	10
19	78	76	154	1.026	8.105
16	60	55	115	1.091	7.188
20	86	81	167	1.062	8.35
15	80	68	148	1.176	9.867
25	89	82	171	1.085	6.84
22	104	92	196	1.13	8.909

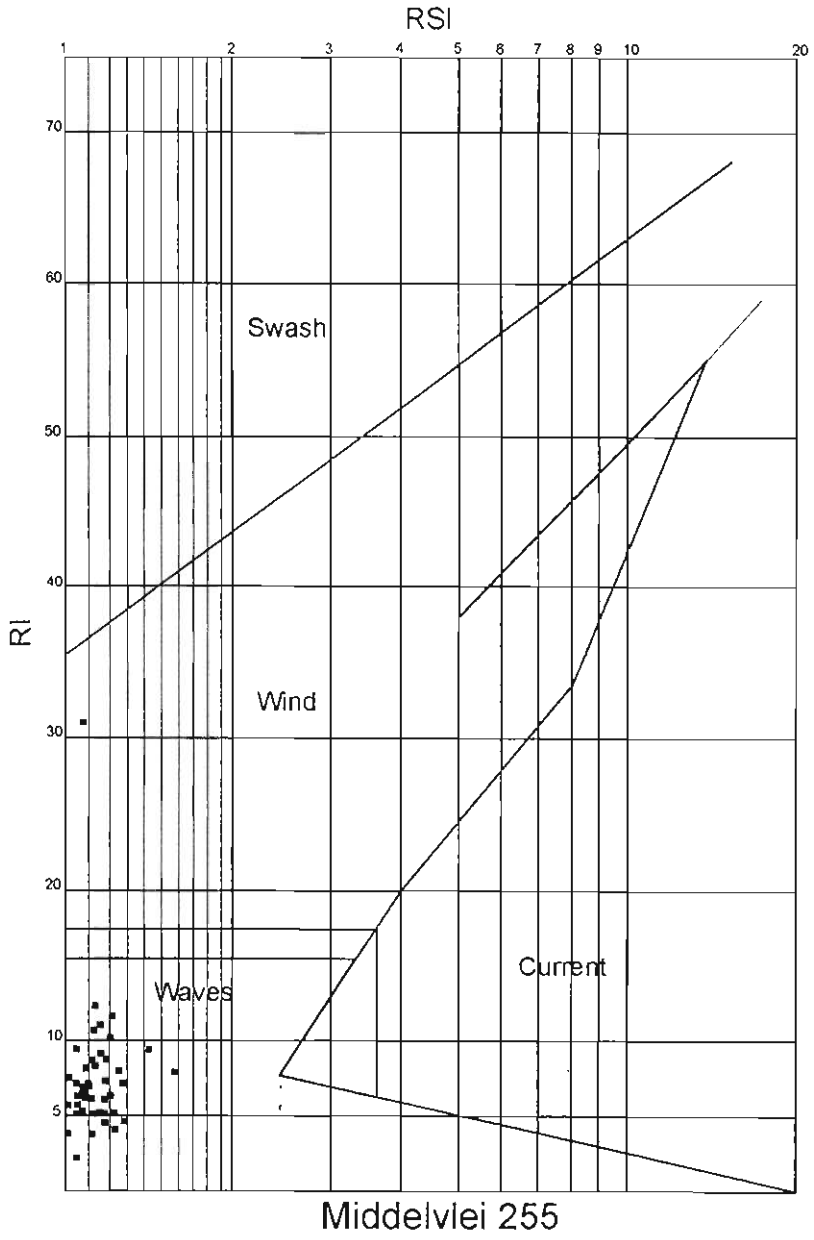

Middelvlei 255

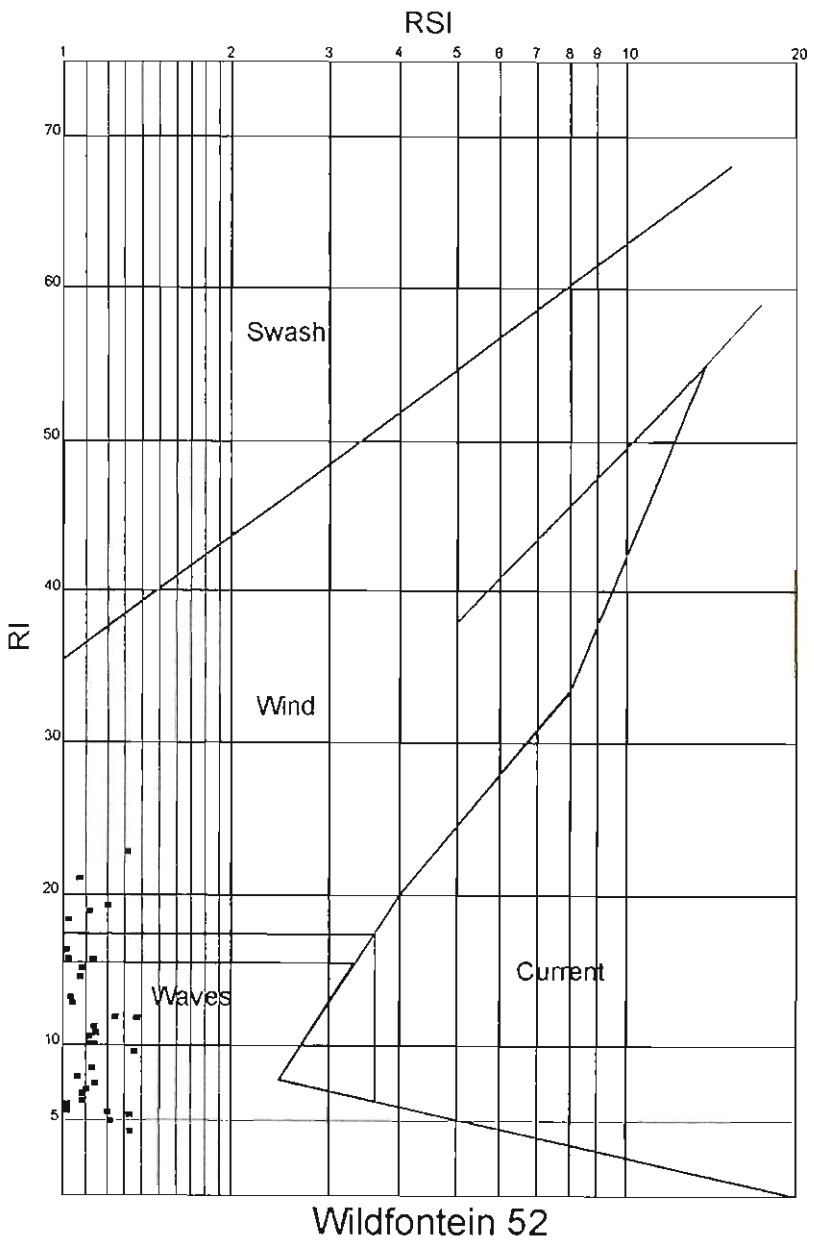

Wildfontein 52

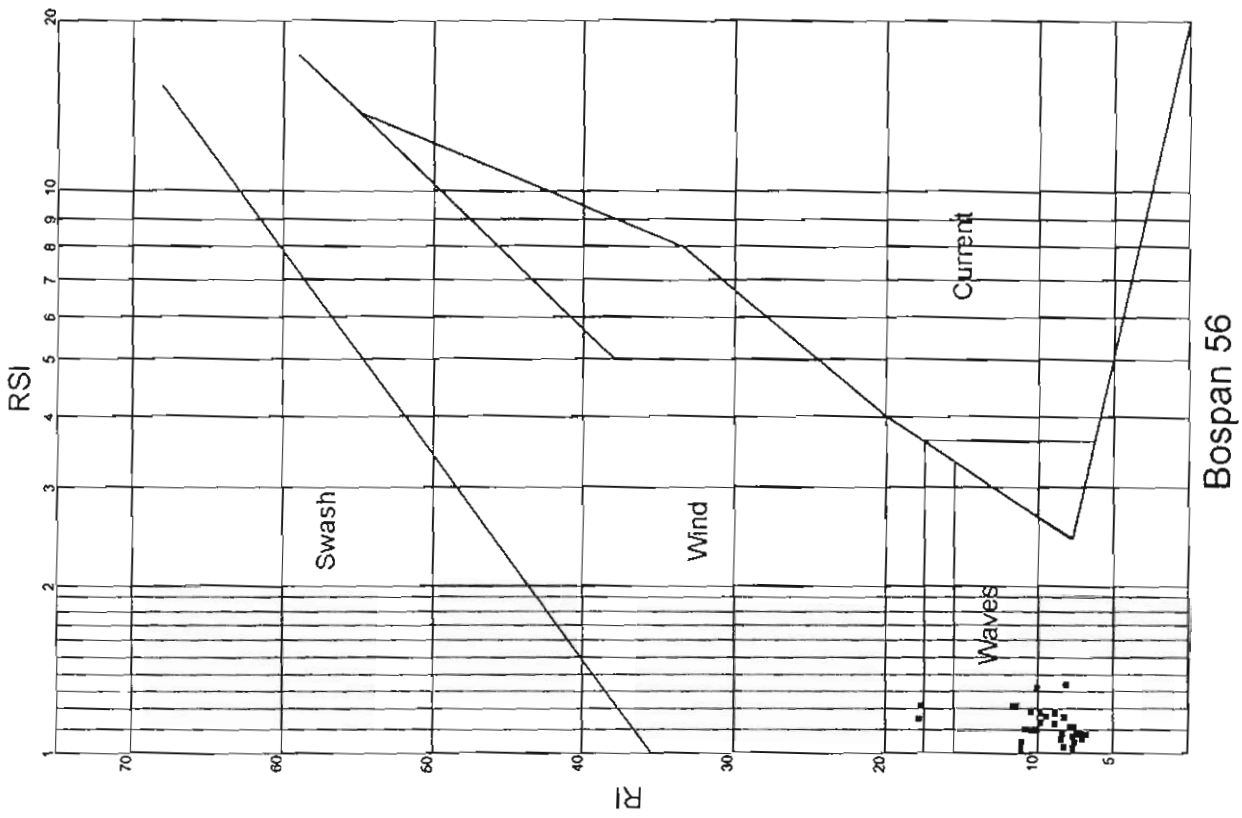
RSI
RI
Swash
Wind
Current
Waves
Bospan 56

Appendix 3

Markov Analysis

Transition Count Matrix

	Pebbly flaser-bedded quartzite	Pebbly lenticular-bedded quartzite	Pebbly quartzite	Lenticular-bedded quartzite	Flaser-bedded quartzite	Mudstone	Quartzite	Conglomerate	Pre-Transvaal Rocks	Total
Pebbly flaser-bedded quartzite	-	-	5	15	-	7	5	2	-	34
Pebbly lenticular-bedded quartzite	1	-	-	-	1	4	3	-	-	9
Pebbly quartzite	5	-	-	27	9	38	11	3	-	93
Lenticular-bedded quartzite	11	1	24	-	24	13	37	-	-	110
Flaser-bedded quartzite	-	1	10	23	-	25	14	1	-	74
Mudstone	8	2	32	15	23	-	61	1	-	142
Quartzite	6	5	8	34	19	60	-	1	-	133
Conglomerate	2	-	7	1	2	1	1	-	-	14
Pre-Transvaal Rocks	1	-	12	-	1	3	10	6	-	33
									Number of profiles:	31
									Total number of beds:	642

Transition Probability Matrix

	Pebbly flaser-bedded quartzite	Pebbly lenticular-bedded quartzite	Pebbly quartzite	Lenticular-bedded quartzite	Flaser-bedded quartzite	Mudstone	Quartzite	Conglomerate	Pre-Transvaal Rocks
Pebbly flaser-bedded quartzite	-	-	0.15	0.44	-	0.21	0.15	0.06	-
Pebbly lenticular-bedded quartzite	0.11	-	-	-	0.11	0.44	0.33	-	-
Pebbly quartzite	0.05	-	-	0.29	0.10	0.41	0.12	0.03	-
Lenticular-bedded quartzite	0.10	0.01	0.22	-	0.22	0.12	0.34	-	-
Flaser-bedded quartzite	-	0.01	0.14	0.31	-	0.34	0.19	0.01	-
Mudstone	0.06	0.01	0.23	0.11	0.16	-	0.43	0.01	-
Quartzite	0.05	0.04	0.06	0.26	0.14	0.45	-	0.01	-
Conglomerate	0.14	-	0.50	0.07	0.14	0.07	0.07	-	-
Pre-Transvaal Rocks	0.03	-	0.36	-	0.03	0.09	0.30	0.18	-

Relative frequency of occurrence										
	Pebbly flaser-bedded quartzite	Pebbly lenticular-bedded quartzite	Pebbly quartzite	Lenticular-bedded quartzite	Flaser-bedded quartzite	Mudstone	Quartzite	Conglomerate	Pre-Transvaal Rocks	Total
Pebbly flaser-bedded quartzite	-	-	0 0078	0.0234	-	0 0109	0.0078	0.0031	-	0 0530
Pebbly lenticular-bedded quartzite	0.0016	-	-	-	0.0016	0 0062	0 0047	-	-	0 0140
Pebbly quartzite	0.0078	-	-	0 0421	0.0140	0.0592	0.0171	0 0047	-	0 1449
Lenticular-bedded quartzite	0 0171	0.0016	0 0374	-	0.0374	0 0202	0.0576	-	-	0 1713
Flaser-bedded quartzite	-	0 0016	0.0156	0.0358	-	0 0389	0.0218	0.0016	-	0.1153
Mudstone	0 0125	0.0031	0 0498	0.0234	0 0358	-	0 0950	0 0016	-	0.2212
Quartzite	0 0093	0.0078	0.0125	0 0530	0.0296	0 0935	-	0.0016	-	0.2072
Conglomerate	0.0031	-	0.0109	0.0016	0.0031	0 0016	0.0016	-	-	0 0218
Pre-Transvaal Rocks	0.0016	-	0.0187	-	0.0016	0 0047	0.0156	0.0093	-	0.0514

Appendix 4

Thickness Data

Thickness data for the Black Reef Quartzite Formation							
	Quartzite Thickness (m)	Mudstone Thickness (m)	Conglomerate Thickness (m)	Total Thickness (m)	Percentage Quartzite	Percentage Mudstone	Percentage Conglomerate
mn1	9.23	15.21	0.48	24.92	37.0	61.0	1.9
mn6a	9.42	10.33	0	19.75	47.7	52.3	0.0
mn13	7.85	4.64	0.18	12.67	62.0	36.6	1.4
mn24	10.71	1.29	0	12	89.3	10.8	0.0
mn39	7.37	10.2	0.04	17.61	41.9	57.9	0.2
mn44	6.82	13.83	0	20.65	33.0	67.0	0.0
mn76	7.61	11.71	0	19.32	39.4	60.6	0.0
mn87	14.91	22.63	0	37.54	39.7	60.3	0.0
mn90	6.97	14.28	0	21.25	32.8	67.2	0.0
mn105	4.61	14.96	0	19.57	23.6	76.4	0.0
mn70-57	3.57	4.5	0	8.07	44.2	55.8	0.0
mn72-49	3.93	17.11	0	21.04	18.7	81.3	0.0
ms3	3.99	10.38	0.47	14.84	26.9	69.9	3.2
ms23	5.13	19.17	0.46	24.76	20.7	77.4	1.9
ms33	8.75	11.04	0	19.79	44.2	55.8	0.0
ms37	6.01	16.23	0	22.24	27.0	73.0	0.0
ms50	5.11	16.08	0	21.19	24.1	75.9	0.0
ms56	11.01	12.67	0	23.68	46.5	53.5	0.0
bel3	14.05	4.16	0.21	18.42	76.3	22.6	1.1
bl2	11.17	1.86	0	13.03	85.7	14.3	0.0
bl4	22.13	1.17	0.44	23.74	93.2	4.9	1.9
bl7	17.59	0.16	0	17.75	99.1	0.9	0.0
bl8	9.02	1.88	0	10.9	82.8	17.2	0.0
bl9	10.07	2.46	0	12.53	80.4	19.6	0.0
bw1	17.9	6.85	1.56	26.31	68.0	26.0	5.9
ge25	4.07	9.03	0	13.1	31.1	68.9	0.0
n4	6.13	8.84	0	14.97	40.9	59.1	0.0
rk3	5.18	5.8	0	10.98	47.2	52.8	0.0
rt1	10.06	3.09	0	13.15	76.5	23.5	0.0
wbl1	4.48	6.37	0.06	10.91	41.1	58.4	0.5
wbl3	5.51	7.61	0	13.12	42.0	58.0	0.0
wbl4	4.63	6.61	0	11.24	41.2	58.8	0.0
wfn9	11.36	0.12	0	11.48	99.0	1.0	0.0
Mean	8.677273	8.856667	0.118182	17.65212	51.6	47.8	0.5

Appendix 5

Palaeocurrent Data

Data of trough cross-bedding measurements

	Trough axis		Transport direction	Tectonic dip		Trough dimensions
	Direction	Plunge	relative to plunge	Dip angle	Dip direction	(cm)
Data Station 1:	255	0	With	6	355	50
Varkenskraal 93	280	10	With	7	325	50
	260	0	With	0		50
	264	5	With	4	325	40
	49	22	With	0		40
	56	1	With	0		30
	305	0	With	0		100
	Vector Mean = 294.2				334.8960906	
	n = 7					

	Trough axis		Transport direction	Tectonic dip		Trough dimensions
	Direction	Plunge	relative to plunge	Dip angle	Dip direction	(cm)
Data Station 2:	0	10	With	8	8	10
Varkenskraal 93 & Rooipan 96	5	3	With	0		20
	21	4	With	0		7
	2	2	With	0		12
	23	5	With	0		14
	6	10	With	12	16	13
	16	8	With	8	13	10
	17	8	With	8	16	25
	15	12	With	12	16	10
	354	1	With	0		8
	340	12	With	15	330	9
	333	5	With	4	340	18
	348	5	With	4	340	4
	352	15	With	15	330	13
	350	14	With	14	15	8
	13	10	With	14	15	6
	7	10	With	7	10	8
	352	9	With	9	350	8
	341	10	With	9	350	8
	18	14	With	14	15	8
	358	4	With	0		10
	15	2	With	0		8
	0	3	With	0		6
	354	5	With	0		6
	351	10	With	9	351	7
	351	9	With	9	351	6
	348	6	With	6	348	4
	3	4	With	0		6
	5	12	With	9	355	15
	355	1	With	0		11
	Vector Mean = 359.6				358.437515	
	n = 30					

	Trough axis		Transport direction	Tectonic dip		Trough dimensions
	Direction	Plunge	relative to plunge	Dip angle	Dip direction	(cm)
Data Station 3:	0	17	With	12	340	24
Rooipan 96	15	16	With	12	340	27
	350	12	With	12	340	21
	332	18	With	12	340	38
	322	30	With	12	340	30
	348	18	With	18	345	19
	284	25	With	26	340	24
	134	13	With	13	134	16
	14	14	With	14	30	20
	45	8	With	8	45	18
	145	10	With	10	155	30
	285	0	With	0		30
	Vector Mean = 351.8				0.332161093	
	n = 12					

	Trough axis		Transport direction	Tectonic dip		Trough dimensions
	Direction	Plunge	relative to plunge	Dip angle	Dip direction	(cm)
Data Station 4:	345	8	With	8	340	24
Leeuwpan 58	156	12	Against	12	355	45
	132	14	Against	14	10	52
	227	8	With	8	197	25
	278	0	With	0		27
	232	0	With	0		24
	218	0	With	0		?
	241	0	With	0		27
	Vector Mean = 225.6				344.4153759	
	n = 8					

	Trough axis		Transport direction	Tectonic dip		Trough dimensions
	Direction	Plunge	relative to plunge	Dip angle	Dip direction	(cm)
Data Station 6:	142	15	With	15	140	32
Wildfontein 52	145	18	Against	18	145	25
	145	0	With	0		75
	125	25	Against	25	295	30
	135	12	Against	12	303	
	60	20	With	20	280	40
	116	21	Against	21	255	
	280	9	With	9	250	30
	255	19	Against	21	90	28
	272	10	With	10	280	40
	310	19	With	19	300	50
	137	0		0		35
	240	6		6	328	34
	340	15	With	15	320	30
	308	14	With	14	280	27
	10	5	With	10	310	30
	165	15	With	17	70	36
	278	9	With	6	45	44
	300	0	With	0		?
	285	9	With	9	345	40
	281	0		0		28
	350	9	With	9	340	75
	354	11	With	11	305	38
	351	18	With	18	340	45
	322	14	With	14	330	30
	335	11	With	11	315	30
	0	20	With	20	340	25
	310	14	With	13	338	75
	315	12	With	13	338	40
	325	12	With	13	338	40
	315	14	With	13	338	38
	315	14	With	13	338	40
	228	4	With	11	300	19
	260	12	With	11	300	22
	300	14	With	14	300	32
	335	0		0		14
	325	12	With	12	255	39
	250	22	With	12	255	35
	325	11	With	6	305	11
	315	11	With	6	303	?
	340	6	With	6	303	50
	100	15	With	15	105	32
	325	10	With	10	60	14
	324	10	With	10	60	20
	270	15	With	12	52	16
	275	6	With	6	10	13
	Vector Mean = 128.3				322.932976	
	n = 10					
	Vector Mean = 307.6					
	n = 33					

	Trough axis		Transport direction	Tectonic dip		Trough dimensions
	Direction	Plunge	relative to plunge	Dip angle	Dip direction	(cm)
Data Station 7:	304	19	With	19	270	30
Elandsfontein 277	345	26	With	23	294	70
	325	6	With	8	293	30
	315	7	With	17	284	40
	Vector Mean = 322.2				285.2809191	
	n = 4					

Data Station 8:
Blaauwbank 278

Trough axis		Transport direction	Tectonic dip		Trough dimensions
Direction	Plunge	relative to plunge	Dip angle	Dip direction	(cm)
195	5	With	18	145	30
226	7	Against	20	90	10
185	12	Against	13	68	30
212	12	Against	13	68	30
202	1	With	9	101	40
193	3	Against	5	294	20
182	4	With	8	97	30
186	10	Against	11	352	30
198	4	With	5	92	40
161	3	With	8	51	40
211	5	Against	2	98	40
204	10	Against	5	65	20
195	3	Against	5	65	20
224	12	Against	12	43	20
213	1	With	0		30
226	12	With	12	226	50
216	4	Against	0		40
222	4	With	0		10
209	5	Against	5	94	50
235	5	With	5	94	30
218	3	With	5	24	10
222	2	With	5	24	10
200	9	Against	12	35	50

Vector Mean = 204.3
n = 24
68.40478999

Data Station 9:
Blaauwbank 278

Trough axis		Transport direction	Tectonic dip		Trough dimensions
Direction	Plunge	relative to plunge	Dip angle	Dip direction	(cm)
232	4	With	3	195	100
160	3	With	3	195	50
196	3	With	3	326	50
198	4	With	3	175	50
200	3	With	3	175	100
196	1	With	31	196	70
197	6	With	6	195	20
226	8	With	6	195	80
215	11	With	11	215	75
218	2	Against	2	38	50
232	8	With	3	186	60
195	4	With	3	186	20
286	12	With	12	286	50
275	15	With	12	286	20
270	4	With	12	286	50
223	0		0		30
230	3	With	0		20
278	0		0		10
196	15	Against	15	16	30
275	8	Against	6	95	
294	4	Against	4	95	
295	8	With	3	65	
240	0		0		100
205	25	With	24	196	30
170	25	With	23	164	30
212	5	With	11	149	30
256	9	With	14	215	30
285	2	With	5	20	20

Vector Mean = 229.8
n = 28
188.4921975

Data Station10:
Blaauwbank 278

Trough axis		Transport direction	Tectonic dip		Trough dimensions
Direction	Plunge	relative to plunge	Dip angle	Dip direction	(cm)
162	15	With	16	200	70
25	11	Against	16	200	20
15	10	Against	16	200	30
340	3	Against	0		40
115	0	Against	0		
25	8	Against	10	210	20
337	2	With	0		30
36	10	Against	13	210	20
357	9	Against	13	210	20
40	0		0		40

Data Station10 (cont.):

Trough axis		Transport direction	Tectonic dip		Trough dimensions
Direction	Plunge	relative to plunge	Dip angle	Dip direction	(cm)
50	6	Against	9	230	20
218	11	Against	15	240	20
0	0		0		20
5	3	Against	0		10
335	8	Against	15	31	20
20	8	With	12	30	20
0	4	With	12	30	25
48	11	With	13	45	20
354	20	With	22	345	20
198	30	With	30	178	30
43	5	Against	8	210	20
12	15	With	17	20	20
20	5	Against	15	220	20
16	8	Against	14	200	10
38	0		0		10
38	0		0		20
16	8	With	8	15	30
39	16	With	18	40	10
46	14	With	18	40	10
180	0		0		20
175	0		0		30
191	4	With	4	191	10
25	4	With	14	20	10
0	5	With	14	20	10
31	12	With	14	20	10
357	3	Against	0		20
359	2	With	0		
50	2	With	0		

Vector Mean = 18.1
n = 31
Vector Mean = 178.2
n = 7

237.2516445

Data Station 11:
Rietfontein 256

Trough axis		Transport direction	Tectonic dip		Trough dimensions
Direction	Plunge	relative to plunge	Dip angle	Dip direction	(cm)
113	7	With	0		10
351	1	With	0		20
356	7	With	4	49	20
65	5	With	6	120	10
85	3	With	6	120	20
87	13	With	7	85	10
131	11	With	11	140	50
160	11	With	11	130	50
126	15	With	15	135	30
115	8	With	8	135	
145	6	With	6	138	30
100	10	With	10	110	30
125	20	With	20	130	40
140	12	With	12	133	30
105	15	With	15	135	70
340	0		0		70
160	3	With	3	150	50
155	9	With	9	130	100
145	9	With	9	140	30
100	9	With	9	115	20
135	7	With	7	130	
123	19	With	19	115	20
152	7	With	7	140	40
160	5	With	16	135	30
130	15	With	30	125	30
110	15	With	15	136	
110	0		12	177	30
129	20	With	10	185	25
157	0		0		22

Vector Mean = 349.0
n = 3
Vector Mean = 125.9
n = 26

130.173818

	Trough axis		Transport direction	Tectonic dip		Trough dimensions
	Direction	Plunge	relative to plunge	Dip angle	Dip direction	(cm)
Data Station 12:	138	21	With	16	138	10
Middelvlei 255	115	10	With	10	115	10
	116	15	With	19	50	20
	125	5	With	25	210	10
	120	13	With	13	40	10
	115	12	With	12	115	
	Vector Mean = 121.5				107.1385338	
	n = 6					

	Trough axis		Transport direction	Tectonic dip		Trough dimensions
	Direction	Plunge	relative to plunge	Dip angle	Dip direction	(cm)
Data Station 13:	255	0		0		20
Middelvlei 255	270	0		0		15
	261	12	With	12	250	10
	228	11	With	8	207	12
	242	10	With	8	207	11
	295	4	With	8	207	15
	235	13	With	13	235	30
	210	28	With	28	210	20
	250	6	With	0		12
	235	0		0		12
	250	12	With	12	250	15
	244	0	With	0		30
	228	0	With	0		20
	237	8	With	12	205	11
	262	0	With	0		9
	230	0	With	0		8
	258	25	With	23	260	10
	270	20	With	25	260	10
	250	14	With	12	245	10
	231	0	With	0		10
	Vector Mean = 246.9				230.5243908	
	n = 20					

	Trough axis		Transport direction	Tectonic dip		Trough dimensions
	Direction	Plunge	relative to plunge	Dip angle	Dip direction	(cm)
Data Station 14:	52	11	With	10	40	15
Middelvlei 255	272	7	With	8	42	13
	295	7	With	8	42	20
	78	11	With	12	40	10
	228	15	Against	20	40	12
	225	20	Against	20	40	21
	254	13	Against	15	40	20
	40	9	With	9	40	50
	215	2	Against	0		
	41	4	With	4	45	
	230	14	With	15	220	
	44	14	With	14	75	28
	74	12	With	16	75	
	86	12	With	12	75	30
	188	0	With	0		20
	198	6	Against	0		19
	Vector Mean = 59.2				50.1840415	
	n = 7					
	Vector Mean = 233					
	n = 9					

	Trough axis		Transport direction	Tectonic dip		Trough dimensions
	Direction	Plunge	relative to plunge	Dip angle	Dip direction	(cm)
Data Station 15:	172	11	With	12	130	34
Middelvlei 255	156	18	With	20	147	15
	161	21	With	15	110	10
	154	5	With	7	154	17
	125	10	With	7	154	12
	154	10	With	11	112	14
	193	19	With	11	112	15
	191	18	With	11	112	17
	200	10	With	10	129	15
	212	14	With	10	129	22
	200	0	With	10	129	10
	153	12	With	10	129	10
	168	14	With	12	115	

Data Station 15 (cont.):

Trough axis		Transport direction	Tectonic dip		Trough dimensions
Direction	Plunge	relative to plunge	Dip angle	Dip direction	(cm)
141	11	With	10	120	21
160	9	With	15	98	15
150	8	With	15	129	25
140	25	With	23	120	35
153	17	With	22	144	17
141	14	With	12	183	14
168	36	With	27	121	20
111	18	With	17	105	
184	8	With	0		14
185	10	With	5	90	14
182	20	With	5	90	
196	0	With	0		26
234	8	With	0		20
165	1	With	0		
230	5	With	0		28
155	10	With	12	112	26

Vector Mean = 169.7
n = 29

123.5560489

Data Station 16:
Middelvlei 255

Trough axis		Transport direction	Tectonic dip		Trough dimensions
Direction	Plunge	relative to plunge	Dip angle	Dip direction	(cm)
185	0		0		36
186	6	With	0		32
200	2	Against	0		20
218	5	With	0		17
164	0		0		45
148	0		0		9
146	0		0		13
150	12	With	0		33
154	4	With	0		19
145	0		0		30
158	0		0		31

Vector Mean = 168.0
n = 11

Data Station 17:
Middelvlei 255

Trough axis		Transport direction	Tectonic dip		Trough dimensions
Direction	Plunge	relative to plunge	Dip angle	Dip direction	(cm)
274	4	With	0		28
110	16	With	12	172	22
25	10	With	10	160	40
2	10	With	10	160	40
9	1	With	0		100
158	7	Against	10	152	20
152	15	With	15	150	25
304	0		5	145	75
349	3	With	0		35
30	3	With	0		100
5	5	With	5	30	50
20	5	With	5	25	75
50	5	With	5	50	60
40	8	With	8	40	60
50	8	With	8	45	60
38	5	With	5	45	70
72	0		0		
90	0		0		40
90	4	With	5	120	30
85	4	With	4	95	60
55	5	With	4	115	75
42	6	With	6	70	50
10	0		0		40
90	15	With	13	95	40
120	10	With	9	120	40
95	6	With	7	120	40
120	6	With	7	120	40
102	10	With	5	145	10
110	0		12	177	30
129	20	With	10	155	25
157	0		0		22

Vector Mean = 17.7
n = 16

111.9249973

Vector Mean = 111.5
n = 15

Data Station 18:
Brandvlei 261

Trough axis		Transport direction	Tectonic dip		Trough dimensions
Direction	Plunge	relative to plunge	Dip angle	Dip direction	(cm)
320	0		0		40
50	0	With	0		38
60	5	With	0		
62	5	Against	5	250	
132	15	With	15	135	
140	15	With	15	135	
137	10	With	15	135	40
135	0		0		
205	0		0		
60	10		10	70	
115	10	With	10	10	
90	3	With	0		
85	6	With	6	90	40
88	2	With	0		30
265	6	With	6	265	31
252	15	With	17	255	
245	9	With	9	255	20
240	7	Against	7	60	
238	5	With	5	215	27
185	25	With	25	160	
120	12	With	12	120	15
100	14	With	15	140	21
100	0		0		22
85	0		0		30
105	5	With	5	110	25
170	6	With	6	170	7
75	7		10	26	
95	0		0		30
80	25	With	25	80	40
115	12	With	12	115	50
76	9		9	76	
320	8	With	18	0	30
100	0		0		24
89	11	With	18	106	12
310	3	Against	0		15
320	0		0		25
300	10	With	10	300	
315	10	With	10	300	10
97	0		0		20
114	0		0		9
320	4	With	0		20
116	12	With	12	135	
67	9	With	11	5	10
Vector Mean = 100.3				111.1522413	
n = 30					
Vector Mean = 282.3					
n = 13					

Data of planar cross-bedding measurements

	Field Readings		Tectonic Dip		Set Thickness	Corrected Readings	
	Dip	Direction	Dip	Direction		Dip	Diection
Data Station 13:	343	32	10	12		25	345
Middelvlei	338	27	10	12		19	340

	Field Readings		Tectonic Dip		Set Thickness	Corrected Readings	
Data Station 14:	Dip	Direction	Dip	Direction		Dip	Direction
Middelvlei	45	24	14	21	46	31	23
	32	8	14	21	46	18	9
	42	23	14	21	46	28	23
	42	23	14	21	46	28	23
	34	15	14	21	46	20	15

Data of ripple crest measurements

	Direction		Plunge	Tectonic dip		Wavelength	Amplitude
				Dip angle	Dip direction	(cm)	(cm)
Data Station 2:	113	293				3	0.3
Varkenskraal 93 & Rooipan 96	75	255				3	0.3
	100	280				3	0.3
	97	277				3	0.3
	93	273				3	0.3
	106	286				3	0.3
	102	282				3	0.3
	94	274				3	0.3
	108	288				3	0.3
	96	276				3	0.3
	90	270				3	0.3
	90	270				3	0.3
	105	285				3	0.3
	94	274				3	0.3
	95	275				3	0.3
	102	282				3	0.3
	100	280				3	0.3
	100	280				3	0.3
	96	276				4	0.3
	83	263				3	0.3
	107	287				3	0.3
	94	274				3	0.3
	100	280				3	0.3
	80	260				5	0.3
Vector Mean = 96.7			/	276.7			
n = 24							

	Direction		Plunge	Tectonic dip		Wavelength	Amplitude
				Dip angle	Dip direction	(cm)	(cm)
Data Station 3:	98	278	10	20	20	9	1
Rooipan 96	92	272	10	15	55	12	2
	64	244	9	14	295	19	1
	55	235	0	0		16	1
	48	228	0	0		16	1
	60	240	0	0		12	2
	70	250	9	9	70	11	1
	68	248	0	0		5	0.5
	70	250	3	0		5	0.5
	74	254	12	10	40	8	0.5
	70	250	0	0		7	0.5
	75	255	0	0		15	2
	65	245	0	0		18	1
	70	250	0	0		18	1
	65	245	0	0		15	1
Vector mean = 69.5			\	249.5			
n = 15							

	Direction		Plunge	Tectonic dip		Wavelength	Amplitude
				Dip angle	Dip direction	(cm)	(cm)
Data Station 4:	38	218	0	0		9	0.5
Leeuwpan 58	22	202	0	0		9	0.5
	35	215	0	0		9	0.5
	30	210	0	0		9	0.5
	48	228	0	0		?	?
	54	234	0	0		?	?
Vector Mean = 37.8			\	217.8			
n = 6							

	Direction		Plunge	Tectonic dip		Wavelength	Amplitude
				Dip angle	Dip direction	(cm)	(cm)
Data Station 5:	70	250	15	15	70	8	1
Bospan 56	70	250	0	10	150	15	2
	65	245	0	10	150	15	2
	73	253	0	18	320	16	2
	62	242	0	10	305	17	2
	90	270	10	10	90	24	2
	50	230	0	0		15	2
	92	272	0	0		13	2
	72	252	5	5	45	10	1
	60	240	0	4	10	16	2

Data Station 5 (cont.):

Direction		Plunge	Tectonic dip		Wavelength	Amplitude
			Dip angle	Dip direction	(cm)	(cm)
57	237	4	4	330	11	1
65	245	6	5	285	14	3
38	218	0	5	318	20	3
72	252	0	0	0	15	2
75	255	5	8	0	18	3
74	254	0	8	348	17	3
75	255	5	5	24	24	3
69	249	0	8	335	17	3
75	255	4	9	350	14	2
94	274	1	10	335	10	1
60	240	1	5	325	11	1
68	248	2	7	325	17	2
74	254	1	10	345	18	2
75	255	1	1	340	15	2
55	235	2	8	165	20	2
79	259	5	6	290	13	2
75	255	2	5	315	17	3
50	230	0	8	315	24	4
84	264	2	15	345	18	2
76	256	0	0		14	2
78	258	1	0		10	1
76	256	2	14	350	17	2
62	242	6	8	5	27	2
77	257	3	10	328	18	2
95	275	5	15	345	19	3
75	255	8	10	355	10	2
78	258	0	0		17	3
80	260	10	11	35	20	2
78	258	8	8	40	25	5
76	256	8	7	20	15	2
86	266	5	9	10	25	3
86	266	0	6	15	13	2
65	245	11	14	25	20	2
81	261	10	10	50	22	3
73	253	5	6	240	20	5
75	255	0	0		50	8
161	341	6	6	333	2.5	0.5
180	360	6	6	333	2	0.5
191	11	6	6	333	2	0.5
169	349	6	6	333	2.5	0.5
160	340	6	6	333	2.5	0.5
176	356	6	6	333	2	0.5
Vector Mean = 72.5		\	252.5			
n = 46						
Vector Mean = 172.8		\	352.8			
n = 6						

Data Station 6:
Wildfontein 52

Direction		Plunge	Tectonic dip		Wavelength	Amplitude
			Dip angle	Dip direction	(cm)	(cm)
45	225	4	4	10	25	3
47	227	10	10	40	25	5
52	232	3	3	18	20	3
57	237	4	4	22	30	3
48	228	5	5	45	23	5
52	232	6	6	40	21	5
45	225	6	6	40	20	5
45	225	5	5	40	18	5
43	223	6	5	35	25	5
43	223	5	5	35	25	5
70	250	0	0		3.5	0.5
75	255	0	0		3.5	0.5
70	250	0	0		6	1
10	190	0	0		5	0.5
15	195	0	0		5	0.5
15	195	0	0		5	0.5
55	235	7	7	275	16	3
50	230	15	15	230	13	2
80	260	15	15	270	12	2
50	230	0	0		31	5
42	222	5	19	285	30	5
140	320	11	11	255	25	2.5
46	226	0	0		20	2.5

Data Station 6 (cont.)

Direction		Plunge	Tectonic dip		Wavelength (cm)	Amplitude (cm)
			Dip angle	Dip direction		
115	295	0	0		50	8
112	292	0	0		50	8
50	230	0	0		29	5
55	235	0	0		15	3
180	360	0	0		12	1
140	320	3	0		8	0.5
65	245	0	0		10	1

Vector Mean = 59.8 \ 239.8
n = 30

Data Station 8: Blaauwbank 278

Direction		Plunge	Tectonic dip		Wavelength	Amplitude
			Dip angle	Dip direction		
58	238					
50	230					
45	225					
38	218					
50	230					
48	228					
44	224					
48	228					
55	235					
60	240					

Vector Mean = 49.6 \ 229.6
n = 10

Data Station 9: Blaauwbank 278

Direction		Plunge	Tectonic dip		Wavelength (cm)	Amplitude (cm)
			Dip angle	Dip direction		
68	248				6	4

Data Station 13: Middelvlei 255

Direction		Plunge	Tectonic dip		Wavelength (cm)	Amplitude (cm)
			Dip angle	Dip direction		
130	310				4	0.5
125	305				4	0.5
125	305				8	0.5
130	310				4	0.5
90	270				4	0.5
128	308				5	0.5
115	295				6	0.5
110	290				5	0.5
100	280				5	0.5
110	290				5	0.5
122	302				4	0.5
110	290				9	1
108	288				10	1
115	295				4	0.5
115	295				28	5
122	302				7	0.5
125	305				5	0.5
123	303				8	1
125	305				9	1
117	297				12	3
106	286				17	3.5
128	308				11	2.5
116	296				15	2.5
123	303				9	0.5
127	307				5	0.5
120	300	25	30	175	7	0.5
120	300	20	33	48	8	0.5
124	304				12	4.5
115	295	28	27	130	6	0.5
114	294	12	12	114	10	2
122	302				14	3
110	290	12	12	110	10	3
125	305				6	1.5
88	268	10	10	88	12	3
122	302				10	3
125	305				7	1
113	293				11	3

Vector Mean = 117.4 \ 197.4
n = 37

	Direction		Plunge	Tectonic dip		Wavelength	Amplitude
				Dip angle	Dip direction	(cm)	(cm)
Data Station14:	72	252	0	0			
Middelvlei 255	90	270	12	12	40	12	1
	86	266	9	10	40	14	3
	85	265	8	10	40	11	3
	79	259	8	10	40	12	3
	89	269	3	10	40	14	3.5
	125	305	4	9	45	46	8
	108	288	15	8	75	23	7
	85	265	26	26	75	20	5
	103	283	16	17	75	13	3
	102	282	4	15	220	26	5
	109	289	12	12	75	15	2
	92	272	17	17	75	12	3
	178	358	0	2	75	17	6
	85	265	15	15	75	15	3
	131	311	0	0		17	4
	176	356	0	0		12	1.5
	90	270	13	0		9	0.8
	111	291	0	0		14	3
	106	286	5	0		8	0.5
	65	245	7	0		15	1
	126	306	12	12	38	20	3
Vector Mean = 102.7			\	182.7			
n = 22							

	Direction		Plunge	Tectonic dip		Wavelength	Amplitude
				Dip angle	Dip direction	(cm)	(cm)
Data Station17:	70	250	7	4	135	8	0.5
Middelvlei 255	80	260	3	4	135	8	0.5
Vector Mean = 75.0			\	255			
n = 2							

	Direction		Plunge	Tectonic dip		Wavelength	Amplitude
				Dip angle	Dip direction	(cm)	(cm)
Data Station18:	15	195	0	0		10	1.5
Brandvlei 261	135	315	6	6	265	10	2
	130	310	6	6	265	11	2
	135	315	0	0		18	2
	65	245	0	0		3	0.5
	65	245	0	0		4	0.5
	45	225	0	0		4	0.5
	70	250	18	18	70	6	1
Vector Mean = 52.4			\	232.4			
n = 5							
Vector Mean = 133.3			\	313.3			
n = 3							

Appendix 6

Pebble Size, Pebble Composition and Pebble Roundness

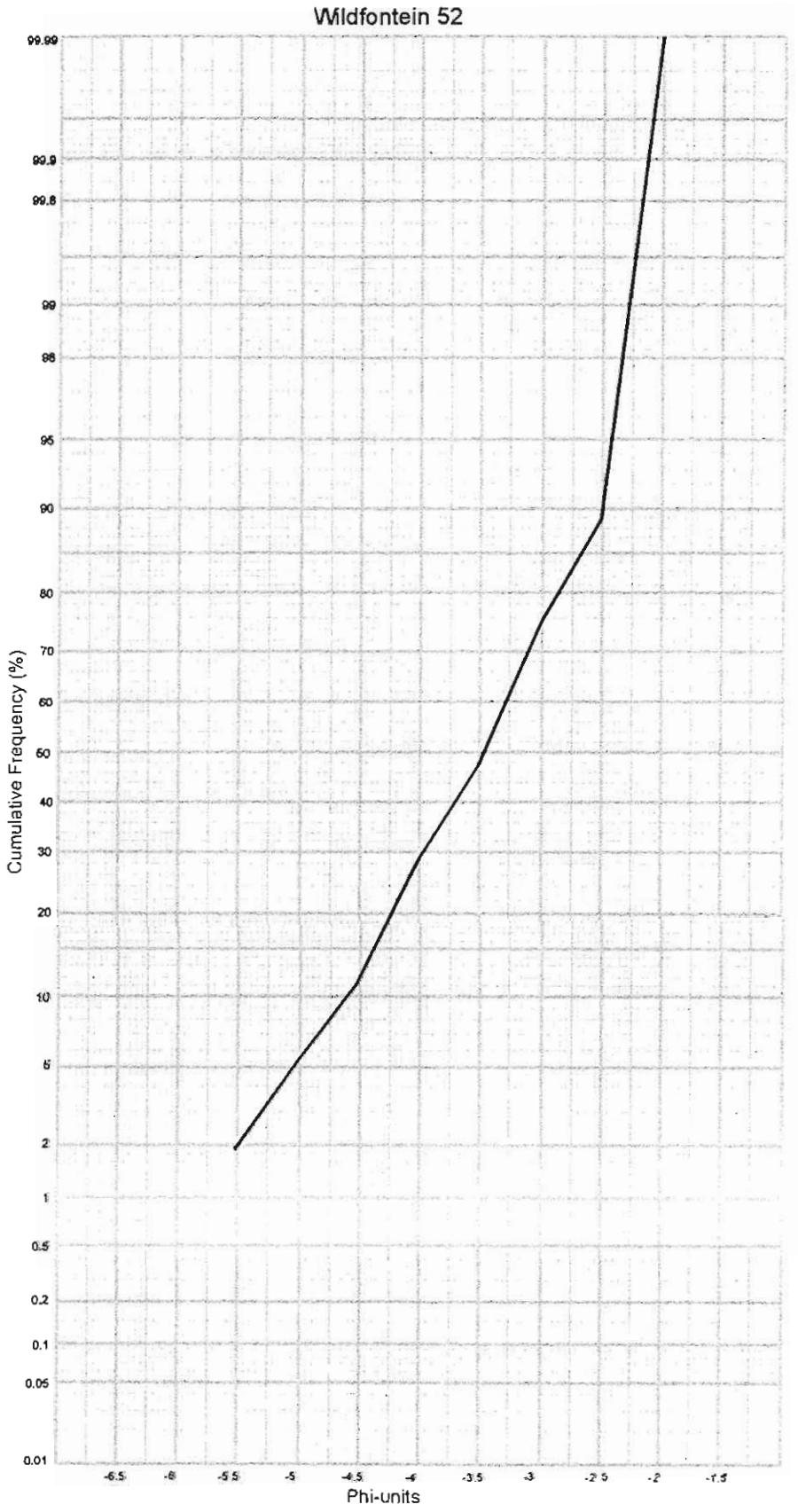
Wildfontein 52
Cumulative Frequency (%)
99.99
99.9
99.8
99
98
95
90
80
70
60
50
40
30
20
10
5
2
1
0.5
0.2
0.1
0.05
0.01
-6.5
-6
-5.5
-5
-4.5
-4
-3.5
-3
-2.5
-2
-1.5
Phi-units

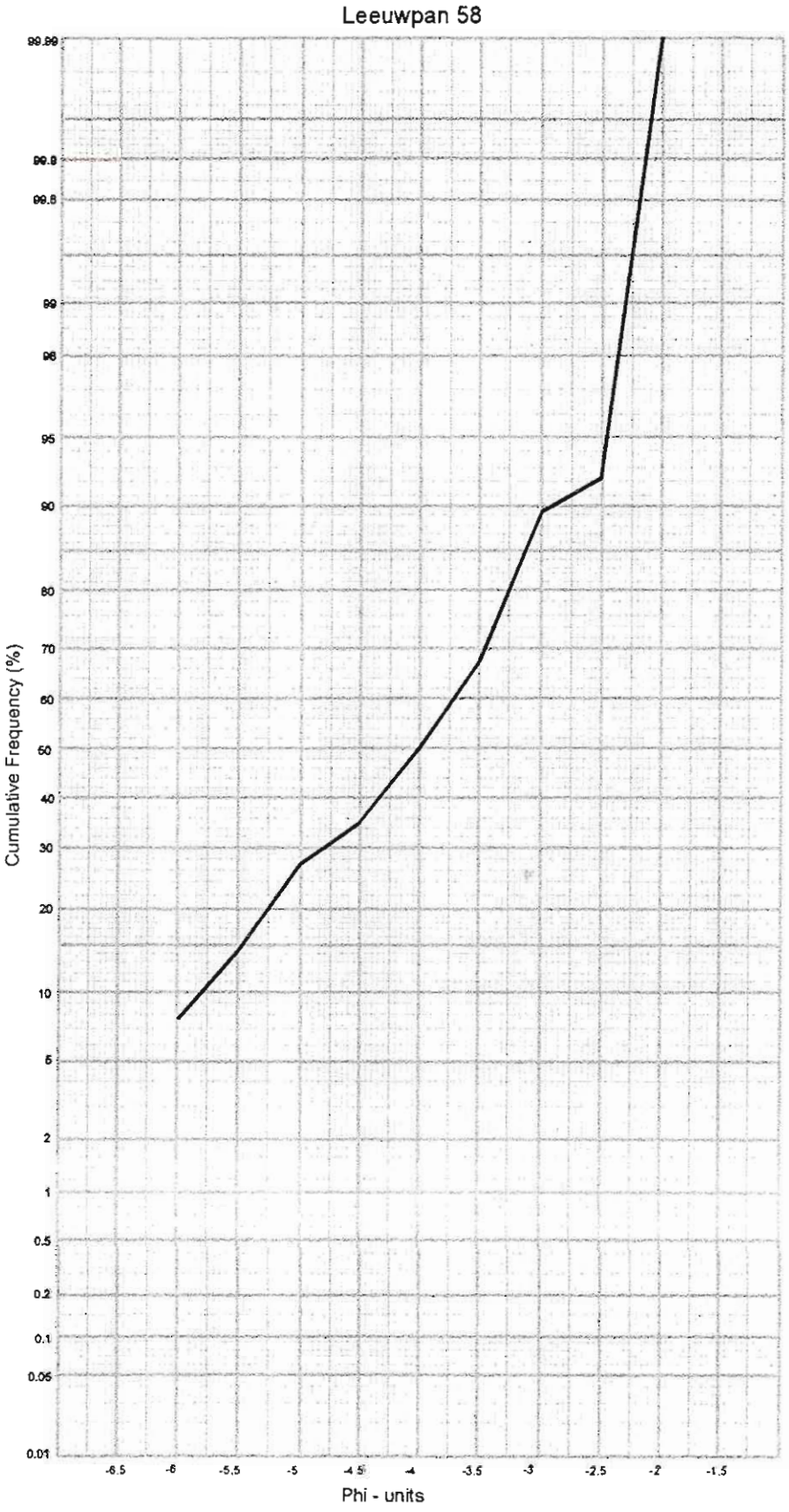
Leeuwpan 58
Cumulative Frequency (%)
99.99
99.9
99.8
99
98
95
90
80
70
60
50
40
30
20
10
5
2
1
0.5
0.2
0.1
0.05
0.01
-6.5
-6
-5.5
-5
-4.5
-4
-3.5
-3
-2.5
-2
-1.5
Phi - units

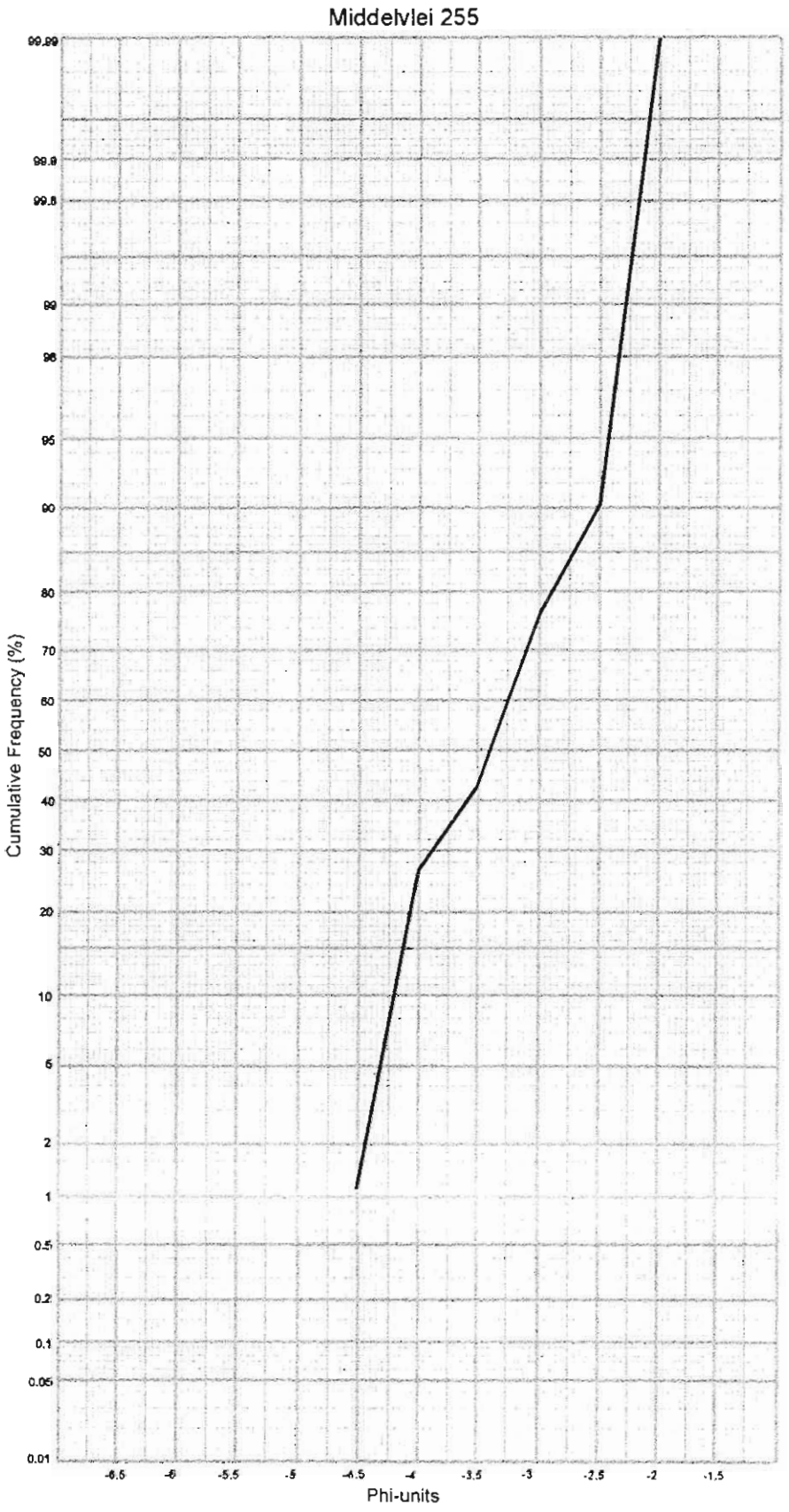
Middelvlei 255
Cumulative Frequency (%)
99.99
99.9
99.8
99
98
95
90
80
70
60
50
40
30
20
10
5
2
1
0.5
0.2
0.1
0.05
0.01
-6.5
-6
-5.5
-5
-4.5
-4
-3.5
-3
-2.5
-2
-1.5
Phi-units

Pebble roundness statistics of the Black Reef Quartzite Formation					
Wildfontein 52	**Bospan 58**	**Middelvlei 225**	**Wildfontein 52**	**Bospan 58**	**Middelvlei 225**
0.5	0.5	0.4	0.4	0.3	0.6
0.4	0.5	0.7	0.4	0.2	0.6
0.5	0.6	0.4	0.5	0.4	0.5
0.5	0.5	0.5	0.7	0.3	0.5
0.6	0.6	0.5	0.5	0.3	0.5
0.4	0.5	0.4	0.5	0.4	0.5
0.5	0.4	0.7	0.4	0.5	0.6
0.4	0.4	0.6	0.6	0.3	0.3
0.5	0.5	0.5	0.6	0.4	0.4
0.5	0.4	0.4	0.6	0.3	0.5
0.4	0.4	0.3	0.6	0.4	0.5
0.5	0.4	0.3	0.4	0.4	0.5
0.9	0.4	0.6	0.4	0.6	0.6
0.5	0.5	0.9	0.5	0.5	0.5
0.5	0.4	0.6	0.4	0.5	0.3
0.6	0.3	0.5	0.4	0.4	0.6
0.4	0.3	0.5	0.6	0.4	0.4
0.5	0.3	0.5	0.5	0.5	0.5
0.4	0.4	0.6	0.4	0.5	0.6
0.4	0.4	0.6	0.3	0.5	0.3
0.3	0.3	0.6	0.6	0.6	0.5
0.4	0.4	0.5	0.5	0.3	0.3
0.5	0.4	0.6	0.4	0.4	0.6
0.6	0.4	0.6	0.3	0.4	0.4
0.4	0.4	0.6	0.4	0.5	0.4
0.7	0.5	0.7	0.4		0.3
0.4	0.4	0.6	0.4		0.4
0.4	0.4	0.5	0.4		0.4
0.5	0.6	0.5	0.5		0.3
0.4	0.4	0.4	0.4		0.6
0.5	0.4	0.4	0.6		0.6
0.5	0.4	0.4	0.4		0.3
0.7	0.4	0.5	0.4		0.4
0.4	0.3	0.7	0.5		0.6
0.6	0.3	0.8	0.3		0.6
0.6	0.5	0.6	0.3		0.4
0.5	0.6	0.4	0.4		0.4
0.5	0.3	0.6	0.4		0.6
0.6	0.5	0.5	0.5		0.3
0.4	0.3	0.6	0.5		0.4
0.5	0.3	0.7	0.3		0.3
0.4	0.5	0.5	0.4		0.5
0.7	0.3	0.7	0.4		0.4
0.5	0.7	0.4	0.5		0.3
0.5	0.7	0.4	0.5		0.5
0.7	0.5	0.5	0.4		0.3
0.4	0.3	0.7	0.3		0.5
0.4	0.6	0.6	0.5		0.5
0.3	0.5	0.5	0.5		
0.5	0.5	0.5	0.5		
0.5	0.5	0.4	0.6		
0.3	0.5	0.5	0.4		
	Mean Pebble Roundness:		0.47	0.43	0.50

Middelvlei 255

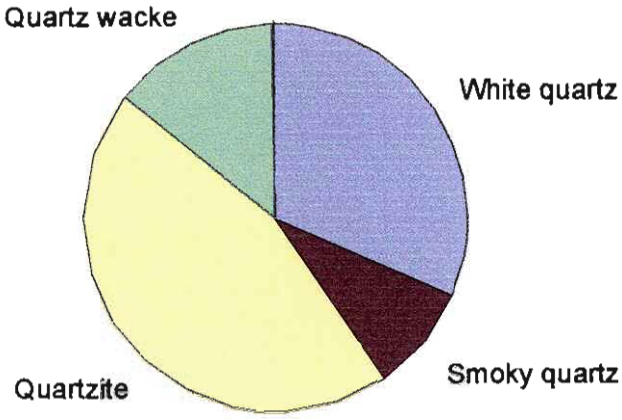

Wildfontein 52

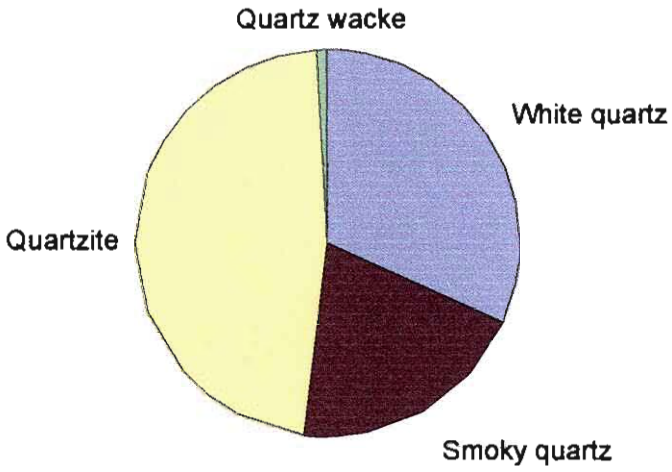

Leeuwfontein 58

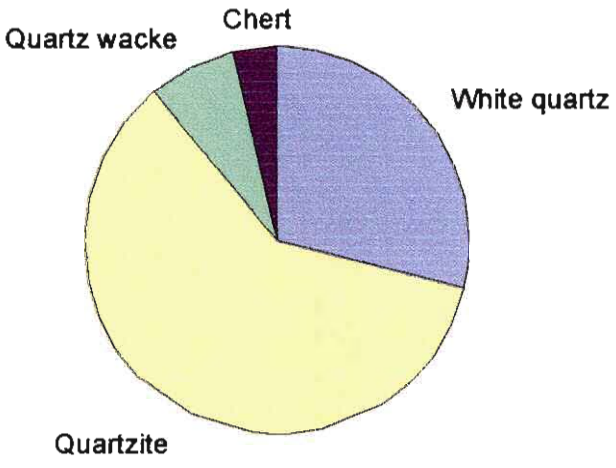

Appendix 7

Modal Analysis of Quartzites

Modal analysis of Quartzites in the Black Reef Quartzite Formation											
			Framework					Matrix			
Unit no.	Depth		Mono Quartz	Poli-quartz	Chert	Cloritoite	Opaque	Undifferentiable	Dolomite	Sericite	
1	390.33	500	40.2		0.8		0.2		58.4	0.4	
2	392.33	500	55.2	16	0.4		0.4		28		
3	393.16	500	5		1			2.2	92.8		
4	394.27	500	1.6					33.6	64.8		
5	394.88	500	79	4.4	5.6				11		
6	395.64	500	95.6	1.2					3.2		
7	396.11	500	58.4	10	15.4		0.2	9.2	5	1.8	
8	396.49	500	93.2	5	0.2		1.6				
9	398.48	500	90.2	2.4	6.2			1.2			
10	398.15	500	93	5.4	0.2		0.4				
11	399.54	500	82.4	5.4	1.8	1.2	0.6	6.4	2		
12	400.82	500	87.4	2.6	0.8		0.4	3.6	5.2		
13	401.4	500	67.2	3.4			0.2		29.2		
14	401.71	500	50.6	1.6				37.2		10.6	
15	401.96	500	96	2	0.4		0.2		1.4		
16	402.72	500	96.6	4.2			0.2				
17	403.24	500	96.4	2.4		0.2	0.4		0.6		
18	404.93	500	96	4							
19	405.02	500	79.2	2.8	1.8		0.4			15.8	

Classification of quartzites					
No.	Quartz	Lithic	Feldspar	Matrix	Class
1	97.6	2.4	0	58.8	Quartzwacke
2	98.9	1.1	0	28	Quartzwacke
3	83.3	16.7	0	95	Mudstone
4	100.0	0.0	0	98.4	Mudstone
5	93.7	6.3	0	11	Sublitharenite
6	100.0	0.0	0	3.2	Quartz arenite
7	81.4	18.6	0	16	Lithic greywacke
8	98.2	1.8	0	0	Quartz arenite
9	93.7	6.3	0	1.2	Lithic arenite
10	99.4	0.6	0	0	Quartz arenite
11	96.1	3.9	0	8.4	Quartz arenite
12	98.7	1.3	0	8.8	Quartz arenite
13	99.7	0.3	0	29.2	Quartzwacke
14	100.0	0.0	0	47.8	Quartzwacke
15	99.4	0.6	0	1.4	Quartz arenite
16	99.8	0.2	0	0	Quartz arenite
17	99.4	0.6	0	0.6	Quartz arenite
18	100.0	0.0	0	0	Quartz arenite
19	97.4	2.6	0	15.8	Quartzwacke

Appendix 8

Grain-size Data

Individual grain-size measurements for the different quartz beds in borehole BL8

1		2		3		5		6		7		8		9		10		11		12		13		14		15		16		17		18		19	
Long dimension (mm)	Short Dimension (mm)	Long dimension (mm)	Short Dimension (mm)	Long dimension (mm)	Short Dimension (mm)	Long dimension (mm)	Short Dimension (mm)	Long dimension (mm)	Short Dimension (mm)	Long dimension (mm)	Short Dimension (mm)	Long dimension (mm)	Short Dimension (mm)	Long dimension (mm)	Short Dimension (mm)	Long dimension (mm)	Short Dimension (mm)	Long dimension (mm)	Short Dimension (mm)	Long dimension (mm)	Short Dimension (mm)	Long dimension (mm)	Short Dimension (mm)	Long dimension (mm)	Short Dimension (mm)	Long dimension (mm)	Short Dimension (mm)	Long dimension (mm)	Short Dimension (mm)	Long dimension (mm)	Short Dimension (mm)	Long dimension (mm)	Short Dimension (mm)	Long dimension (mm)	Short Dimension (mm)
1.85	0.65	1.5	0.75	0.6	0.35	1.1	0.55	1.7	0.75	3.15	0.25	1.8	0.95	3.4	2.3	3.3	0.3	1.4	1	2.05	1.45	1.85	1.1	0.25	0.2	1.55	0.75	2.95	1.4	0.85	0.4	0.8	0.6	1.95	0.75
1.8	0.85	1.35	1.3	0.6	0.3	1.05	0.85	1.5	0.85	0.85	0.25	1.3	0.8	2.5	1.65	2.85	1.55	1.35	0.8	2.05	1.4	1.75	1.5	0.25	0.1	1.5	1.25	2.25	1.8	0.7	0.6	0.75	0.6	1.55	0.75
1.75	1.2	1.35	0.9	0.6	0.25	0.9	0.55	1.35	0.4	0.8	0.35	1.25	0.75	2.45	1.55	2.6	1.75	1.25	1.1	2	1.1	1.55	0.85	0.25	0.1	1.25	0.85	1.95	1.05	0.65	0.35	0.65	0.3	1.4	0.85
1.75	0.9	1.35	1.3	0.5	0.4	0.9	0.5	1.25	0.6	0.7	0.5	1.2	0.85	2.45	1.25	2.25	1.5	1.25	1.05	1.95	1	1.5	1.3	0.2	0.1	0.85	0.2	1.7	1.15	0.6	0.45	0.6	0.4	1.35	0.7
1.65	1.05	1.3	1.2	0.45	0.15	0.85	0.65	1.15	0.55	0.6	0.35	1.1	0.75	2.45	0.9	2.1	1.55	1.15	0.75	1.95	1.45	0.95	0.9	0.2	0.15	0.65	0.3	1.6	1.35	0.6	0.35	0.55	0.4	1.25	1
1.6	1.1	1.25	0.45	0.45	0.25	0.85	0.6	1.15	0.7	0.6	0.15	1.05	0.95	2.3	1.45	2	0.75	1.15	0.75	1.9	0.85	0.95	0.7	0.2	0.1	0.65	0.35	1.55	1.1	0.6	0.35	0.55	0.45	1.25	0.7
1.5	1.05	1.25	0.55	0.45	0.3	0.8	0.55	1.1	0.6	0.6	0.25	1	0.6	2.05	1.55	1.95	1.9	1.15	0.6	1.85	0.8	0.9	0.6	0.2	0.05	0.6	0.4	1.45	1.35	0.6	0.4	0.5	0.25	1.2	0.8
1.5	1.35	1.15	0.8	0.4	0.15	0.75	0.5	1.1	0.8	0.55	0.3	0.95	0.65	1.95	1.1	1.9	1.85	1.05	0.8	1.8	1.15	0.85	0.65	0.2	0.15	0.8	0.15	1.4	0.85	0.55	0.35	0.5	0.2	1.15	0.85
1.45	1	1.15	0.85	0.4	0.25	0.75	0.5	1.05	0.9	0.5	0.25	0.9	0.5	1.9	1.3	1.85	1.4	1	0.65	1.7	0.8	0.85	0.5	0.2	0.1	0.6	0.55	1.3	0.65	0.55	0.4	0.5	0.3	1.1	1.1
1.4	1.05	1.15	0.7	0.4	0.2	0.75	0.5	1.05	0.7	0.5	0.3	0.8	0.4	1.8	0.95	1.75	1.5	0.85	0.55	1.7	1	0.8	0.55	0.2	0.15	0.55	0.4	1.25	0.9	0.55	0.3	0.5	0.25	1.05	0.7
1.4	0.95	1.15	0.85	0.4	0.25	0.75	0.25	1.05	0.85	0.45	0.15	0.75	0.5	1.75	0.9	1.7	1.0	0.8	0.55	1.7	1.05	0.8	0.65	0.2	0.05	0.55	0.35	1.1	0.55	0.55	0.3	0.5	0.3	1	0.45
1.4	1.1	1.15	0.75	0.35	0.15	0.7	0.6	1	0.75	0.45	0.35	0.75	0.35	1.75	1.1	1.65	1.15	0.8	0.75	1.6	0.85	0.75	0.65	0.2	0.1	0.55	0.3	1.1	0.9	0.55	0.3	0.45	0.4	0.9	0.55
1.35	1.15	1.1	0.75	0.35	0.25	0.7	0.45	1	0.6	0.45	0.25	0.75	0.5	1.7	1.65	1.45	0.85	0.8	0.45	1.5	1.05	0.75	0.35	0.2	0.05	0.55	0.5	1	0.7	0.55	0.45	0.45	0.25	0.9	0.6
1.35	1.15	1.05	0.8	0.35	0.15	0.7	0.55	1	0.7	0.45	0.3	0.7	0.4	1.5	1.4	1.4	1	0.75	0.6	1.5	1.3	0.85	0.45	0.2	0.05	0.55	0.45	0.9	0.5	0.55	0.25	0.4	0.2	0.9	0.75
1.3	0.5	1.05	0.3	0.35	0.25	0.7	0.35	0.95	0.75	0.45	0.25	0.65	0.5	1.4	1	1.25	0.9	0.75	0.45	1.5	0.9	0.65	0.35	0.2	0.05	0.5	0.35	0.9	0.4	0.55	0.4	0.4	0.25	0.9	0.4
1.3	1	1.05	0.85	0.35	0.2	0.7	0.55	0.95	0.4	0.45	0.25	0.65	0.35	1.35	1.2	1.25	0.75	0.75	0.45	1.6	0.95	0.55	0.4	0.2	0.1	0.5	0.25	0.85	0.7	0.55	0.35	0.4	0.4	0.9	0.5
1.25	0.75	1	0.75	0.35	0.15	0.65	0.2	0.95	0.5	0.4	0.3	0.65	0.3	1.25	0.9	1.25	1	0.7	0.4	1.45	1	0.5	0.35	0.2	0.05	0.5	0.2	0.75	0.5	0.5	0.3	0.4	0.35	0.9	0.55
1.25	0.85	1	1	0.35	0.1	0.65	0.4	0.9	0.5	0.4	0.25	0.6	0.4	1.25	0.9	1.15	0.7	0.7	0.35	1.4	1.1	0.45	0.3	0.15	0.1	0.5	0.35	0.75	0.5	0.5	0.25	0.4	0.25	0.8	0.55
1.25	1.1	0.95	0.45	0.3	0.15	0.65	0.45	0.9	0.6	0.4	0.25	0.6	0.25	1.2	0.9	1.15	0.6	0.65	0.45	1.4	0.9	0.4	0.3	0.15	0.1	0.5	0.4	0.75	0.6	0.5	0.35	0.4	0.25	0.8	0.45
1.25	0.9	0.9	0.75	0.3	0.15	0.65	0.5	0.9	0.75	0.4	0.25	0.55	0.35	1.2	0.6	1.1	0.6	0.65	0.55	1.4	1.05	0.4	0.25	0.15	0.1	0.5	0.25	0.7	0.45	0.5	0.2	0.4	0.25	0.75	0.55
1.2	1.1	0.9	0.6	0.3	0.1	0.65	0.55	0.9	0.65	0.4	0.2	0.55	0.4	1.2	0.8	1.1	0.8	0.65	0.45	1.35	0.8	0.25	0.1	0.15	0.1	0.45	0.2	0.7	0.35	0.5	0.25	0.4	0.25	0.75	0.35
1.15	1.05	0.9	0.35	0.3	0.1	0.65	0.45	0.9	0.45	0.4	0.2	0.55	0.15	1.2	0.85	1.1	0.65	0.65	0.4	1.35	0.7	0.25	0.15	0.15	0.1	0.45	0.3	0.7	0.6	0.5	0.4	0.4	0.2	0.75	0.5
1.15	0.9	0.85	0.45	0.3	0.15	0.65	0.45	0.9	0.6	0.4	0.35	0.55	0.3	1.1	0.9	1.05	0.85	0.6	0.35	1.3	0.75	0.25	0.25	0.15	0.1	0.45	0.35	0.65	0.25	0.5	0.25	0.35	0.3	0.7	0.65
1.15	0.9	0.85	0.45	0.3	0.2	0.65	0.45	0.9	0.75	0.4	0.2	0.55	0.25	1.05	0.6	1.05	0.65	0.6	0.4	1.3	1.05	0.25	0.15	0.15	0.15	0.45	0.4	0.65	0.25	0.5	0.35	0.35	0.15	0.65	0.5
1.15	0.8	0.85	0.8	0.3	0.2	0.65	0.4	0.9	0.6	0.35	0.1	0.5	0.3	1.05	0.8	1	0.85	0.5	0.35	1.3	0.85	0.25	0.2	0.15	0.05	0.45	0.2	0.6	0.6	0.5	0.25	0.35	0.2	0.65	0.4
1.15	0.75	0.85	0.75	0.3	0.15	0.6	0.4	0.9	0.45	0.35	0.25	0.5	0.35	1.05	0.85	1	0.85	0.5	0.4	1.3	0.95	0.25	0.15	0.15	0.05	0.45	0.2	0.6	0.25	0.45	0.35	0.35	0.2	0.65	0.4
1.1	0.85	0.85	0.65	0.3	0.3	0.6	0.45	0.9	0.4	0.35	0.25	0.5	0.3	1.05	0.7	0.95	0.4	0.5	0.15	1.3	1	0.2	0.15	0.15	0.1	0.45	0.15	0.55	0.15	0.45	0.35	0.35	0.15	0.65	0.4
1.1	0.9	0.85	0.75	0.3	0.2	0.6	0.4	0.85	0.3	0.35	0.25	0.5	0.35	0.95	0.75	0.9	0.65	0.5	0.45	1.3	1.1	0.2	0.15	0.15	0.15	0.45	0.2	0.55	0.35	0.45	0.3	0.35	0.15	0.6	0.3
1.1	0.85	0.85	0.6	0.3	0.2	0.6	0.4	0.85	0.65	0.35	0.15	0.5	0.3	0.95	0.55	0.9	0.45	0.5	0.1	1.3	0.9	0.2	0.1	0.15	0.1	0.45	0.2	0.55	0.4	0.45	0.3	0.35	0.15	0.6	0.2
1.1	1.1	0.8	0.15	0.3	0.25	0.6	0.35	0.85	0.75	0.35	0.2	0.5	0.45	0.9	0.6	0.9	0.65	0.5	0.35	1.3	0.8	0.2	0.15	0.15	0.05	0.45	0.45	0.5	0.25	0.45	0.25	0.35	0.15	0.6	0.3
1.05	0.6	0.8	0.4	0.25	0.1	0.55	0.3	0.85	0.3	0.35	0.25	0.45	0.25	0.8	0.75	0.8	0.7	0.5	0.35	1.25	0.75	0.2	0.1	0.15	0.05	0.4	0.25	0.5	0.2	0.45	0.25	0.35	0.15	0.6	0.45
1.05	0.65	0.8	0.65	0.25	0.15	0.55	0.35	0.85	0.45	0.35	0.2	0.45	0.4	0.8	0.5	0.85	0.6	0.45	0.25	1.25	0.8	0.2	0.15	0.15	0.05	0.4	0.3	0.5	0.35	0.45	0.2	0.35	0.3	0.55	0.35
1	0.65	0.8	0.5	0.25	0.1	0.55	0.4	0.85	0.6	0.35	0.2	0.45	0.15	0.75	0.5	0.85	0.75	0.45	0.25	1.25	0.75	0.2	0.05	0.15	0.1	0.4	0.2	0.5	0.15	0.45	0.3	0.35	0.2	0.55	0.25
1	0.7	0.8	0.6	0.25	0.15	0.55	0.45	0.85	0.5	0.35	0.2	0.45	0.3	0.7	0.65	0.8	0.55	0.4	0.2	1.25	0.55	0.2	0.1	0.15	0.05	0.4	0.25	0.5	0.25	0.45	0.3	0.35	0.3	0.5	0.2
1	0.6	0.8	0.6	0.25	0.2	0.55	0.35	0.85	0.35	0.35	0.2	0.45	0.35	0.7	0.5	0.8	0.45	0.4	0.25	1.25	0.75	0.2	0.1	0.15	0.05	0.4	0.25	0.5	0.5	0.45	0.4	0.35	0.15	0.5	0.35
1	0.85	0.75	0.6	0.25	0.2	0.5	0.45	0.85	0.4	0.3	0.2	0.45	0.2	0.6	0.3	0.75	0.5	0.4	0.2	1.2	1.05	0.2	0.05	0.15	0.05	0.4	0.35	0.45	0.45	0.4	0.3	0.35	0.15	0.5	0.25
1	0.75	0.75	0.5	0.25	0.15	0.5	0.45	0.8	0.75	0.3	0.25	0.45	0.35	0.55	0.35	0.75	0.55	0.4	0.15	1.2	1	0.2	0.1	0.15	0.05	0.4	0.25	0.45	0.3	0.4	0.2	0.35	0.2	0.5	0.25
1	0.9	0.75	0.6	0.25	0.15	0.5	0.2	0.8	0.05	0.3	0.15	0.45	0.25	0.55	0.3	0.75	0.5	0.4	0.35	1.15	0.65	0.2	0.15	0.15	0.1	0.4	0.35	0.45	0.25	0.4	0.25	0.35	0.15	0.5	0.3
0.95	0.7	0.75	0.35	0.25	0.25	0.5	0.2	0.8	0.6	0.3	0.2	0.45	0.25	0.55	0.45	0.75	0.5	0.4	0.2	1.15	1	0.2	0.1	0.15	0.05	0.4	0.3	0.45	0.25	0.4	0.25	0.35	0.3	0.45	0.25
0.95	0.7	0.75	0.4	0.25	0.2	0.5	0.3	0.8	0.45	0.3	0.2	0.45	0.35	0.5	0.25	0.7	0.4	0.4	0.25	1.15	0.4	0.2	0.1	0.15	0.05	0.4	0.35	0.45	0.15	0.4	0.25	0.35	0.2	0.4	0.25
0.95	0.6	0.75	0.5	0.25	0.15	0.5	0.35	0.8	0.65	0.3	0.15	0.4	0.25	0.45	0.3	0.7	0.45	0.4	0.2	1.1	0.65	0.2	0.1	0.15	0.1	0.4	0.35	0.4	0.3	0.4	0.15	0.35	0.3	0.4	0.3
0.9	0.55	0.7	0.35	0.25	0.15	0.5	0.3	0.8	0.35	0.3	0.15	0.4	0.25	0.4	0.3	0.7	0.4	0.4	0.25	1.1	0.65	0.2	0.15	0.15	0.05	0.4	0.2	0.4	0.25	0.4	0.2	0.35	0.25	0.4	0.2
0.9	0.65	0.7	0.4	0.25	0.2	0.5	0.45	0.75	0.55	0.3	0.25	0.4	0.35	0.35	0.2	0.7	0.5	0.4	0.2	1.1	0.65	0.15	0.1	0.15	0.1	0.4	0.35	0.4	0.25	0.4	0.2	0.35	0.25	0.4	0.2
0.9	0.7	0.7	0.5	0.75	0.15	0.45	0.4	0.75	0.7	0.3	0.3	0.4	0.2	0.35	0.25	0.7	0.35	0.4	0.25	1.1	0.6	0.15	0.1	0.15	0.1	0.4	0.2	0.35	0.25	0.4	0.2	0.35	0.25	0.4	0.2

1		2		3		5		6		7		8		9		10		11		12		13		14		15		16		17		18		19	
Long dimension (mm)	Short Dimension (mm)	Long dimension (mm)	Short Dimension (mm)	Long dimension (mm)	Short Dimension (mm)	Long dimension (mm)	Short Dimension (mm)	Long dimension (mm)	Short Dimension (mm)	Long dimension (mm)	Short Dimension (mm)	Long dimension (mm)	Short Dimension (mm)	Long dimension (mm)	Short Dimension (mm)	Long dimension (mm)	Short Dimension (mm)	Long dimension (mm)	Short Dimension (mm)	Long dimension (mm)	Short Dimension (mm)	Long dimension (mm)	Short Dimension (mm)	Long dimension (mm)	Short Dimension (mm)	Long dimension (mm)	Short Dimension (mm)	Long dimension (mm)	Short Dimension (mm)	Long dimension (mm)	Short Dimension (mm)	Long dimension (mm)	Short Dimension (mm)
0.9	0.4	0.7	0.55	0.25	0.2	0.45	0.25	0.75	0.55	0.3	0.15	0.4	0.3	0.35	0.25	0.65	0.4	0.4	0.3	1.1	0.8	0.15	0.05	0.15	0.1	0.35	0.15	0.35	0.2	0.4	0.3	0.3	0.15	0.4	0.25
0.9	0.55	0.7	0.6	0.25	0.25	0.45	0.25	0.75	0.5	0.3	0.1	0.4	0.35	0.3	0.1	0.65	0.5	0.4	0.15	1.1	0.55	0.15	0.1	0.15	0.1	0.35	0.35	0.35	0.2	0.4	0.15	0.3	0.2	0.4	0.35
0.9	0.55	0.65	0.65	0.25	0.15	0.45	0.2	0.75	0.6	0.3	0.1	0.4	0.3	0.3	0.2	0.65	0.3	0.4	0.15	1.05	0.6	0.15	0.1	0.15	0.1	0.35	0.15	0.35	0.15	0.4	0.3	0.3	0.3	0.4	0.35
0.9	0.75	0.65	0.25	0.25	0.2	0.45	0.25	0.75	0.6	0.3	0.2	0.4	0.35	0.3	0.15	0.65	0.5	0.35	0.15	1.05	1	0.15	0.1	0.15	0.1	0.35	0.15	0.35	0.15	0.4	0.35	0.3	0.25	0.4	0.1
0.85	0.55	0.65	0.25	0.25	0.2	0.45	0.35	0.75	0.75	0.3	0.25	0.4	0.25	0.3	0.3	0.65	0.55	0.35	0.2	1.05	0.95	0.15	0.1	0.15	0.15	0.35	0.25	0.35	0.2	0.4	0.25	0.3	0.2	0.4	0.25
0.85	0.8	0.65	0.3	0.25	0.2	0.45	0.35	0.75	0.5	0.3	0.15	0.4	0.25	0.3	0.15	0.65	0.35	0.35	0.15	1.05	0.65	0.15	0.1	0.15	0.15	0.35	0.2	0.35	0.25	0.4	0.15	0.3	0.3	0.4	0.15
0.8	0.6	0.65	0.45	0.25	0.2	0.4	0.25	0.75	0.4	0.3	0.15	0.4	0.3	0.3	0.1	0.65	0.45	0.35	0.25	1.05	0.75	0.15	0.05	0.15	0.1	0.35	0.2	0.35	0.1	0.4	0.15	0.3	0.25	0.4	0.25
0.8	0.6	0.65	0.4	0.25	0.1	0.4	0.2	0.75	0.65	0.3	0.15	0.35	0.3	0.25	0.1	0.6	0.45	0.35	0.3	1.05	0.8	0.15	0.15	0.15	0.1	0.35	0.25	0.35	0.15	0.4	0.25	0.3	0.25	0.35	0.25
0.75	0.5	0.65	0.4	0.25	0.2	0.4	0.3	0.75	0.55	0.3	0.25	0.35	0.35	0.25	0.15	0.6	0.45	0.35	0.2	1	0.8	0.15	0.1	0.15	0.05	0.35	0.2	0.3	0.25	0.4	0.3	0.3	0.2	0.35	0.3
0.75	0.7	0.65	0.25	0.2	0.15	0.4	0.3	0.75	0.55	0.3	0.2	0.35	0.3	0.25	0.1	0.6	0.5	0.35	0.25	1	0.65	0.15	0.05	0.15	0.05	0.35	0.15	0.3	0.2	0.4	0.3	0.3	0.15	0.35	0.35
0.75	0.5	0.65	0.5	0.2	0.2	0.4	0.15	0.75	0.6	0.25	0.1	0.35	0.2	0.25	0.2	0.6	0.3	0.35	0.25	1	0.55	0.15	0.1	0.15	0.05	0.35	0.25	0.3	0.25	0.35	0.25	0.3	0.15	0.35	0.25
0.75	0.65	0.6	0.35	0.2	0.15	0.4	0.3	0.75	0.6	0.25	0.2	0.35	0.3	0.25	0.2	0.6	0.5	0.35	0.3	1	0.75	0.15	0.1	0.1	0.05	0.35	0.15	0.3	0.2	0.35	0.35	0.3	0.2	0.35	0.2
0.75	0.6	0.6	0.3	0.2	0.15	0.4	0.15	0.75	0.45	0.25	0.15	0.35	0.25	0.25	0.15	0.55	0.45	0.35	0.25	1	1	0.15	0.1	0.1	0.1	0.3	0.15	0.3	0.2	0.35	0.3	0.3	0.25	0.35	0.25
0.75	0.5	0.6	0.3	0.2	0.1	0.4	0.3	0.75	0.45	0.25	0.2	0.35	0.2	0.2	0.15	0.55	0.5	0.35	0.2	1	0.8	0.15	0.1	0.1	0.05	0.3	0.2	0.3	0.25	0.35	0.35	0.3	0.2	0.35	0.2
0.75	0.65	0.6	0.45	0.2	0.15	0.35	0.3	0.75	0.4	0.25	0.1	0.35	0.2	0.2	0.15	0.55	0.35	0.35	0.25	1	0.9	0.15	0.1	0.1	0.1	0.3	0.2	0.3	0.2	0.35	0.3	0.3	0.2	0.3	0.2
0.75	0.55	0.6	0.55	0.2	0.15	0.35	0.25	0.75	0.55	0.25	0.2	0.3	0.2	0.2	0.15	0.55	0.45	0.35	0.25	1	0.65	0.15	0.05	0.1	0.05	0.3	0.25	0.3	0.15	0.35	0.25	0.3	0.2	0.3	0.25
0.75	0.4	0.6	0.35	0.2	0.1	0.35	0.15	0.7	0.55	0.25	0.15	0.3	0.15	0.2	0.15	0.55	0.25	0.35	0.2	1	0.9	0.15	0.1	0.1	0.1	0.3	0.25	0.3	0.25	0.35	0.15	0.3	0.25	0.3	0.15
0.75	0.65	0.6	0.3	0.2	0.05	0.35	0.25	0.7	0.45	0.25	0.2	0.3	0.2	0.2	0.15	0.55	0.35	0.35	0.35	1	0.65	0.15	0.05	0.1	0.1	0.3	0.2	0.3	0.2	0.35	0.05	0.3	0.25	0.3	0.2
0.75	0.6	0.55	0.4	0.2	0.15	0.35	0.3	0.7	0.45	0.25	0.1	0.3	0.2	0.2	0.15	0.55	0.4	0.35	0.3	1	0.7	0.15	0.1	0.1	0.1	0.3	0.15	0.3	0.2	0.35	0.2	0.3	0.2	0.3	0.15
0.75	0.7	0.55	0.35	0.2	0.15	0.35	0.15	0.7	0.55	0.25	0.25	0.3	0.25	0.2	0.15	0.55	0.45	0.3	0.2	0.65	0.55	0.15	0.05	0.1	0.05	0.3	0.15	0.3	0.2	0.35	0.3	0.3	0.2	0.3	0.3
0.7	0.4	0.55	0.25	0.2	0.2	0.35	0.25	0.7	0.7	0.25	0.2	0.3	0.25	0.2	0.15	0.5	0.4	0.3	0.25	0.65	0.6	0.15	0.05	0.1	0.05	0.3	0.2	0.3	0.25	0.35	0.2	0.3	0.15	0.3	0.15
0.7	0.55	0.55	0.35	0.2	0.1	0.35	0.35	0.7	0.4	0.25	0.1	0.3	0.2	0.2	0.15	0.5	0.35	0.3	0.2	0.9	0.9	0.15	0.05	0.1	0.05	0.3	0.2	0.3	0.15	0.35	0.25	0.3	0.2	0.3	0.25
0.7	0.45	0.55	0.35	0.2	0.15	0.35	0.3	0.7	0.55	0.25	0.15	0.3	0.1	0.2	0.15	0.5	0.3	0.3	0.15	0.9	0.75	0.15	0.1	0.1	0.05	0.3	0.2	0.3	0.25	0.35	0.15	0.3	0.15	0.3	0.2
0.7	0.6	0.55	0.3	0.2	0.15	0.35	0.3	0.7	0.55	0.25	0.15	0.25	0.1	0.2	0.1	0.5	0.3	0.3	0.2	0.9	0.55	0.15	0.1	0.1	0.05	0.3	0.25	0.25	0.15	0.35	0.15	0.25	0.15	0.3	0.15
0.7	0.7	0.55	0.45	0.2	0.2	0.35	0.25	0.7	0.7	0.25	0.15	0.25	0.15	0.2	0.2	0.5	0.3	0.3	0.25	0.9	0.8	0.15	0.1	0.1	0.1	0.3	0.2	0.25	0.2	0.35	0.2	0.25	0.15	0.3	0.15
0.7	0.4	0.55	0.35	0.2	0.1	0.35	0.3	0.7	0.6	0.25	0.1	0.25	0.15	0.2	0.15	0.5	0.25	0.3	0.25	0.9	0.6	0.15	0.1	0.1	0.05	0.3	0.25	0.25	0.2	0.35	0.25	0.25	0.2	0.25	0.2
0.7	0.35	0.5	0.25	0.2	0.15	0.35	0.2	0.65	0.3	0.25	0.1	0.25	0.2	0.2	0.15	0.5	0.45	0.3	0.15	0.9	0.5	0.15	0.1	0.1	0.05	0.3	0.2	0.25	0.15	0.35	0.3	0.25	0.2	0.25	0.2
0.7	0.6	0.5	0.2	0.2	0.1	0.35	0.25	0.65	0.35	0.25	0.1	0.25	0.2	0.2	0.05	0.5	0.3	0.3	0.2	0.9	0.5	0.15	0.1	0.1	0.1	0.3	0.1	0.25	0.1	0.35	0.15	0.25	0.2	0.25	0.15
0.65	0.55	0.5	0.45	0.2	0.15	0.3	0.2	0.65	0.25	0.25	0.15	0.25	0.25	0.2	0.15	0.5	0.35	0.3	0.25	0.8	0.5	0.15	0.1	0.1	0.05	0.3	0.1	0.25	0.2	0.35	0.25	0.25	0.15	0.25	0.2
0.65	0.55	0.5	0.35	0.2	0.15	0.3	0.25	0.65	0.55	0.25	0.2	0.25	0.2	0.2	0.1	0.45	0.4	0.3	0.25	0.8	0.25	0.15	0.1	0.1	0.05	0.3	0.25	0.25	0.2	0.35	0.2	0.25	0.2	0.25	0.15
0.65	0.55	0.5	0.4	0.2	0.1	0.3	0.1	0.65	0.45	0.25	0.15	0.25	0.15	0.15	0.1	0.45	0.3	0.25	0.2	0.8	0.55	0.15	0.1	0.1	0.05	0.3	0.15	0.25	0.1	0.35	0.3	0.25	0.25	0.25	0.15
0.65	0.45	0.5	0.2	0.2	0.15	0.3	0.15	0.65	0.5	0.2	0.15	0.25	0.15	0.15	0.05	0.45	0.25	0.25	0.15	0.75	0.35	0.15	0.1	0.1	0.05	0.3	0.2	0.25	0.2	0.35	0.2	0.25	0.15	0.25	0.1
0.65	0.3	0.5	0.4	0.2	0.05	0.3	0.2	0.65	0.35	0.2	0.15	0.25	0.1	0.15	0.1	0.45	0.35	0.25	0.1	0.75	0.5	0.15	0.05	0.1	0.1	0.25	0.1	0.25	0.1	0.3	0.3	0.25	0.2	0.25	0.2
0.65	0.4	0.5	0.35	0.2	0.1	0.3	0.15	0.65	0.5	0.2	0.15	0.25	0.1	0.15	0.05	0.45	0.25	0.25	0.2	0.75	0.6	0.15	0.1	0.1	0.05	0.25	0.15	0.25	0.2	0.3	0.15	0.25	0.25	0.25	0.15
0.65	0.35	0.5	0.35	0.2	0.1	0.3	0.2	0.65	0.4	0.2	0.1	0.25	0.15	0.15	0.1	0.4	0.35	0.25	0.2	0.75	0.45	0.15	0.1	0.1	0.05	0.25	0.2	0.25	0.15	0.3	0.25	0.25	0.2	0.25	0.2
0.65	0.5	0.5	0.5	0.2	0.1	0.3	0.2	0.65	0.3	0.2	0.15	0.25	0.2	0.15	0.1	0.4	0.35	0.25	0.1	0.75	0.6	0.15	0.1	0.1	0.05	0.25	0.25	0.2	0.15	0.3	0.2	0.25	0.15	0.25	0.1
0.6	0.35	0.45	0.35	0.2	0.15	0.25	0.1	0.6	0.5	0.2	0.2	0.25	0.2	0.15	0.1	0.4	0.25	0.25	0.15	0.7	0.45	0.15	0.15	0.1	0.05	0.25	0.1	0.2	0.1	0.3	0.2	0.25	0.15	0.25	0.1
0.6	0.4	0.45	0.35	0.2	0.1	0.25	0.2	0.6	0.55	0.2	0.1	0.25	0.25	0.15	0.1	0.4	0.3	0.25	0.2	0.7	0.55	0.15	0.1	0.1	0.05	0.25	0.1	0.2	0.1	0.3	0.2	0.25	0.1	0.25	0.2
0.6	0.55	0.45	0.25	0.15	0.1	0.25	0.15	0.6	0.5	0.2	0.2	0.2	0.1	0.15	0.1	0.4	0.25	0.25	0.1	0.65	0.4	0.1	0.05	0.1	0.05	0.25	0.1	0.2	0.15	0.3	0.2	0.25	0.2	0.25	0.1
0.6	0.35	0.45	0.3	0.15	0.1	0.25	0.15	0.6	0.3	0.2	0.2	0.2	0.15	0.15	0.1	0.4	0.25	0.25	0.15	0.65	0.55	0.1	0.05	0.1	0.05	0.25	0.2	0.2	0.15	0.3	0.2	0.25	0.15	0.25	0.2
0.6	0.35	0.45	0.25	0.15	0.05	0.25	0.2	0.6	0.4	0.2	0.15	0.2	0.2	0.15	0.1	0.4	0.25	0.25	2.2	0.65	0.65	0.1	0.1	0.1	0.1	0.25	0.15	0.2	0.1	0.3	0.2	0.25	0.15	0.25	0.15
0.6	0.5	0.45	0.25	0.15	0.1	0.25	0.2	0.6	0.6	0.2	0.15	0.2	0.2	0.15	0.1	0.4	0.3	0.25	0.2	0.65	0.4	0.1	0.1	0.1	0.1	0.25	0.1	0.2	0.1	0.3	0.2	0.25	0.15	0.2	0.15
0.6	0.45	0.45	0.25	0.15	0.15	0.25	0.2	0.6	0.35	0.2	0.15	0.2	0.15	0.15	0.1	0.35	0.25	0.2	0.15	0.65	0.4	0.1	0.1	0.1	0.05	0.25	0.25	0.2	0.15	0.3	0.2	0.25	0.2	0.2	0.15
0.6	0.5	0.45	0.25	0.15	0.1	0.25	0.15	0.6	0.25	0.2	0.15	0.2	0.1	0.15	0.1	0.35	0.2	0.2	0.1	0.6	0.45	0.1	0.1	0.1	0.05	0.25	0.2	0.2	0.15	0.3	0.25	0.25	0.2	0.2	0.15
0.55	0.25	0.45	0.25	0.15	0.1	0.25	0.15	0.6	0.35	0.2	0.15	0.2	0.15	0.15	0.1	0.35	0.15	0.2	0.1	0.6	0.5	0.1	0.1	0.1	0.05	0.25	0.25	0.2	0.15	0.3	0.25	0.25	0.2	0.2	0.15
0.55	0.45	0.45	0.2	0.15	0.15	0.25	0.25	0.6	0.3	0.2	0.1	0.2	0.15	0.15	0.1	0.35	0.15	0.2	0.15	0.6	0.4	0.1	0.1	0.1	0.1	0.25	0.2	0.2	0.15	0.3	0.15	0.25	0.2	0.2	0.15

1		2		3		5		6		7		8		9		10		11		12		13		14		15		16		17		18		19	
Long dimension (mm)	Short Dimension (mm)	Long dimension (mm)	Short Dimension (mm)	Long dimension (mm)	Short Dimension (mm)	Long dimension (mm)	Short Dimension (mm)	Long dimension (mm)	Short Dimension (mm)	Long dimension (mm)	Short Dimension (mm)	Long dimension (mm)	Short Dimension (mm)	Long dimension (mm)	Short Dimension (mm)	Long dimension (mm)	Short Dimension (mm)	Long dimension (mm)	Short Dimension (mm)	Long dimension (mm)	Short Dimension (mm)	Long dimension (mm)	Short Dimension (mm)	Long dimension (mm)	Short Dimension (mm)	Long dimension (mm)	Short Dimension (mm)	Long dimension (mm)	Short Dimension (mm)	Long dimension (mm)	Short Dimension (mm)	Long dimension (mm)	Short Dimension (mm)
0.55	0.45	0.45	0.25	0.15	0.15	0.25	0.15	0.6	0.4	0.2	0.15	0.2	0.1	0.15	0.1	0.35	0.25	0.2	0.15	0.6	0.25	0.1	0.1	0.1	0.05	0.25	0.2	0.2	0.05	0.3	0.2	0.25	0.2	0.2	0.15
0.55	0.35	0.4	0.25	0.15	0.05	0.25	0.15	0.55	0.35	0.2	0.2	0.2	0.2	0.15	0.1	0.35	0.2	0.2	0.15	0.6	0.4	0.1	0.1	0.1	0.05	0.25	0.1	0.2	0.15	0.3	0.2	0.25	0.2	0.2	0.15
0.55	0.3	0.4	0.25	0.15	0.1	0.25	0.15	0.55	0.45	0.2	0.2	0.2	0.1	0.15	0.1	0.35	0.3	0.2	0.15	0.6	0.4	0.1	0.1	0.1	0.05	0.25	0.15	0.2	0.1	0.3	0.25	0.25	0.2	0.2	0.15
0.55	0.3	0.4	0.25	0.15	0.1	0.25	0.2	0.55	0.35	0.2	0.1	0.2	0.1	0.15	0.1	0.35	0.2	0.2	0.15	0.55	0.5	0.1	0.05	0.1	0.1	0.25	0.15	0.2	0.1	0.3	0.25	0.25	0.15	0.2	0.2
0.5	0.5	0.4	0.25	0.15	0.1	0.2	0.15	0.5	0.35	0.2	0.05	0.2	0.1	0.15	0.1	0.35	0.2	0.2	0.2	0.55	0.3	0.1	0.1	0.1	0.1	0.25	0.2	0.2	0.2	0.25	0.15	0.25	0.2	0.2	0.15
0.5	0.25	0.4	0.35	0.15	0.15	0.2	0.15	0.5	0.35	0.15	0.15	0.2	0.15	0.15	0.15	0.35	0.25	0.2	0.15	0.55	0.3	0.1	0.1	0.1	0.05	0.2	0.2	0.2	0.1	0.25	0.2	0.25	0.2	0.2	0.15
0.5	0.3	0.4	0.25	0.15	0.05	0.2	0.1	0.5	0.3	0.15	0.1	0.2	0.2	0.15	0.1	0.35	0.25	0.2	0.15	0.55	0.35	0.1	0.1	0.1	0.05	0.2	0.2	0.2	0.15	0.25	0.2	0.25	0.15	0.2	0.1
0.5	0.45	0.4	0.35	0.15	0.05	0.2	0.15	0.5	0.45	0.15	0.1	0.2	0.15	0.15	0.1	0.35	0.25	0.2	0.15	0.5	0.3	0.1	0.1	0.1	0.1	0.2	0.2	0.2	0.15	0.25	0.15	0.2	0.15	0.2	0.15
0.45	0.25	0.4	0.3	0.15	0.05	0.2	0.2	0.5	0.3	0.15	0.15	0.2	0.1	0.15	0.05	0.35	0.25	0.2	0.15	0.5	0.35	0.1	0.1	0.1	0.05	0.2	0.25	0.15	0.15	0.25	0.25	0.2	0.15	0.2	0.1
0.45	0.45	0.4	0.25	0.15	0.1	0.2	0.15	0.5	0.5	0.15	0.1	0.2	0.1	0.15	0.15	0.35	0.15	0.2	0.1	0.45	0.45	0.1	0.05	0.1	0.05	0.2	0.15	0.15	0.15	0.25	0.2	0.2	0.15	0.2	0.1
0.45	0.3	0.4	0.25	0.15	0.1	0.2	0.15	0.5	0.35	0.15	0.15	0.2	0.1	0.15	0.15	0.35	0.3	0.2	0.1	0.45	0.2	0.1	0.05	0.1	0.05	0.2	0.15	0.15	0.05	0.25	0.2	0.2	0.2	0.15	0.15
0.45	0.35	0.4	0.3	0.15	0.05	0.2	0.15	0.5	0.35	0.15	0.15	0.2	0.1	0.15	0.1	0.35	0.25	0.2	0.1	0.45	0.35	0.1	0.1	0.1	0.1	0.2	0.15	0.15	0.1	0.25	0.2	0.2	0.15	0.15	0.1
0.45	0.45	0.4	0.35	0.15	0.1	0.2	0.15	0.5	0.5	0.15	0.15	0.2	0.15	0.1	0.05	0.35	0.2	0.2	0.15	0.45	0.25	0.1	0.05	0.1	0.1	0.2	0.15	0.15	0.15	0.25	0.2	0.2	0.2	0.15	0.15
0.4	0.25	0.4	0.15	0.15	0.1	0.2	0.15	0.5	0.4	0.15	0.15	0.2	0.1	0.1	0.05	0.35	0.3	0.2	0.15	0.45	0.3	0.1	0.1	0.1	0.05	0.2	0.15	0.15	0.1	0.25	0.2	0.2	0.15	0.15	0.1
0.4	0.35	0.4	0.3	0.15	0.1	0.2	0.15	0.5	0.35	0.15	0.1	0.2	0.1	0.1	0.05	0.35	0.2	0.2	0.15	0.45	0.3	0.1	0.1	0.1	0.05	0.2	0.1	0.15	0.15	0.25	0.15	0.2	0.2	0.15	0.1
0.4	0.3	0.4	0.25	0.15	0.15	0.2	0.2	0.5	0.35	0.15	0.05	0.2	0.1	0.1	0.05	0.3	0.2	0.2	0.15	0.4	0.3	0.1	0.05	0.1	0.05	0.2	0.1	0.15	0.05	0.25	0.2	0.2	0.15	0.15	0.1
0.4	0.15	0.4	0.25	0.15	0.1	0.2	0.15	0.45	0.3	0.15	0.1	0.2	0.1	0.1	0.1	0.3	0.15	0.2	0.15	0.4	0.3	0.1	0.1	0.1	0.05	0.2	0.2	0.15	0.1	0.25	0.25	0.2	0.2	0.15	0.15
0.4	0.3	0.35	0.3	0.1	0.2	0.2	0.15	0.45	0.2	0.15	0.1	0.2	0.15	0.1	0.1	0.3	0.2	0.2	0.15	0.4	0.25	0.1	0.1	0.1	0.05	0.2	0.2	0.15	0.05	0.25	0.2	0.2	0.15	0.15	0.15
0.35	0.15	0.35	0.15	0.1	0.05	0.2	0.15	0.45	0.25	0.15	0.15	0.15	0.05	0.1	0.1	0.3	0.1	0.2	0.1	0.4	0.3	0.1	0.05	0.1	0.05	0.2	0.15	0.15	0.15	0.25	0.1	0.2	0.15	0.15	0.05
0.35	0.2	0.35	0.25	0.1	0.05	0.2	0.15	0.45	0.25	0.15	0.1	0.15	0.1	0.1	0.05	0.3	0.3	0.2	0.2	0.4	0.3	0.1	0.05	0.1	0.05	0.2	0.15	0.15	0.15	0.25	0.25	0.2	0.2	0.15	0.1
0.35	0.25	0.35	0.25	0.1	0.05	0.2	0.2	0.4	0.35	0.15	0.15	0.15	0.1	0.1	0.05	0.3	0.25	0.15	0.15	0.4	0.25	0.1	0.05	0.1	0.05	0.2	0.15	0.15	0.15	0.25	0.15	0.2	0.15	0.15	0.15
0.35	0.25	0.35	0.2	0.1	0.05	0.2	0.2	0.4	0.25	0.15	0.1	0.15	0.1	0.1	0.1	0.3	0.3	0.15	0.1	0.4	0.2	0.1	0.15	0.1	0.05	0.2	0.2	0.15	0.1	0.25	0.15	0.2	0.15	0.15	0.1
0.35	0.2	0.35	0.25	0.1	0.1	0.2	0.15	0.4	0.35	0.15	0.1	0.15	0.05	0.1	0.1	0.3	0.2	0.15	0.1	0.4	0.25	0.1	0.1	0.05	0.05	0.2	0.15	0.15	0.15	0.25	0.2	0.2	0.15	0.15	0.1
0.3	0.15	0.35	0.15	0.1	0.05	0.15	0.1	0.4	0.35	0.15	0.05	0.15	0.15	0.1	0.1	0.3	0.15	0.15	0.1	0.4	0.2	0.1	0.1	0.05	0.05	0.2	0.1	0.15	0.1	0.25	0.2	0.2	0.15	0.15	0.15
0.3	0.25	0.35	0.2	0.1	0.05	0.15	0.1	0.4	0.25	0.15	0.1	0.15	0.1	0.1	0.1	0.3	0.2	0.15	0.1	0.4	0.3	0.1	0.05	0.05	0.05	0.15	0.15	0.15	0.15	0.25	0.15	0.2	0.1	0.15	0.05
0.3	0.25	0.35	0.2	0.1	0.05	0.15	0.05	0.4	0.4	0.15	0.1	0.15	0.1	0.1	0.05	0.3	0.25	0.15	0.1	0.4	0.25	0.1	0.05	0.05	0.05	0.15	0.1	0.15	0.15	0.25	0.15	0.2	0.15	0.15	0.05
0.3	0.25	0.35	0.15	0.1	0.05	0.15	0.1	0.4	0.25	0.15	0.15	0.15	0.1	0.1	0.1	0.25	0.2	0.15	0.15	0.4	0.3	0.1	0.1	0.05	0.05	0.15	0.1	0.15	0.15	0.25	0.15	0.2	0.1	0.15	0.15
0.3	0.25	0.35	0.25	0.1	0.05	0.15	0.1	0.4	0.2	0.1	0.05	0.15	0.1	0.1	0.05	0.25	0.2	0.15	0.05	0.35	0.2	0.1	0.1	0.05	0.05	0.15	0.1	0.15	0.1	0.25	0.15	0.2	0.15	0.15	0.15
0.25	0.15	0.35	0.35	0.1	0.1	0.15	0.15	0.4	0.25	0.1	0.05	0.15	0.15	0.1	0.1	0.25	0.2	0.15	0.1	0.35	0.1	0.1	0.1	0.05	0.05	0.15	0.1	0.15	0.1	0.25	0.25	0.2	0.1	0.15	0.15
0.25	0.15	0.3	0.25	0.1	0.1	0.15	0.1	0.35	0.15	0.1	0.05	0.15	0.1	0.1	0.05	0.25	0.16	0.15	0.15	0.35	0.2	0.1	0.1	0.05	0.05	0.15	0.1	0.15	0.1	0.25	0.25	0.2	0.15	0.15	0.15
0.25	0.15	0.3	0.2	0.1	0.05	0.15	0.1	0.35	0.15	0.1	0.1	0.15	0.15	0.1	0.1	0.25	0.25	0.15	0.1	0.35	0.2	0.1	0.1	0.05	0.05	0.15	0.15	0.15	0.1	0.25	0.2	0.2	0.2	0.1	0.05
0.25	0.15	0.3	0.1	0.1	0.05	0.15	0.1	0.35	0.25	0.1	0.05	0.15	0.1	0.1	0.1	0.25	0.1	0.15	0.1	0.35	0.2	0.1	0.05	0.05	0.05	0.15	0.1	0.15	0.1	0.2	0.15	0.2	0.15	0.1	0.1
0.25	0.1	0.3	0.25	0.1	0.05	0.15	0.05	0.35	0.15	0.1	0.1	0.15	0.1	0.1	0.1	0.25	0.1	0.15	0.15	0.35	0.3	0.1	0.1	0.05	0.05	0.15	0.05	0.15	0.05	0.2	0.05	0.2	0.15	0.1	0.05
0.25	0.2	0.3	0.2	0.1	0.1	0.15	0.15	0.35	0.3	0.1	0.1	0.15	0.1	0.1	0.1	0.25	0.15	0.15	0.1	0.35	0.25	0.1	0.05	0.05	0.05	0.15	0.05	0.15	0.15	0.2	0.15	0.2	0.15	0.1	0.1
0.25	0.2	0.3	0.2	0.1	0.1	0.15	0.1	0.3	0.2	0.1	0.05	0.15	0.1	0.1	0.05	0.25	0.2	0.15	0.1	0.35	0.25	0.05	0.05	0.05	0.05	0.15	0.1	0.15	0.15	0.2	0.15	0.2	0.1	0.1	0.05
0.25	0.15	0.3	0.2	0.1	0.1	0.15	0.15	0.3	0.25	0.1	0.05	0.15	0.1	0.1	0.1	0.25	0.1	0.1	0.1	0.35	0.35	0.05	0.05	0.05	0.05	0.15	0.15	0.15	0.1	0.2	0.1	0.2	0.15	0.1	0.1
0.25	0.05	0.3	0.3	0.1	0.05	0.15	0.15	0.3	0.25	0.1	0.05	0.15	0.15	0.1	0.1	0.25	0.15	0.1	0.05	0.35	0.25	0.05	0.05	0.05	0.05	0.15	0.1	0.1	0.1	0.2	0.15	0.2	0.15	0.1	0.05
0.25	0.1	0.3	0.25	0.1	0.1	0.15	0.05	0.3	0.2	0.1	0.05	0.15	0.1	0.1	0.1	0.25	0.2	0.1	0.1	0.3	0.25	0.05	0.05	0.05	0.05	0.15	0.1	0.1	0.05	0.2	0.15	0.2	0.15	0.1	0.05
0.2	0.1	0.3	0.2	0.1	0.1	0.15	0.05	0.3	0.05	0.1	0.1	0.15	0.1	0.1	0.1	0.25	0.2	0.1	0.05	0.3	0.2	0.05	0.05	0.05	0.05	0.15	0.1	0.1	0.1	0.2	0.15	0.2	0.1	0.1	0.1
0.2	0.1	0.3	0.25	0.1	0.05	0.15	0.15	0.3	1.55	0.1	0.1	0.15	0.15	0.1	0.1	0.25	0.15	0.1	0.05	0.3	0.2	0.05	0.05	0.05	0.05	0.15	0.1	0.1	0.1	0.2	0.15	0.15	0.15	0.1	0.05
0.2	0.15	0.3	0.2	0.05	0.05	0.15	0.15	0.3	0.1	0.1	0.1	0.15	0.1	0.1	0.1	0.25	0.25	0.1	0.1	0.3	0.1	0.05	0.05	0.05	0.05	0.15	0.15	0.1	0.1	0.2	0.2	0.15	0.15	0.1	0.1
0.2	0.15	0.3	0.25	0.05	0.05	0.15	0.15	0.25	0.15	0.1	0.05	0.15	0.15	0.1	0.1	0.2	0.1	0.1	0.05	0.3	0.15	0.05	0.05	0.05	0.05	0.15	0.1	0.1	0.05	0.2	0.1	0.15	0.1	0.1	0.1
0.2	0.15	0.25	0.15	0.05	0.05	0.15	0.1	0.25	0.2	0.1	0.1	0.15	0.1	0.1	0.05	0.2	0.15	0.1	0.1	0.3	0.2	0.05	0.05	0.05	0.05	0.15	0.1	0.1	0.1	0.2	0.2	0.15	0.1	0.1	0.1
0.2	0.1	0.25	0.15	0.05	0.05	0.1	0.05	0.25	0.1	0.1	0.1	0.15	0.1	0.1	0.05	0.2	0.2	0.1	0.1	0.3	0.25	0.05	0.05	0.05	0.05	0.15	0.1	0.1	0.1	0.2	0.15	0.15	0.1	0.1	0.05
0.2	0.15	0.25	0.2	0.05	0.05	0.1	0.05	0.25	0.15	0.05	0.05	0.15	0.15	0.1	0.1	0.2	0.2	0.1	0.05	0.3	0.2	0.05	0.05	0.05	0.05	0.15	0.05	0.1	0.05	0.2	0.1	0.15	0.1	0.1	0.1
0.2	0.2	0.25	0.2	0.05	0.05	0.1	0.05	0.25	0.15	0.05	0.05	0.15	0.15	0.1	0.1	0.2	0.2	0.1	0.05	0.25	0.2	0.05	0.05	0.05	0.05	0.15	0.05	0.1	0.1	0.2	0.15	0.15	0.1	0.05	0.05

1		2		3		5		6		7		8		9		10		11		12		13		14		15		16		17		18		19	
Long dimension (mm)	Short Dimension (mm)	Long dimension (mm)	Short Dimension (mm)	Long dimension (mm)	Short Dimension (mm)	Long dimension (mm)	Short Dimension (mm)	Long dimension (mm)	Short Dimension (mm)	Long dimension (mm)	Short Dimension (mm)	Long dimension (mm)	Short Dimension (mm)	Long dimension (mm)	Short Dimension (mm)	Long dimension (mm)	Short Dimension (mm)	Long dimension (mm)	Short Dimension (mm)	Long dimension (mm)	Short Dimension (mm)	Long dimension (mm)	Short Dimension (mm)	Long dimension (mm)	Short Dimension (mm)	Long dimension (mm)	Short Dimension (mm)	Long dimension (mm)	Short Dimension (mm)	Long dimension (mm)	Short Dimension (mm)	Long dimension (mm)	Short Dimension (mm)	Long dimension (mm)	Short Dimension (mm)
0.2	0.1	0.2	0.1	0.05	0.05	0.1	0.05	0.25	0.15	0.05	0.05	0.15	0.15	0.1	0.1	0.2	0.15	0.1	0.1	0.25	0.2	0.05	0.05	0.05	0.05	0.15	0.1	0.1	0.05	0.2	0.2	0.15	0.1	0.05	0.05
0.2	0.15	0.2	0.2	0.05	0.05	0.1	0.05	0.25	0.15	0.05	0.05	0.15	0.1	0.1	0.1	0.2	0.15	0.1	0.1	0.25	0.2	0.05	0.05	0.05	0.05	0.15	0.1	0.1	0.1	0.15	0.05	0.15	0.1	0.05	0.05
0.2	0.1	0.2	0.1	0.05	0.05	0.1	0.05	0.2	0.15	0.05	0.05	0.15	0.1	0.1	0.05	0.2	0.1	0.1	0.1	0.25	0.2	0.05	0.05	0.05	0.05	0.15	0.05	0.1	0.1	0.15	0.1	0.15	0.1	0.05	0.05
0.15	0.15	0.2	0.15	0.05	0.05	0.1	0.1	0.2	0.15	0.05	0.05	0.1	0.05	0.1	0.05	0.2	0.1	0.1	0.1	0.25	0.1	0.05	0.05	0.05	0.05	0.15	0.15	0.1	0.1	0.15	0.1	0.15	0.1	0.05	0.05
0.15	0.1	0.2	0.15	0.05	0.05	0.1	0.1	0.15	0.1	0.05	0.05	0.1	0.1	0.1	0.05	0.2	0.2	0.1	0.1	0.25	0.2	0.05	0.05	0.05	0.05	0.1	0.05	0.1	0.1	0.15	0.05	0.15	0.15	0.05	0.05
0.15	0.1	0.2	0.1	0.05	0.05	0.1	0.05	0.15	0.15	0.05	0.05	0.1	0.1	0.1	0.1	0.2	0.15	0.1	0.1	0.25	0.2	0.05	0.05	0.05	0.05	0.1	0.05	0.1	0.1	0.15	0.1	0.15	0.1	0.05	0.05
0.15	0.1	0.2	0.2	0.05	0.05	0.1	0.05	0.15	0.15	0.05	0.05	0.1	0.1	0.1	0.1	0.2	0.15	0.1	0.1	0.25	0.2	0.05	0.05	0.05	0.05	0.1	0.05	0.1	0.05	0.15	0.15	0.15	0.05	0.05	0.05
0.15	0.05	0.15	0.1	0.05	0.05	0.1	0.1	0.15	0.15	0.05	0.05	0.1	0.1	0.05	0.05	0.2	0.15	0.1	0.05	0.25	0.2	0.05	0.05	0.05	0.05	0.1	0.05	0.1	0.1	0.15	0.15	0.15	0.1	0.05	0.05
0.15	0.1	0.15	0.1	0.05	0.05	0.1	0.05	0.15	0.15	0.05	0.05	0.1	0.1	0.05	0.05	0.2	0.2	0.1	0.1	0.25	0.2	0.05	0.1	0.05	0.05	0.1	0.1	0.1	0.05	0.15	0.05	0.15	0.1	0.05	0.05
0.15	0.15	0.15	0.1	0.05	0.05	0.1	0.05	0.15	0.1	0.05	0.05	0.1	0.1	0.05	0.05	0.2	0.15	0.1	0.1	0.25	0.2	0.05	0.2	0.05	0.05	0.1	0.05	0.1	0.1	0.15	0.1	0.15	0.1	0.05	0.05
0.15	0.1	0.15	0.05	0.05	0.05	0.1	0.1	0.15	0.15	0.05	0.05	0.1	0.1	0.05	0.05	0.2	0.1	0.1	0.1	0.25	0.2	0.05	0.05	0.05	0.05	0.1	0.1	0.1	0.05	0.15	0.1	0.15	0.1	0.05	0.05
0.15	0.1	0.15	0.1	0.05	0.05	0.1	0.1	0.15	0.1	0.05	0.05	0.1	0.1	0.05	0.05	0.2	0.2	0.05	0.05	0.25	0.2	0.05	0.05	0.05	0.05	0.1	0.1	0.1	0.1	0.15	0.1	0.15	0.1	0.05	0.05
0.15	0.1	0.15	0.1	0.05	0.05	0.1	0.05	0.1	0.1	0.05	0.05	0.1	0.1	0.05	0.05	0.15	0.15	0.05	0.05	0.2	0.15	0.05	0.05	0.05	0.05	0.1	0.05	0.1	0.1	0.1	0.1	0.15	0.1	0.05	0.05
0.15	0.05	0.1	0.1	0.05	0.05	0.1	0.05	0.1	0.1	0.05	0.05	0.1	0.1	0.05	0.05	0.15	0.1	0.05	0.05	0.2	0.15	0.05	0.05	0.05	0.05	0.1	0.1	0.1	0.1	0.1	0.05	0.1	0.1	0.05	0.05
0.15	0.1	0.1	0.05	0.05	0.05	0.05	0.05	0.1	0.1	0.05	0.05	0.1	0.1	0.05	0.05	0.15	0.15	0.05	0.05	0.2	0.15	0.05	0.05	0.05	0.05	0.1	0.1	0.1	0.1	0.1	0.1	0.1	0.1	0.05	0.05
0.1	0.1	0.1	0.1	0.05	0.05	0.05	0.05	0.1	0.05	0.05	0.05	0.1	0.1	0.05	0.05	0.15	0.15	0.05	0.05	0.2	0.15	0.05	0.05	0.05	0.05	0.1	0.05	0.1	0.1	0.1	0.05	0.1	0.1	0.05	0.05
0.1	0.05	0.1	0.05	0.05	0.05	0.05	0.05	0.1	0.1	0.05	0.05	0.1	0.1	0.05	0.05	0.15	0.15	0.05	0.05	0.2	0.15	0.05	0.05	0.05	0.05	0.1	0.1	0.05	0.05	0.1⊢	0.1	0.1	0.05	0.05	0.05
0.1	0.05	0.1	0.1	0.05	0.05	0.05	0.05	0.1	0.1	0.05	0.05	0.1	0.05	0.05	0.05	0.15	0.15	0.05	0.05	0.2	0.15	0.05	0.05	0.05	0.05	0.1	0.1	0.05	0.05	0.1	0.05	0.1	0.1	0.05	0.05
0.1	0.05	0.1	0.05	0.05	0.05	0.05	0.05	0.1	0.1	0.05	0.05	0.1	0.1	0.05	0.05	0.15	0.1	0.05	0.05	0.15	0.1	0.05	0.05	0.05	0.05	0.1	0.05	0.05	0.05	0.1	0.05	0.1	0.1	0.05	0.05
0.1	0.05	0.1	0.05	0.05	0.05	0.05	0.05	0.1	0.1	0.05	0.05	0.1	0.1	0.05	0.05	0.15	0.1	0.05	0.05	0.15	0.1	0.05	0.05	0.05	0.05	0.05	0.05	0.05	0.05	0.1	0.1	0.1	0.1	0.05	0.05
0.1	0.1	0.1	0.1	0.05	0.05	0.05	0.05	0.1	0.1	0.05	0.05	0.1	0.1	0.05	0.05	0.1	0.05	0.05	0.05	0.15	0.15	0.05	0.05	0.05	0.05	0.05	0.05	0.05	0.05	0.1	0.1	0.1	0.1	0.05	0.05
0.05	0.05	0.1	0.1	0.05	0.05	0.05	0.05	0.1	0.1	0.05	0.05	0.05	0.05	0.05	0.05	0.1	0.1	0.05	0.05	0.05	0.05	0.05	0.05	0.05	0.05	0.05	0.05	0.05	0.05	0.05	0.05	0.1	0.1	0.05	0.05
0.05	0.05	0.05	0.05	0.05	0.05	0.05	0.05	0.05	0.05	0.05	0.05	0.05	0.05	0.05	0.05	0.1	0.05	0.05	0.05	0.05	0.05	0.05	0.05	0.05	0.05	0.05	0.05	0.05	0.05	0.05	0.05	0.1	0.1	0.05	0.05
0.05	0.05	0.05	0.05	0.05	0.05	0.05	0.05	0.05	0.05	0.05	0.05	0.05	0.05	0.05	0.05	0.1	0.1	0.05	0.05	0.05	0.05	0.05	0.05	0.05	0.05	0.05	0.1	0.05	0.05	0.05	0.05	0.05	0.05	0.05	0.05

Long Dimension (Phi-units)																	
1	2	3	5	6	7	8	9	10	11	12	13	14	15	16	17	18	19
-0.888	-0.585	0.737	-0.138	-0.766	-1.655	-0.848	-1.766	-1.722	-0.485	-1.036	-0.888	2.000	-0.632	-1.406	0.234	0.322	-0.963
-0.848	-0.433	0.737	-0.070	-0.585	0.234	-0.379	-1.322	-1.511	-0.433	-1.036	-0.807	2.000	-0.585	-1.170	0.515	0.415	-0.632
-0.807	-0.433	0.737	0.152	-0.433	0.322	-0.322	-1.293	-1.379	-0.322	-1.000	-0.632	2.000	-0.322	-0.963	0.621	0.621	-0.485
-0.807	-0.433	1.000	0.152	-0.322	0.515	-0.263	-1.293	-1.170	-0.322	-0.963	-0.585	2.322	0.621	-0.766	0.737	0.737	-0.433
-0.722	-0.379	1.152	0.234	-0.202	0.737	-0.138	-1.293	-1.070	-0.202	-0.963	0.074	2.322	0.621	-0.678	0.737	0.862	-0.322
-0.678	-0.322	1.152	0.234	-0.202	0.737	-0.070	-1.202	-1.000	-0.202	-0.926	0.074	2.322	0.621	-0.632	0.737	0.862	-0.322
-0.585	-0.322	1.152	0.322	-0.138	0.737	0.000	-1.036	-0.963	-0.202	-0.888	0.152	2.322	0.737	-0.536	0.737	1.000	-0.263
-0.585	-0.202	1.322	0.415	-0.138	0.862	0.074	-0.963	-0.926	-0.070	-0.848	0.234	2.322	0.737	-0.485	0.862	1.000	-0.202
-0.536	-0.202	1.322	0.415	-0.070	1.000	0.152	-0.926	-0.888	0.000	-0.766	0.234	2.322	0.737	-0.379	0.862	1.000	-0.138
-0.485	-0.202	1.322	0.415	-0.070	1.000	0.322	-0.848	-0.807	0.234	-0.766	0.322	2.322	0.862	-0.322	0.862	1.000	-0.070
-0.485	-0.202	1.322	0.415	-0.070	1.152	0.415	-0.807	-0.766	0.322	-0.766	0.322	2.322	0.862	-0.138	0.862	1.000	0.000
-0.485	-0.202	1.515	0.515	0.000	1.152	0.415	-0.807	-0.722	0.322	-0.678	0.415	2.322	0.862	-0.138	0.862	1.152	0.152
-0.433	-0.138	1.515	0.515	0.000	1.152	0.415	-0.766	-0.536	0.322	-0.585	0.415	2.322	0.862	0.000	0.862	1.152	0.152
-0.433	-0.070	1.515	0.515	0.000	1.152	0.515	-0.585	-0.485	0.415	-0.585	0.621	2.322	0.862	0.152	0.862	1.322	0.152
-0.379	-0.070	1.515	0.515	0.074	1.152	0.621	-0.485	-0.322	0.415	-0.585	0.621	2.322	1.000	0.152	0.862	1.322	0.152
-0.379	-0.070	1.515	0.515	0.074	1.152	0.621	-0.433	-0.322	0.415	-0.585	0.862	2.322	1.000	0.234	0.862	1.322	0.152
-0.322	0.000	1.515	0.621	0.074	1.322	0.621	-0.322	-0.322	0.515	-0.536	1.000	2.322	1.000	0.415	1.000	1.322	0.152
-0.322	0.000	1.515	0.621	0.152	1.322	0.737	-0.322	-0.202	0.515	-0.485	1.152	2.737	1.000	0.415	1.000	1.322	0.322
-0.322	0.074	1.737	0.621	0.152	1.322	0.737	-0.263	-0.202	0.621	-0.485	1.322	2.737	1.000	0.415	1.000	1.322	0.322
-0.322	0.152	1.737	0.621	0.152	1.322	0.862	-0.263	-0.138	0.621	-0.485	1.322	2.737	1.000	0.515	1.000	1.322	0.415
-0.263	0.152	1.737	0.621	0.152	1.322	0.862	-0.263	-0.138	0.621	-0.433	2.000	2.737	1.152	0.515	1.000	1.322	0.415
-0.202	0.152	1.737	0.621	0.152	1.322	0.862	-0.263	-0.138	0.621	-0.433	2.000	2.737	1.152	0.515	1.000	1.322	0.415
-0.202	0.234	1.737	0.621	0.152	1.322	0.862	-0.138	-0.070	0.737	-0.379	2.000	2.737	1.152	0.621	1.000	1.515	0.515
-0.202	0.234	1.737	0.621	0.152	1.322	0.862	-0.070	-0.070	0.737	-0.379	2.000	2.737	1.152	0.621	1.000	1.515	0.621
-0.202	0.234	1.737	0.621	0.152	1.515	1.000	-0.070	0.000	1.000	-0.379	2.000	2.737	1.152	0.737	1.000	1.515	0.621
-0.202	0.234	1.737	0.737	0.152	1.515	1.000	-0.070	0.000	1.000	-0.379	2.000	2.737	1.152	0.737	1.152	1.515	0.621
-0.138	0.234	1.737	0.737	0.152	1.515	1.000	-0.070	0.074	1.000	-0.379	2.322	2.737	1.152	0.862	1.152	1.515	0.621
-0.138	0.234	1.737	0.737	0.234	1.515	1.000	0.074	0.152	1.000	-0.379	2.322	2.737	1.152	0.862	1.152	1.515	0.737
-0.138	0.234	1.737	0.737	0.234	1.515	1.000	0.074	0.152	1.000	-0.379	2.322	2.737	1.152	0.862	1.152	1.515	0.737
-0.138	0.322	1.737	0.737	0.234	1.515	1.000	0.152	0.152	1.000	-0.379	2.322	2.737	1.152	1.000	1.152	1.515	0.737
-0.070	0.322	2.000	0.862	0.234	1.515	1.152	0.152	0.152	1.000	-0.322	2.322	2.737	1.322	1.000	1.152	1.515	0.737
-0.070	0.322	2.000	0.862	0.234	1.515	1.152	0.322	0.234	1.152	-0.322	2.322	2.737	1.322	1.000	1.152	1.515	0.862
0.000	0.322	2.000	0.862	0.234	1.515	1.152	0.415	0.234	1.152	-0.322	2.322	2.737	1.322	1.000	1.152	1.515	0.862
0.000	0.322	2.000	0.862	0.234	1.515	1.152	0.515	0.322	1.322	-0.322	2.322	2.737	1.322	1.000	1.152	1.515	1.000
0.000	0.322	2.000	0.862	0.234	1.515	1.152	0.515	0.322	1.322	-0.322	2.322	2.737	1.322	1.000	1.152	1.515	1.000
0.000	0.415	2.000	1.000	0.234	1.737	1.152	0.737	0.415	1.322	-0.263	2.322	2.737	1.322	1.152	1.322	1.515	1.000
0.000	0.415	2.000	1.000	0.322	1.737	1.152	0.862	0.415	1.322	-0.263	2.322	2.737	1.322	1.152	1.322	1.515	1.000
0.000	0.415	2.000	1.000	0.322	1.737	1.152	0.862	0.415	1.322	-0.202	2.322	2.737	1.322	1.152	1.322	1.515	1.000
0.074	0.415	2.000	1.000	0.322	1.737	1.152	0.862	0.415	1.322	-0.202	2.322	2.737	1.322	1.152	1.322	1.515	1.152
0.074	0.415	2.000	1.000	0.322	1.737	1.152	1.000	0.515	1.322	-0.202	2.322	2.737	1.322	1.152	1.322	1.515	1.322
0.074	0.415	2.000	1.000	0.322	1.737	1.322	1.152	0.515	1.322	-0.138	2.322	2.737	1.322	1.322	1.322	1.515	1.322
0.152	0.515	2.000	1.000	0.322	1.737	1.322	1.322	0.515	1.322	-0.138	2.322	2.737	1.322	1.322	1.322	1.515	1.322
0.152	0.515	2.000	1.000	0.415	1.737	1.322	1.515	0.515	1.322	-0.138	2.737	2.737	1.322	1.322	1.322	1.515	1.322
0.152	0.515	2.000	1.152	0.415	1.737	1.322	1.515	0.515	1.322	-0.138	2.737	2.737	1.322	1.515	1.322	1.515	1.322
0.152	0.515	2.000	1.152	0.415	1.737	1.322	1.515	0.621	1.322	-0.138	2.737	2.737	1.515	1.515	1.322	1.737	1.322
0.152	0.515	2.000	1.152	0.415	1.737	1.322	1.737	0.621	1.322	-0.138	2.737	2.737	1.515	1.515	1.322	1.737	1.322
0.152	0.621	2.000	1.152	0.415	1.737	1.322	1.737	0.621	1.322	-0.070	2.737	2.737	1.515	1.515	1.322	1.737	1.322
0.152	0.621	2.000	1.152	0.415	1.737	1.322	1.737	0.621	1.515	-0.070	2.737	2.737	1.515	1.515	1.322	1.737	1.322
0.234	0.621	2.000	1.152	0.415	1.737	1.322	1.737	0.621	1.515	-0.070	2.737	2.737	1.515	1.515	1.322	1.737	1.322

Long Dimension (Phi-units)																	
1	2	3	5	6	7	8	9	10	11	12	13	14	15	16	17	18	19
0.234	0.621	2.000	1.152	0.415	1.737	1.322	1.737	0.621	1.515	-0.070	2.737	2.737	1.515	1.515	1.322	1.737	1.322
0.322	0.621	2.000	1.322	0.415	1.737	1.322	1.737	0.621	1.515	-0.070	2.737	2.737	1.515	1.515	1.322	1.737	1.322
0.322	0.621	2.000	1.322	0.415	1.737	1.515	2.000	0.737	1.515	-0.070	2.737	2.737	1.515	1.515	1.322	1.737	1.515
0.415	0.621	2.000	1.322	0.415	1.737	1.515	2.000	0.737	1.515	0.000	2.737	2.737	1.515	1.737	1.322	1.737	1.515
0.415	0.621	2.322	1.322	0.415	1.737	1.515	2.000	0.737	1.515	0.000	2.737	2.737	1.515	1.737	1.322	1.737	1.515
0.415	0.621	2.322	1.322	0.415	2.000	1.515	2.000	0.737	1.515	0.000	2.737	2.737	1.515	1.737	1.515	1.737	1.515
0.415	0.737	2.322	1.322	0.415	2.000	1.515	2.000	0.737	1.515	0.000	2.737	3.322	1.515	1.737	1.515	1.737	1.515
0.415	0.737	2.322	1.322	0.415	2.000	1.515	2.000	0.862	1.515	0.000	2.737	3.322	1.737	1.737	1.515	1.737	1.515
0.415	0.737	2.322	1.322	0.415	2.000	1.515	2.322	0.862	1.515	0.000	2.737	3.322	1.737	1.737	1.515	1.737	1.515
0.415	0.737	2.322	1.515	0.415	2.000	1.515	2.322	0.862	1.515	0.000	2.737	3.322	1.737	1.737	1.515	1.737	1.737
0.415	0.737	2.322	1.515	0.415	2.000	1.737	2.322	0.862	1.515	0.000	2.737	3.322	1.737	1.737	1.515	1.737	1.737
0.415	0.737	2.322	1.515	0.515	2.000	1.737	2.322	0.862	1.515	0.000	2.737	3.322	1.737	1.737	1.515	1.737	1.737
0.415	0.737	2.322	1.515	0.515	2.000	1.737	2.322	0.862	1.515	0.000	2.737	3.322	1.737	1.737	1.515	1.737	1.737
0.415	0.862	2.322	1.515	0.515	2.000	1.737	2.322	0.862	1.515	0.000	2.737	3.322	1.737	1.737	1.515	1.737	1.737
0.415	0.862	2.322	1.515	0.515	2.000	1.737	2.322	0.862	1.737	0.074	2.737	3.322	1.737	1.737	1.515	1.737	1.737
0.515	0.862	2.322	1.515	0.515	2.000	1.737	2.322	1.000	1.737	0.074	2.737	3.322	1.737	1.737	1.515	1.737	1.737
0.515	0.862	2.322	1.515	0.515	2.000	1.737	2.322	1.000	1.737	0.152	2.737	3.322	1.737	1.737	1.515	1.737	1.737
0.515	0.862	2.322	1.515	0.515	2.000	1.737	2.322	1.000	1.737	0.152	2.737	3.322	1.737	1.737	1.515	1.737	1.737
0.515	0.862	2.322	1.515	0.515	2.000	2.000	2.322	1.000	1.737	0.152	2.737	3.322	1.737	2.000	1.515	2.000	1.737
0.515	0.862	2.322	1.515	0.515	2.000	2.000	2.322	1.000	1.737	0.152	2.737	3.322	1.737	2.000	1.515	2.000	1.737
0.515	0.862	2.322	1.515	0.515	2.000	2.000	2.322	1.000	1.737	0.152	2.737	3.322	1.737	2.000	1.515	2.000	2.000
0.515	1.000	2.322	1.515	0.621	2.000	2.000	2.322	1.000	1.737	0.152	2.737	3.322	1.737	2.000	1.515	2.000	2.000
0.515	1.000	2.322	1.515	0.621	2.000	2.000	2.322	1.000	1.737	0.152	2.737	3.322	1.737	2.000	1.515	2.000	2.000
0.621	1.000	2.322	1.737	0.621	2.000	2.000	2.322	1.000	1.737	0.322	2.737	3.322	1.737	2.000	1.515	2.000	2.000
0.621	1.000	2.322	1.737	0.621	2.000	2.000	2.322	1.152	1.737	0.322	2.737	3.322	1.737	2.000	1.515	2.000	2.000
0.621	1.000	2.322	1.737	0.621	2.000	2.000	2.737	1.152	2.000	0.322	2.737	3.322	1.737	2.000	1.515	2.000	2.000
0.621	1.000	2.322	1.737	0.621	2.322	2.000	2.737	1.152	2.000	0.415	2.737	3.322	1.737	2.000	1.515	2.000	2.000
0.621	1.000	2.322	1.737	0.621	2.322	2.000	2.737	1.152	2.000	0.415	2.737	3.322	2.000	2.000	1.737	2.000	2.000
0.621	1.000	2.322	1.737	0.621	2.322	2.000	2.737	1.152	2.000	0.415	2.737	3.322	2.000	2.000	1.737	2.000	2.000
0.621	1.000	2.322	1.737	0.621	2.322	2.000	2.737	1.322	2.000	0.415	2.737	3.322	2.000	2.000	1.737	2.000	2.000
0.621	1.000	2.322	1.737	0.621	2.322	2.000	2.737	1.322	2.000	0.415	2.737	3.322	2.000	2.322	1.737	2.000	2.000
0.737	1.152	2.322	2.000	0.737	2.322	2.000	2.737	1.322	2.000	0.515	2.737	3.322	2.000	2.322	1.737	2.000	2.000
0.737	1.152	2.322	2.000	0.737	2.322	2.000	2.737	1.322	2.000	0.515	2.737	3.322	2.000	2.322	1.737	2.000	2.000
0.737	1.152	2.737	2.000	0.737	2.322	2.322	2.737	1.322	2.000	0.621	3.322	3.322	2.000	2.322	1.737	2.000	2.000
0.737	1.152	2.737	2.000	0.737	2.322	2.322	2.737	1.322	2.000	0.621	3.322	3.322	2.000	2.322	1.737	2.000	2.000
0.737	1.152	2.737	2.000	0.737	2.322	2.322	2.737	1.322	2.000	0.621	3.322	3.322	2.000	2.322	1.737	2.000	2.000
0.737	1.152	2.737	2.000	0.737	2.322	2.322	2.737	1.322	2.000	0.621	3.322	3.322	2.000	2.322	1.737	2.000	2.322
0.737	1.152	2.737	2.000	0.737	2.322	2.322	2.737	1.515	2.322	0.621	3.322	3.322	2.000	2.322	1.737	2.000	2.322
0.737	1.152	2.737	2.000	0.737	2.322	2.322	2.737	1.515	2.322	0.737	3.322	3.322	2.000	2.322	1.737	2.000	2.322
0.862	1.152	2.737	2.000	0.737	2.322	2.322	2.737	1.515	2.322	0.737	3.322	3.322	2.000	2.322	1.737	2.000	2.322
0.862	1.152	2.737	2.000	0.737	2.322	2.322	2.737	1.515	2.322	0.737	3.322	3.322	2.000	2.322	1.737	2.000	2.322
0.862	1.152	2.737	2.000	0.737	2.322	2.322	2.737	1.515	2.322	0.737	3.322	3.322	2.000	2.322	1.737	2.000	2.322
0.862	1.322	2.737	2.000	0.862	2.322	2.322	2.737	1.515	2.322	0.737	3.322	3.322	2.000	2.322	1.737	2.000	2.322
0.862	1.322	2.737	2.000	0.862	2.322	2.322	2.737	1.515	2.322	0.737	3.322	3.322	2.000	2.322	1.737	2.000	2.322
0.862	1.322	2.737	2.000	0.862	2.322	2.322	2.737	1.515	2.322	0.862	3.322	3.322	2.000	2.322	1.737	2.000	2.322
1.000	1.322	2.737	2.322	1.000	2.322	2.322	2.737	1.515	2.322	0.862	3.322	3.322	2.000	2.322	2.000	2.000	2.322
1.000	1.322	2.737	2.322	1.000	2.737	2.322	2.737	1.515	2.322	0.862	3.322	3.322	2.322	2.322	2.000	2.000	2.322
1.000	1.322	2.737	2.322	1.000	2.737	2.322	2.737	1.515	2.322	0.862	3.322	3.322	2.322	2.322	2.000	2.000	2.322
1.000	1.322	2.737	2.322	1.000	2.737	2.322	2.737	1.515	2.322	1.000	3.322	3.322	2.322	2.322	2.000	2.322	2.322

Long Dimension (Phi-units)																	
1	2	3	5	6	7	8	9	10	11	12	13	14	15	16	17	18	19
1.152	1.322	2.737	2.322	1.000	2.737	2.322	2.737	1.515	2.322	1.000	3.322	3.322	2.322	2.737	2.000	2.322	2.322
1.152	1.322	2.737	2.322	1.000	2.737	2.322	2.737	1.515	2.322	1.152	3.322	3.322	2.322	2.737	2.000	2.322	2.322
1.152	1.322	2.737	2.322	1.000	2.737	2.322	2.737	1.515	2.322	1.152	3.322	3.322	2.322	2.737	2.000	2.322	2.737
1.152	1.322	2.737	2.322	1.000	2.737	2.322	2.737	1.515	2.322	1.152	3.322	3.322	2.322	2.737	2.000	2.322	2.737
1.152	1.322	2.737	2.322	1.000	2.737	2.322	3.322	1.515	2.322	1.152	3.322	3.322	2.322	2.737	2.000	2.322	2.737
1.322	1.322	2.737	2.322	1.000	2.737	2.322	3.322	1.515	2.322	1.152	3.322	3.322	2.322	2.737	2.000	2.322	2.737
1.322	1.322	2.737	2.322	1.000	2.737	2.322	3.322	1.515	2.322	1.152	3.322	3.322	2.322	2.737	2.000	2.322	2.737
1.322	1.322	2.737	2.322	1.000	2.737	2.322	3.322	1.737	2.322	1.322	3.322	3.322	2.322	2.737	2.000	2.322	2.737
1.322	1.322	2.737	2.322	1.152	2.737	2.322	3.322	1.737	2.322	1.322	3.322	3.322	2.322	2.737	2.000	2.322	2.737
1.322	1.515	3.322	2.322	1.152	2.737	2.322	3.322	1.737	2.322	1.322	3.322	3.322	2.322	2.737	2.000	2.322	2.737
1.515	1.515	3.322	2.322	1.152	2.737	2.737	3.322	1.737	2.322	1.322	3.322	3.322	2.322	2.737	2.000	2.322	2.737
1.515	1.515	3.322	2.322	1.152	2.737	2.737	3.322	1.737	2.322	1.322	3.322	3.322	2.322	2.737	2.000	2.322	2.737
1.515	1.515	3.322	2.322	1.322	2.737	2.737	3.322	1.737	2.737	1.322	3.322	3.322	2.322	2.737	2.000	2.322	2.737
1.515	1.515	3.322	2.322	1.322	2.737	2.737	3.322	1.737	2.737	1.322	3.322	3.322	2.322	2.737	2.000	2.322	2.737
1.515	1.515	3.322	2.322	1.322	2.737	2.737	3.322	1.737	2.737	1.322	3.322	4.322	2.322	2.737	2.000	2.322	2.737
1.737	1.515	3.322	2.737	1.322	2.737	2.737	3.322	1.737	2.737	1.322	3.322	4.322	2.322	2.737	2.000	2.322	2.737
1.737	1.515	3.322	2.737	1.322	2.737	2.737	3.322	1.737	2.737	1.322	3.322	4.322	2.737	2.737	2.000	2.322	2.737
1.737	1.515	3.322	2.737	1.322	2.737	2.737	3.322	1.737	2.737	1.322	3.322	4.322	2.737	2.737	2.000	2.322	2.737
1.737	1.515	3.322	2.737	1.322	2.737	2.737	3.322	2.000	2.737	1.322	3.322	4.322	2.737	2.737	2.000	2.322	2.737
1.737	1.515	3.322	2.737	1.322	3.322	2.737	3.322	2.000	2.737	1.515	3.322	4.322	2.737	2.737	2.000	2.322	2.737
2.000	1.515	3.322	2.737	1.322	3.322	2.737	3.322	2.000	2.737	1.515	3.322	4.322	2.737	2.737	2.000	2.322	2.737
2.000	1.737	3.322	2.737	1.515	3.322	2.737	3.322	2.000	2.737	1.515	3.322	4.322	2.737	2.737	2.000	2.322	2.737
2.000	1.737	3.322	2.737	1.515	3.322	2.737	3.322	2.000	2.737	1.515	3.322	4.322	2.737	2.737	2.000	2.322	3.322
2.000	1.737	3.322	2.737	1.515	3.322	2.737	3.322	2.000	2.737	1.515	3.322	4.322	2.737	2.737	2.322	2.322	3.322
2.000	1.737	3.322	2.737	1.515	3.322	2.737	3.322	2.000	2.737	1.515	3.322	4.322	2.737	2.737	2.322	2.322	3.322
2.000	1.737	3.322	2.737	1.515	3.322	2.737	3.322	2.000	2.737	1.515	3.322	4.322	2.737	2.737	2.322	2.322	3.322
2.000	1.737	3.322	2.737	1.737	3.322	2.737	3.322	2.000	2.737	1.515	4.322	4.322	2.737	2.737	2.322	2.322	3.322
2.000	1.737	3.322	2.737	1.737	3.322	2.737	3.322	2.000	3.322	1.515	4.322	4.322	2.737	2.737	2.322	2.322	3.322
2.000	1.737	3.322	2.737	1.737	3.322	2.737	3.322	2.000	3.322	1.515	4.322	4.322	2.737	3.322	2.322	2.322	3.322
2.000	1.737	3.322	2.737	1.737	3.322	2.737	3.322	2.000	3.322	1.737	4.322	4.322	2.737	3.322	2.322	2.322	3.322
2.322	1.737	3.322	2.737	1.737	3.322	2.737	3.322	2.000	3.322	1.737	4.322	4.322	2.737	3.322	2.322	2.322	3.322
2.322	1.737	3.322	2.737	1.737	3.322	2.737	3.322	2.000	3.322	1.737	4.322	4.322	2.737	3.322	2.322	2.737	3.322
2.322	1.737	4.322	2.737	1.737	3.322	2.737	3.322	2.000	3.322	1.737	4.322	4.322	2.737	3.322	2.322	2.737	3.322
2.322	1.737	4.322	2.737	2.000	3.322	2.737	3.322	2.322	3.322	1.737	4.322	4.322	2.737	3.322	2.322	2.737	3.322
2.322	2.000	4.322	2.737	2.000	3.322	2.737	3.322	2.322	3.322	1.737	4.322	4.322	2.737	3.322	2.322	2.737	3.322
2.322	2.000	4.322	3.322	2.000	3.322	2.737	3.322	2.322	3.322	1.737	4.322	4.322	2.737	3.322	2.322	2.737	3.322
2.322	2.000	4.322	3.322	2.000	4.322	2.737	3.322	2.322	3.322	1.737	4.322	4.322	2.737	3.322	2.322	2.737	3.322
2.322	2.000	4.322	3.322	2.000	4.322	2.737	3.322	2.322	3.322	2.000	4.322	4.322	2.737	3.322	2.322	2.737	4.322
2.322	2.322	4.322	3.322	2.000	4.322	2.737	3.322	2.322	3.322	2.000	4.322	4.322	2.737	3.322	2.322	2.737	4.322
2.322	2.322	4.322	3.322	2.000	4.322	2.737	3.322	2.322	3.322	2.000	4.322	4.322	2.737	3.322	2.737	2.737	4.322
2.322	2.322	4.322	3.322	2.322	4.322	2.737	3.322	2.322	3.322	2.000	4.322	4.322	2.737	3.322	2.737	2.737	4.322
2.737	2.322	4.322	3.322	2.322	4.322	3.322	3.322	2.322	3.322	2.000	4.322	4.322	2.737	3.322	2.737	2.737	4.322
2.737	2.322	4.322	3.322	2.737	4.322	3.322	3.322	2.322	3.322	2.000	4.322	4.322	3.322	3.322	2.737	2.737	4.322
2.737	2.322	4.322	3.322	2.737	4.322	3.322	3.322	2.322	3.322	2.000	4.322	4.322	3.322	3.322	2.737	2.737	4.322
2.737	2.322	4.322	3.322	2.737	4.322	3.322	3.322	2.322	3.322	2.000	4.322	4.322	3.322	3.322	2.737	2.737	4.322
2.737	2.737	4.322	3.322	2.737	4.322	3.322	4.322	2.322	3.322	2.000	4.322	4.322	3.322	3.322	2.737	2.737	4.322
2.737	2.737	4.322	3.322	2.737	4.322	3.322	4.322	2.322	3.322	2.000	4.322	4.322	3.322	3.322	2.737	2.737	4.322
2.737	2.737	4.322	3.322	2.737	4.322	3.322	4.322	2.322	3.322	2.000	4.322	4.322	3.322	3.322	2.737	2.737	4.322
2.737	2.737	4.322	3.322	2.737	4.322	3.322	4.322	2.322	3.322	2.000	4.322	4.322	3.322	3.322	2.737	2.737	4.322

Long Dimension (Phi-units)																	
1	2	3	5	6	7	8	9	10	11	12	13	14	15	16	17	18	19
2.737	2.737	4.322	3.322	2.737	4.322	3.322	4.322	2.322	4.322	2.000	4.322	4.322	3.322	3.322	2.737	2.737	4.322
2.737	2.737	4.322	3.322	3.322	4.322	3.322	4.322	2.737	4.322	2.322	4.322	4.322	3.322	3.322	3.322	2.737	4.322
2.737	3.322	4.322	3.322	3.322	4.322	3.322	4.322	2.737	4.322	2.322	4.322	4.322	3.322	3.322	3.322	3.322	4.322
2.737	3.322	4.322	4.322	3.322	4.322	3.322	4.322	2.737	4.322	2.322	4.322	4.322	3.322	3.322	3.322	3.322	4.322
3.322	3.322	4.322	4.322	3.322	4.322	3.322	4.322	2.737	4.322	2.322	4.322	4.322	3.322	3.322	3.322	3.322	4.322
3.322	3.322	4.322	4.322	3.322	4.322	3.322	4.322	2.737	4.322	2.322	4.322	4.322	3.322	4.322	3.322	3.322	4.322
3.322	3.322	4.322	4.322	3.322	4.322	3.322	4.322	2.737	4.322	2.322	4.322	4.322	3.322	4.322	3.322	3.322	4.322
3.322	3.322	4.322	4.322	3.322	4.322	3.322	4.322	2.737	4.322	2.737	4.322	4.322	3.322	4.322	3.322	3.322	4.322
3.322	3.322	4.322	4.322	3.322	4.322	3.322	4.322	2.737	4.322	2.737	4.322	4.322	4.322	4.322	3.322	3.322	4.322
3.322	3.322	4.322	4.322	3.322	4.322	3.322	4.322	3.322	4.322	2.737	4.322	4.322	4.322	4.322	3.322	3.322	4.322
4.322	3.322	4.322	4.322	3.322	4.322	4.322	4.322	3.322	4.322	4.322	4.322	4.322	4.322	4.322	4.322	3.322	4.322
4.322	4.322	4.322	4.322	4.322	4.322	4.322	4.322	3.322	4.322	4.322	4.322	4.322	4.322	4.322	4.322	3.322	4.322
4.322	4.322	4.322	4.322	4.322	4.322	4.322	4.322	3.322	4.322	4.322	4.322	4.322	4.322	4.322	4.322	4.322	4.322

Thin section grain-size parameters in Phi-units															
	percentile 0.1	percentile 2	percentile 5	percentile 9	percentile 16	percentile 25	percentile 36	percentile 50	percentile 64	percentile 75	percentile 84	percentile 91	percentile 95	percentile 98	percentile 99.9
1	-0.887	-0.792	-0.538	-0.379	-0.173	0.074	0.415	0.6792	1.152	2	2.3219	2.737	3.3219	3.3219	4.3219
2	-0.583	-0.423	-0.202	-0.07	0.2345	0.415	0.737	1.076	1.3219	1.737	2	2.737	3.3219	3.3219	4.3219
3	0.737	1.0274	1.3219	1.5146	1.737	2	2.3219	2.3219	2.737	3.3219	4.3219	4.3219	4.3219	4.3219	4.3219
5	-0.136	0.1668	0.415	0.5146	0.737	1	1.3682	1.8685	2.3219	2.737	3.3219	3.3219	4.3219	4.3219	4.3219
6	-0.763	-0.3	-0.074	0.074	0.152	0.3219	0.415	0.6792	1	1.5146	2	2.737	3.3219	3.3219	4.3219
7	-1.625	0.5546	0.9931	1.152	1.5146	1.737	2	2.3219	2.737	3.3219	3.8819	4.3219	4.3219	4.3219	4.3219
8	-0.841	-0.24	0.1481	0.6215	1	1.2794	1.5146	2	2.3219	2.737	2.737	3.3219	3.3219	3.3219	4.3219
9	-1.758	-1.293	-0.928	-0.469	-0.07	1.114	2.3219	2.737	3.1815	3.3219	3.3219	4.3219	4.3219	4.3219	4.3219
10	-1.719	-1.152	-0.889	-0.322	0.0326	0.5146	0.8625	1.3219	1.5146	2	2.3219	2.3219	2.737	3.2166	3.3219
11	-0.485	-0.3	-0.004	0.415	1	1.3219	1.5146	2	2.3219	2.737	3.3219	3.3219	4.3219	4.3219	4.3219
12	-1.036	-0.963	-0.77	-0.585	-0.379	-0.154	0	0.4648	1.152	1.5146	1.737	2	2.3219	2.737	4.3219
13	-0.886	-0.466	0.2345	0.6962	2.1416	2.3219	2.737	2.737	3.3219	3.3219	4.3219	4.3219	4.3219	4.3219	4.3219
14	2	2.3219	2.3219	2.3219	2.737	2.737	3.3219	3.3219	3.3219	4.3219	4.3219	4.3219	4.3219	4.3219	4.3219
15	-0.632	0.6215	0.737	1	1.152	1.3219	1.737	2	2.3219	2.737	2.737	3.3219	3.3219	4.3219	4.3219
16	-1.402	-0.75	-0.384	0.1776	0.7922	1.2794	1.737	2.3219	2.737	2.737	3.3219	3.3219	3.3719	4.3219	4.3219
17	0.2389	0.737	0.8625	0.8625	1.152	1.3219	1.5146	1.737	2	2	2.3219	2.737	3.3219	3.3219	4.3219
18	0.3234	0.7596	1	1.3219	1.5146	1.5146	1.737	2	2.3219	2.3219	2.737	2.737	3.3219	3.3219	4.306
19	-0.958	-0.413	-0.141	0.152	0.6215	1.3219	1.5679	2	2.737	2.8832	3.3219	4.3219	4.3219	4.3219	4.3219

Sieve-equivalent grain-size parameters in Phi-units													
	percentile 2	percentile 5	percentile 9	percentile 16	percentile 25	percentile 36	percentile 50	percentile 64	percentile 75	percentile 84	percentile 91	percentile 95	percentile 98
1	-0.737	-0.435	-0.225	-0.059	0.1957	0.5314	0.8206	1.3703	2.229	2.5301	2.8945	3.4329	3.5469
2	-0.317	-0.065	0.103	0.3791	0.5586	0.8708	1.2293	1.5349	1.9786	2.242	2.8945	3.4329	3.5469
3	1.3321	1.6062	1.7925	1.9942	2.245	2.5413	2.5126	2.9061	3.4875	4.3201	4.2354	4.2339	4.3169
5	0.3537	0.6113	0.7265	0.9192	1.181	1.536	2.0455	2.5039	2.9306	3.4251	3.3894	4.2339	4.3169
6	-0.177	0.0751	0.2569	0.2904	0.4595	0.5314	0.8206	1.223	1.7669	2.242	2.8945	3.4329	3.5469
7	0.7946	1.2455	1.406	1.7552	1.9651	2.202	2.5126	2.9061	3.4875	3.9263	4.2354	4.2339	4.3169
8	-0.109	0.3185	0.8405	1.202	1.4783	1.6904	2.181	2.5039	2.9306	2.9016	3.3894	3.4329	3.5469
9	-1.306	-0.862	-0.322	0.0513	1.3023	2.5413	2.9401	3.3369	3.4875	3.4251	4.2354	4.2339	4.3169
10	-1.146	-0.82	-0.165	0.162	0.6645	1.0031	1.4826	1.7216	2.229	2.5301	2.5434	2.9643	3.4658
11	-0.177	0.1521	0.6204	1.202	1.5235	1.6904	2.181	2.5039	2.9306	3.4251	3.3894	4.2339	4.3169
12	-0.931	-0.688	-0.446	-0.28	-0.046	0.094	0.5997	1.3703	1.7669	2.0066	2.271	2.6319	3.0965
13	-0.366	0.4132	0.9202	2.4293	2.5875	2.9788	2.9401	3.4729	3.4875	4.3201	4.2354	4.2339	4.3169
14	2.804	2.7032	2.6532	3.0692	3.0291	3.5953	3.5426	3.4729	4.4395	4.3201	4.2354	4.2339	4.3169
15	0.8706	0.9645	1.244	1.3654	1.5235	1.9248	2.181	2.5039	2.9306	2.9016	3.3894	3.4329	4.3169
16	-0.689	-0.265	0.3673	0.9786	1.4783	1.9248	2.5126	2.9061	2.9306	3.4251	3.3894	3.4729	4.3169
17	1.0019	1.1022	1.0974	1.3654	1.5235	1.6904	1.9101	2.192	2.229	2.5301	2.8945	3.4329	3.5469
18	1.0276	1.253	1.5872	1.7552	1.7285	1.9248	2.181	2.5039	2.5355	2.9016	2.8945	3.4329	3.5469
19	-0.306	0.0016	0.34	0.7951	1.5235	1.7466	2.181	2.9061	3.0698	3.4251	4.2354	4.2339	4.3169

Thin section grain-size parameters in Phi-units								
	Mean	Median	Mode	Standard Deviation	Skewness	Kurtosis	75 Percentile	25 Percentile
1	0.9916	0.6792	0.415	1.1857	0.6812	-0.213	2	0.074
2	1.1647	1.076	1.3219	0.9898	0.7972	0.6056	1.737	0.415
3	2.6951	2.3219	4.3219	0.9824	0.3676	-0.766	3.3219	2
5	1.9187	1.8685	2.737	1.1027	0.3966	-0.515	2.737	1
6	1.0185	0.6792	0.415	1.0237	1.1809	0.8683	1.5146	0.3219
7	2.4321	2.3219	4.3219	1.1089	0.132	0.2201	3.3219	1.737
8	1.9624	2	2.737	1.0025	-0.291	-0.167	2.737	1.2794
9	2.1489	2.737	3.3219	1.6006	-0.738	-0.489	3.3219	1.114
10	1.1436	1.3219	1.5146	1.0718	-0.377	-0.227	2	0.5146
11	2.04	2	2.3219	1.1718	0.0918	-0.377	2.737	1.3219
12	0.6771	0.4648	2	1.0987	0.7434	0.5522	1.5146	-0.154
13	2.8748	2.737	3.3219	1.2124	-1.058	1.107	3.3219	2.3219
14	3.3707	3.3219	3.3219	0.7087	0.1388	-1.169	4.3219	2.737
15	2.0032	2	2.737	0.9009	0.1704	0.5334	2.737	1.3219
16	2.0133	2.3219	2.737	1.2383	-0.482	-0.028	2.737	1.2794
17	1.7902	1.737	2	0.7486	0.976	1.3345	2	1.3219
18	2.018	2	2.3219	0.6431	0.3089	0.6774	2.3219	1.5146
19	2.1113	2	4.3219	1.3711	0.0339	-0.733	2.8832	1.3219

BL8-2
Cumulative Frequency (%)
Phi-units
Thin-section
Sieve-equivalent
BL8-1
Cumulative Frequency (%)
Phi-units

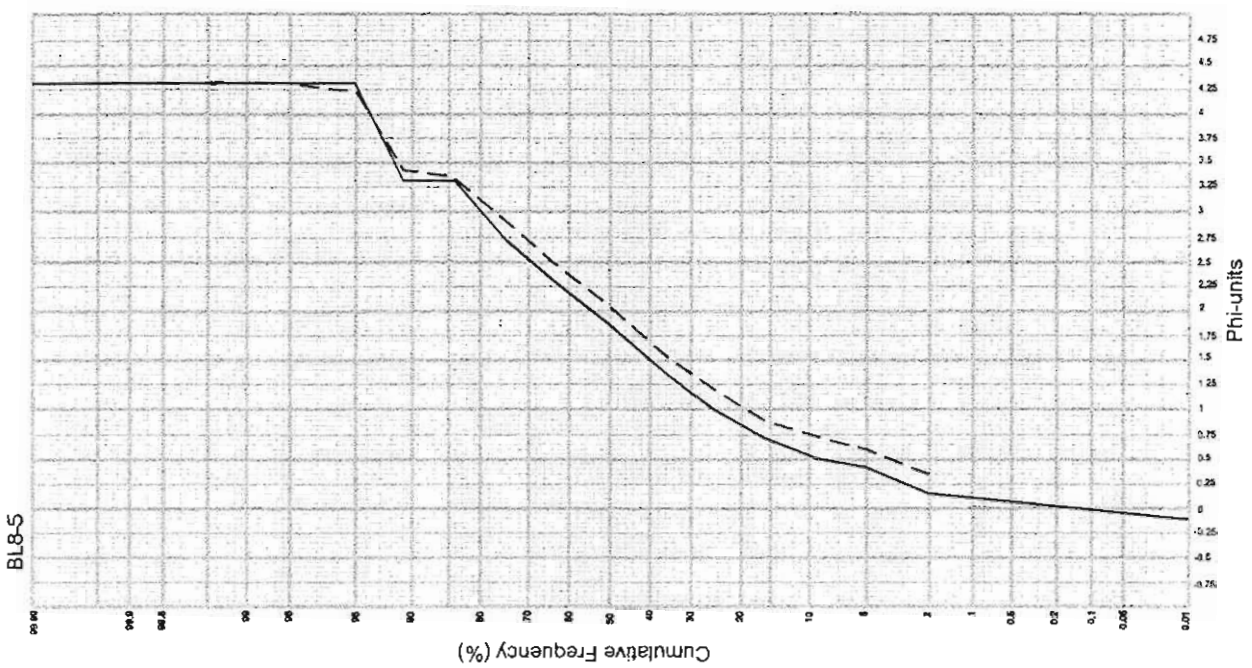
BL8-5
Cumulative Frequency (%)
Phi-units

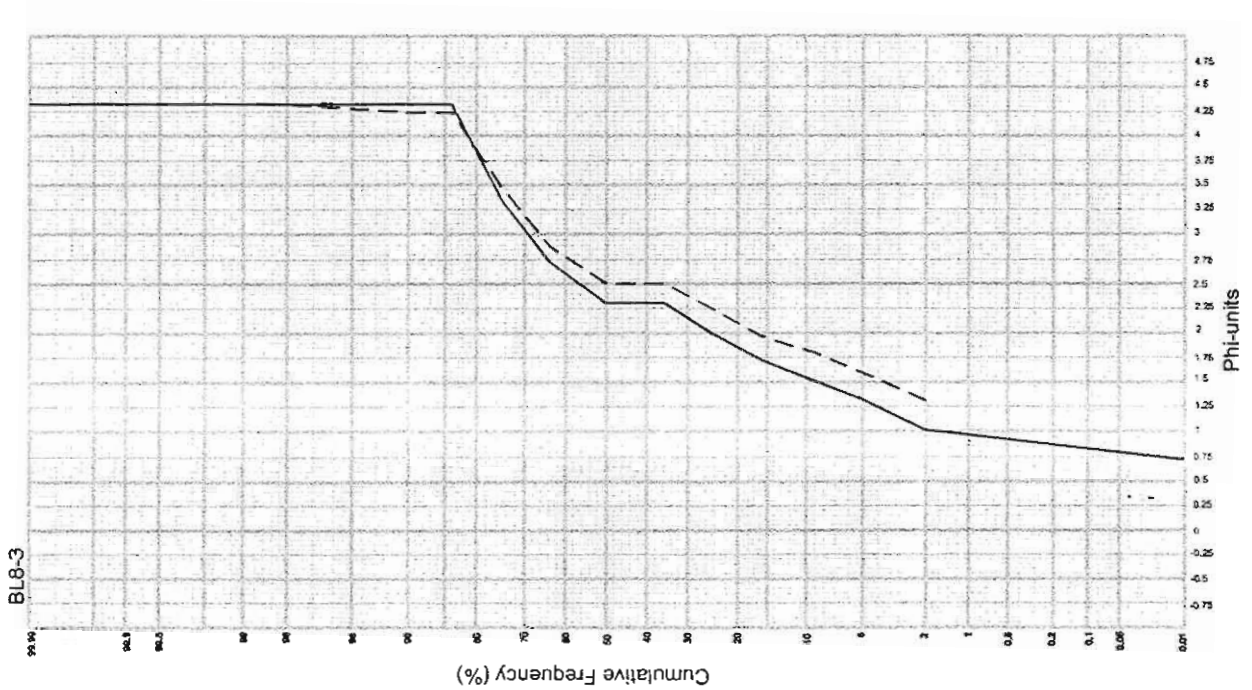
BL8-3
Cumulative Frequency (%)
Phi-units

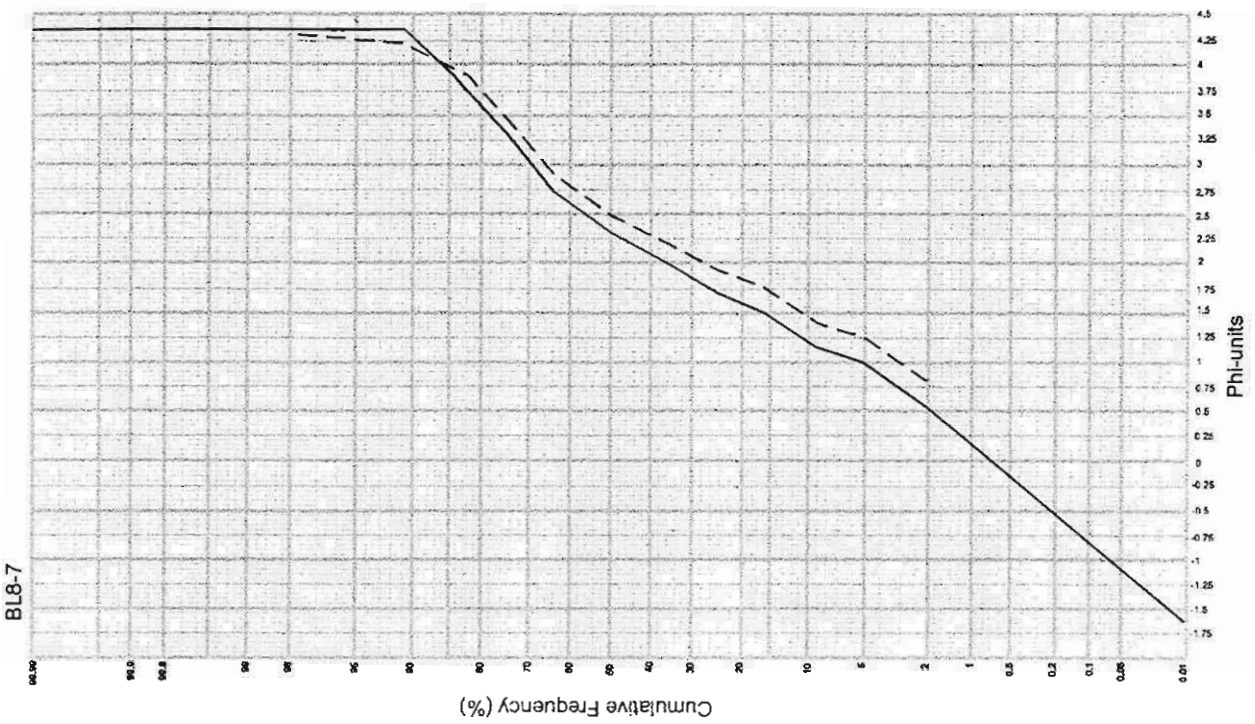
BL8-7
Phi-units
Cumulative Frequency (%)

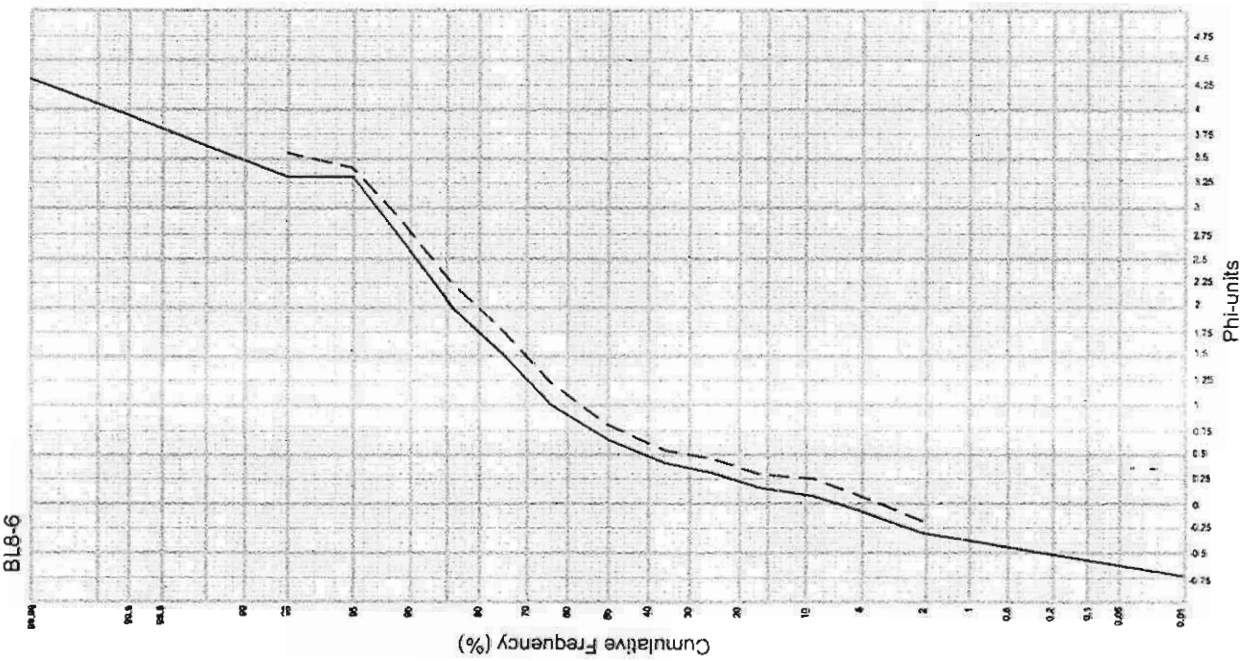
BL8-6
Phi-units
Cumulative Frequency (%)

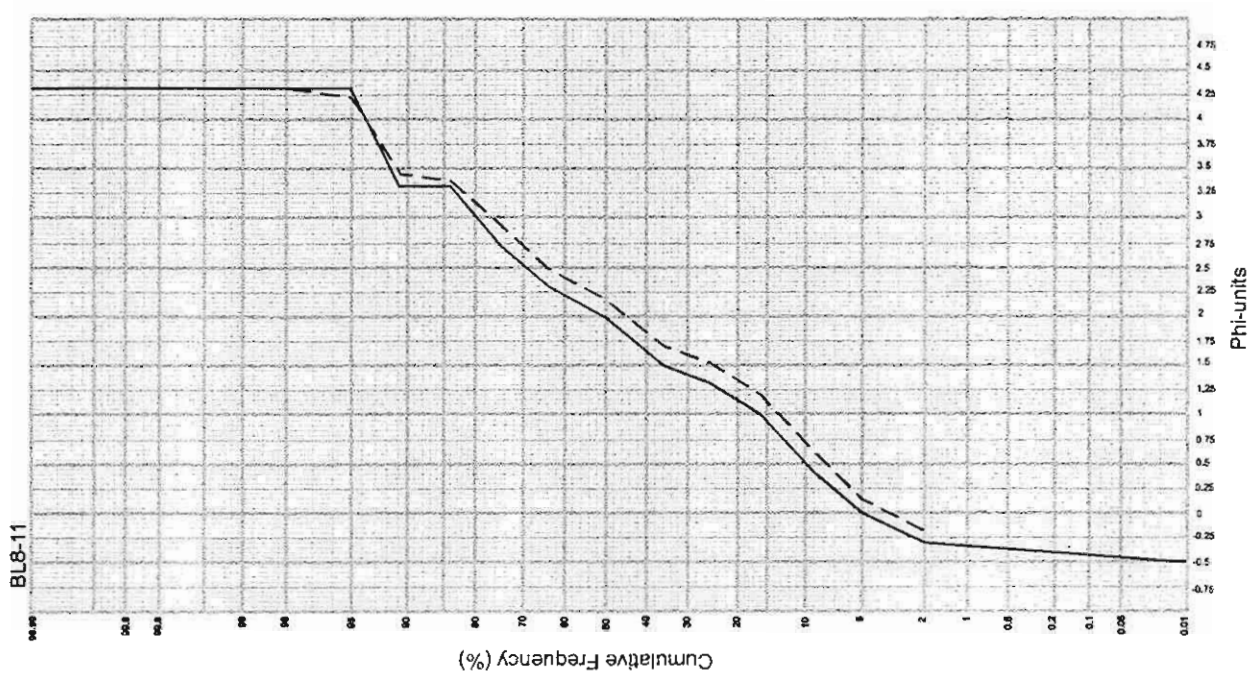
BL8-11
Cumulative Frequency (%)
Phi-units

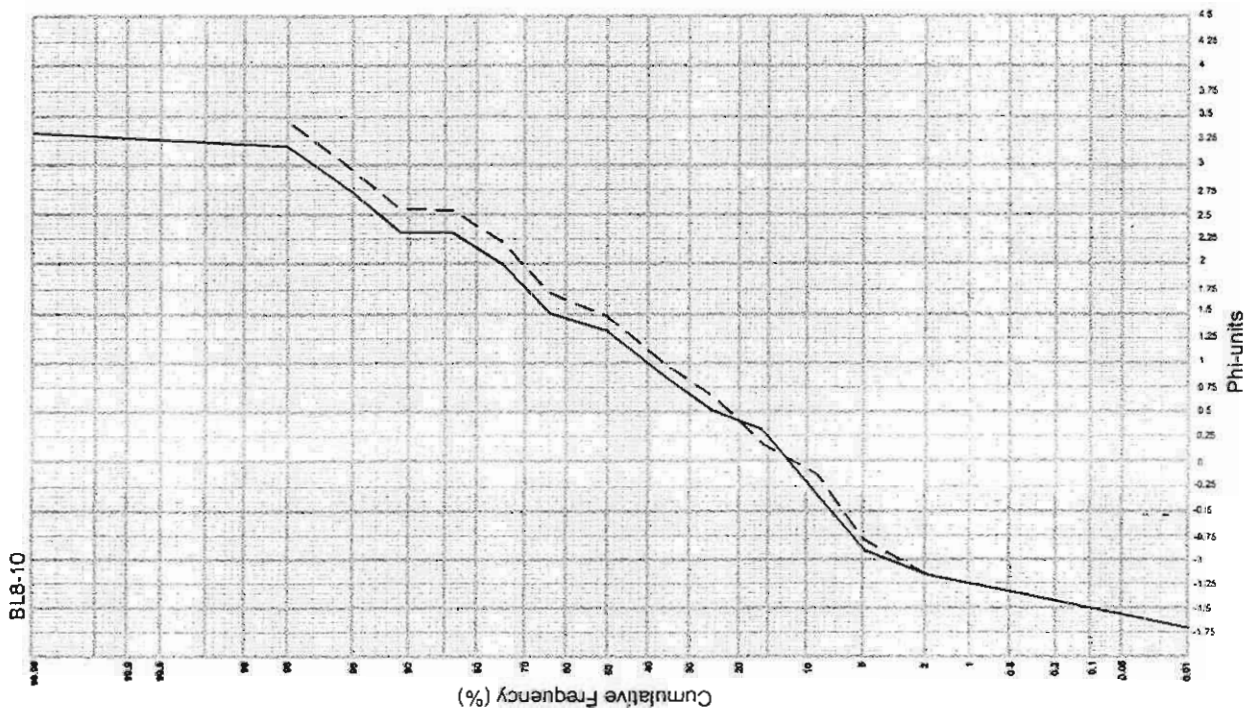
BL8-10
Cumulative Frequency (%)
Phi-units

BL8-13
Cumulative Frequency (%)
Phi-units

BL8-12
Cumulative Frequency (%)
Phi-units

BL8-15
Cumulative Frequency (%)
Phi-units

BL8-14
Cumulative Frequency (%)
Phi-units

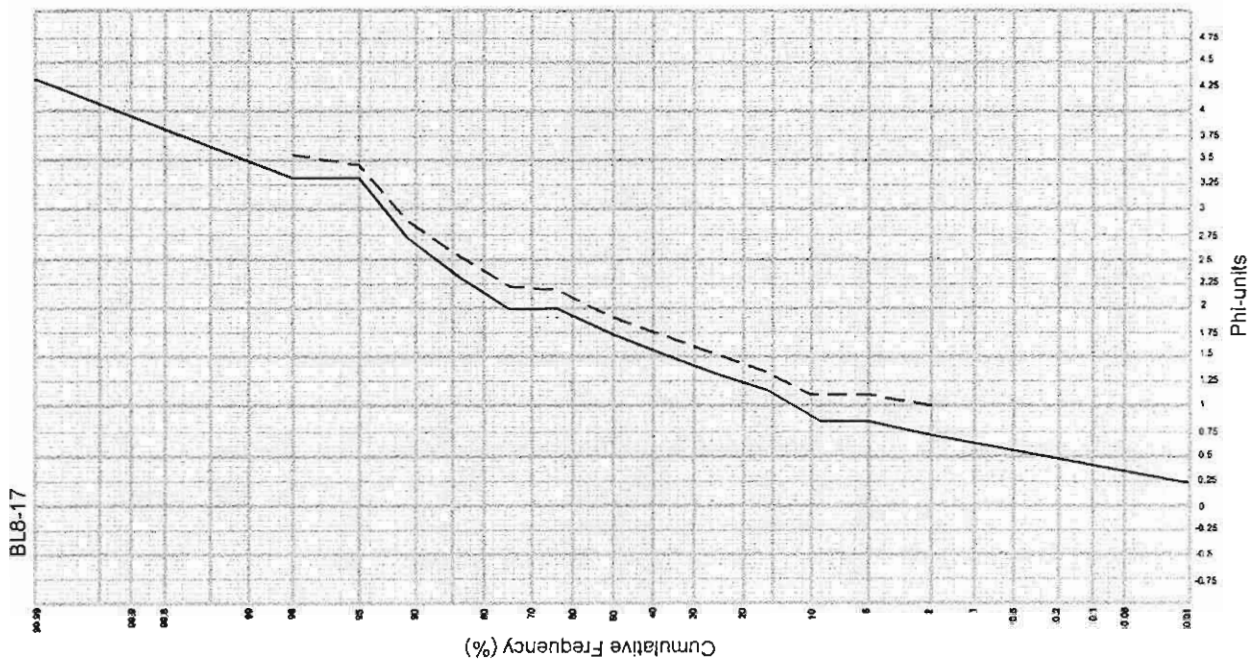
BL8-17
Cumulative Frequency (%)
Phi-units

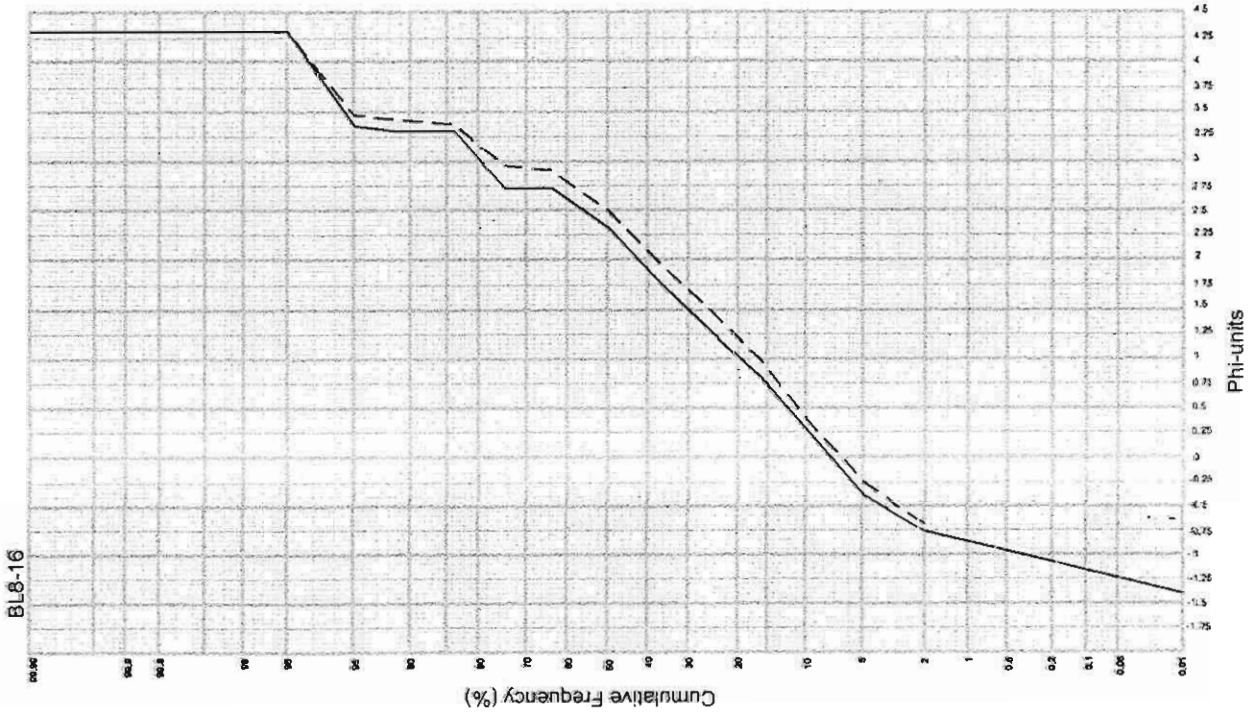
BL8-16
Cumulative Frequency (%)
Phi-units

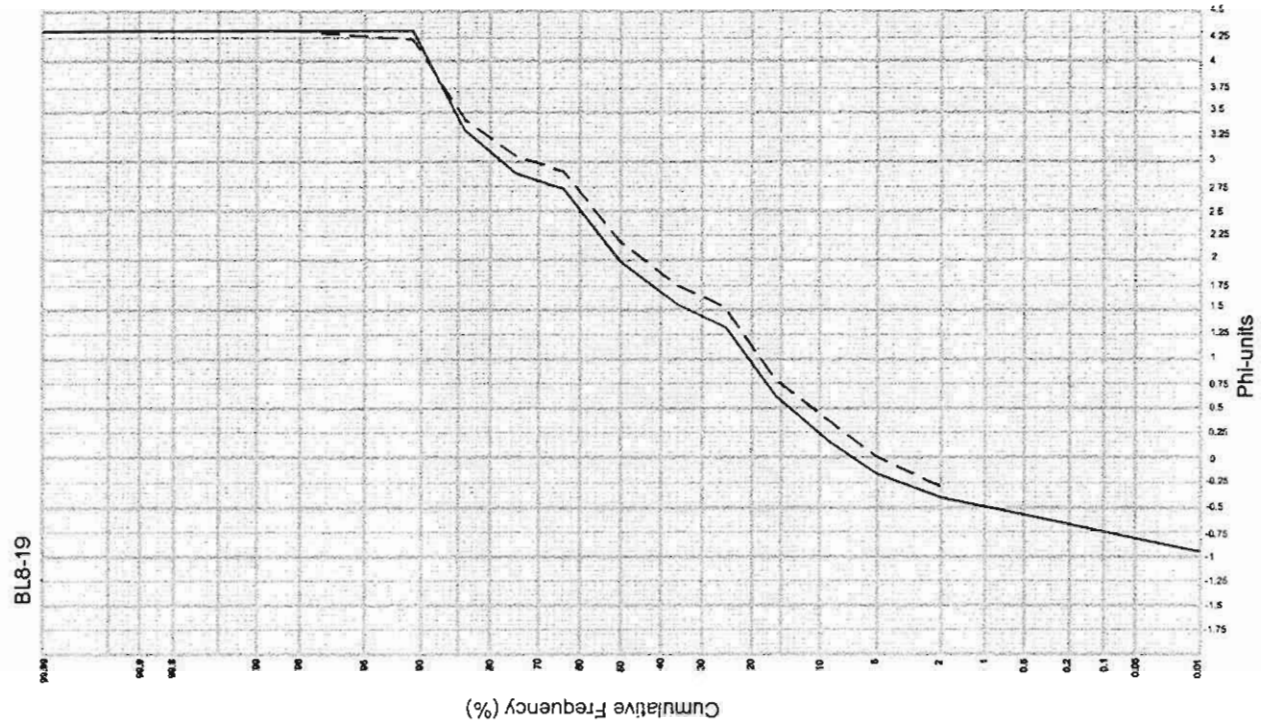
BL8-19
Phi-units
Cumulative Frequency (%)

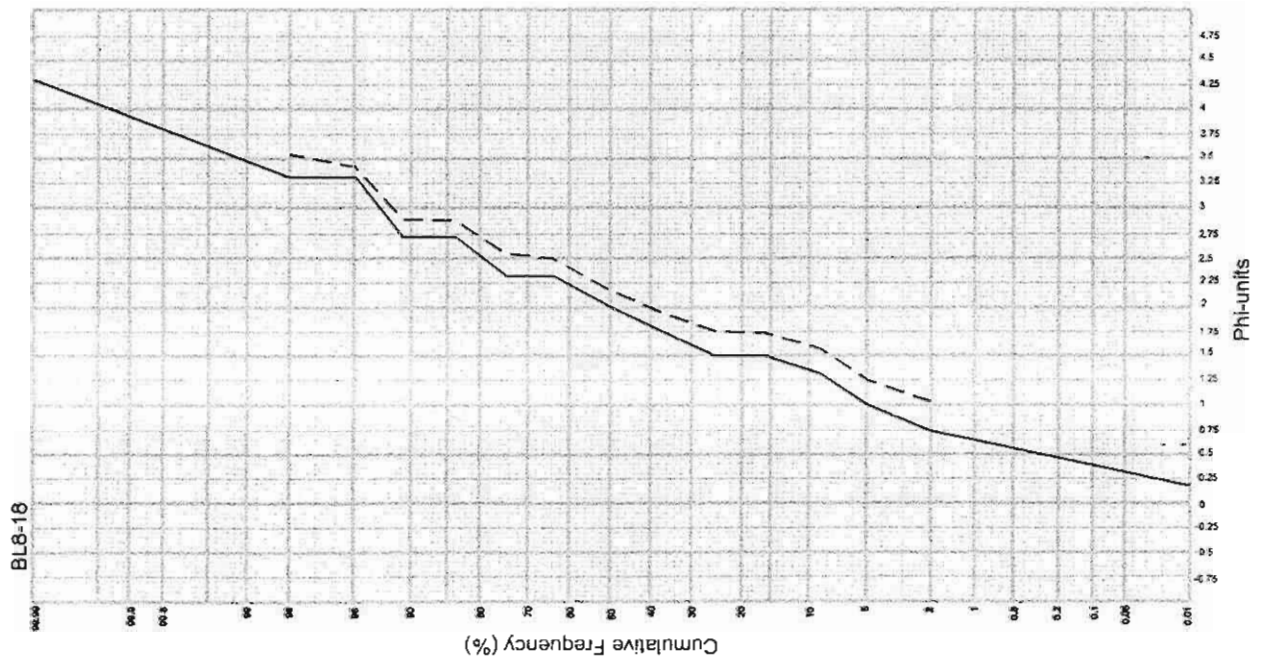
BL8-18
Phi-units
Cumulative Frequency (%)